MOLECULAR CHARACTERIZATION OF 52K PROTEIN OF BOVINE ADENOVIRUS TYPE 3

A Thesis
Submitted to the Faculty of Graduate Studies and Research
in Partial Fulfillment of the Requirements for
the Degree of Doctor of Philosophy
in the
Department of Veterinary Microbiology
University of Saskatchewan
Saskatoon

By
Carolyn Patricia Paterson

PERMISSION TO USE

In presenting this thesis in partial fulfillment of the requirements for a postgraduate degree from the University of Saskatchewan, I agree that the libraries of this university may make it freely available for inspection. I further agree that permission for copying of this thesis in any manner, whole or in part, for scholarly purposes may be granted by the professors who supervised my thesis work or in their absence, the Head of the Department or the Dean of the college in which my thesis work was done. It is understood that any copying or publication or use of this thesis or parts therof for financial gain shall not be allowed without any written permission. It is also understood that due recognition shall be given to me and to the University of Saskatchewan in any scholarly use which may be made of any material in my thesis.

Request for permission to copy or to make other use of material in this thesis in whole or part should be addressed to:

Head of the Department of Veterinary Microbiology
University of Saskatchewan
Saskatoon, Saskatchewan, S7N 5B4

ABSTRACT

Bovine adenovirus (BAdV)-3 is a non-enveloped, icosahedral virus with a double-stranded DNA genome, and is being developed as a vector for vaccination of animals and humans (Rasmussen et al., 1999; Zakhartchouk et al., 1999). Expression of viral genes is divided into early, intermediate, and late phases. The late genes of BAdV-3 are grouped into seven families (L1 to L7) based on usage of common polyadenylation site(s). The L1 region of BAdV-3 encodes the 52K protein, a non-structural protein conserved among members of the family *Adenoviridae*. In human adenovirus (HAdV) -5, the 52K protein is involved in packaging of the viral DNA into the capsid. The N-terminal half of the protein has been proposed to mediate serotype specificity of DNA packaging. The objective of this study was to characterize the 52K protein of BAdV-3.

DNA sequence analysis revealed that the BAdV-3 52K open reading frame encodes a protein of 370 amino acids rather than 331 amino acids as previously reported (Reddy et al., 1998). Western blotting with anti-52K serum detected the expression of a 40kDa protein at 24 to 72 hrs post-infection. BAdV-3 52K localized predominantly to the nucleus in BAdV-3 infected cells and in transfected cells in the absence of other viral proteins. Analysis of mutant 52K proteins revealed that residues 102-110 were necessary but not sufficient for nuclear import. This suggests that residues upstream or downstream of the identified 52K nuclear localization signal (NLS) are required, or that the function of the NLS is dependent on its conformation within 52K.

The nuclear import of 52K is significantly, but not completely, dependent on soluble factors, ATP, and temperature. A peptide competing for binding to importin β and a peptide encoding the NLS of Ycbp80 were also able to inhibit nuclear import of 52K. However, a dominant negative mutant of Ran was unable to block 52K nuclear import. These results suggest that 52K uses a classical importin α/importin β pathway for nuclear import. In support of this, a specific interaction between 52K and importin α3 was detected. In addition, 52K was able to accumulate in the nucleus in the absence of soluble factors and ATP when the nuclear membrane was permeabilized with detergent. This suggests that, in addition to nuclear import by the importin α/importin β pathway, 52K is able to accumulate in the nucleus by binding to nuclear components.

A yeast two-hybrid system identified interactions between BAdV-3 52K and pV, pVI, pVII, and IVa2. However, only the interaction with pVII could be confirmed by GST pulldown. 52K

and pVII also interact during BAdV-3 infection. An interaction between 52K and pVII has previously been shown in HAdV-5 infected cells (Zhang and Arcos, 2005).

Mass spectrometry analysis of proteins co-precipitating with BAdV-3 52K identified a cellular protein, NFκB-binding protein (NFBP), which interacted with 52K. The interaction between NFBP and 52K was confirmed *in vitro* and *in vivo*. NFBP has been shown to be essential for ribosomal RNA (rRNA) processing. While NFBP is normally localized in the nucleolus, co-expression with 52K results in the redistribution of NFBP from the nucleolus to other parts of the nucleus. While this suggested that redistribution of NFBP by 52K could inhibit rRNA processing during BAdV-3 infection, we were unable to detect a difference in rRNA processing in cells expressing truncated or full-length 52K in the absence of other viral proteins. Since NFBP is a multi-functional protein, future experiments should focus on other possible biological functions of the interaction of NFBP with BAdV-3 52K.

ACKNOWLEDGMENTS

First and foremost, I would like to thank my supervisor, Dr. Suresh Tikoo, for giving me the opportunity to pursue my graduate degree in his laboratory. Your support, encouragement, and advice during my graduate studies were greatly appreciated. I would also like to thank the members of my advisory committee, Dr. Lorne Babiuk, Dr. Lambert Loh, Dr. Alexander Zakhartchouk, and Dr. Vikram Misra for their valuable input and assistance during the course of my program.

I would also like to thank the past and present members of the Vectored Vaccines group for their help, suggestions, and support. In particular, the technical assistance of Satyender Hansra, Jill Van Kessel, and Kyla Shea was invaluable. I also owe thanks to the multitude of support staff at the Vaccine & Infectious Disease Organization for assisting with everything from peptide synthesis to administrative paperwork. It has been a pleasure to work with all of you.

I would like to thank my friends and fellow graduate students for their moral support and friendship. Our scientific discussions were always a great help in troubleshooting experiments, and our non-scientific ones were always a great help in maintaining my sanity. Amanda, Jean, Candice, Erin, Megan, Tara, Ellen, Patricia, and everyone else who has come and gone in our basement office, thank you for making my time as a graduate student much more enjoyable.

Finally, I would like to thank my parents, Guy and Sharon, and my brother Greg. I am immensely grateful for all your love, support, and encouragement over the years. I couldn't have done it without you.

TABLE OF CONTENTS

LIST OF TABLES

LIST OF FIGURES

ABBREVIATIONS USED IN THIS WORK

[^{32}P]	[^{32}P]-orthophosphate
ADP	Adenovirus death protein
ALG-4	Apoptosis-linked gene 4
AP	Alkaline phosphatase
ARM	Armadillo
ATP	Adenosine triphosphate
BAdV	Bovine adenovirus
BIB	Beta-like import receptor binding
βME	Beta-mercaptoethanol
Bp	Base pairs
BSA	Bovine serum albumin
CAdV	Canine adenovirus
CAR	Coxsackie and adenovirus receptor
CAS	Cellular apoptosis susceptibility protein
CBF	CCAAT-binding factor
CDK	Cyclin-dependent kinase
CDP	CCAAT-displacement protein
CPE	Cytopathic effects
COUP-TF	Chicken ovalbumin upstream promoter transcription factor
CR	Conserved region
DAPI	4',6-diamino-2-phenylindole
DBP	DNA binding protein
DMEM	Dulbecco's modified Eagle's medium
DTT	Dithiothreitol
EDTA	Ethylenediamine-tetraacetic acid
EGTA	Ethylene bis-(β-aminoethylether)-N,N,N',N-tetra-acetic acid
ETS	External transcribed spacer
EYFP	Enhanced yellow fluorescent protein
FBS	Fetal bovine serum
FG	Phenylalanine-glycine

GFP	Green fluorescent protein
GFPβGal	Green fluorescent protein-beta galactosidase
gp19K	19-kilodalton glycoprotein
GON	Group of nine hexons
GST	Glutathione-S-transferase
GTP	Guanosine triphosphate
HA	Hemagglutinin
HAdV	Human adenovirus
HEAT	Huntington, elongation factor 3, A subunit of protein phosphatase A, Tor1 kinase
HIV	Human immunodeficiency virus
HSV	Herpes simplex virus
IBB	Importin β binding
IPTG	isopropyl-β-D-thiogalactopyranoside
IRES	Internal ribosome entry site
ITR	Inverted terminal repeat
ITS	Internal transcribed spacer
Kb	Kilobases
kDa	Kilodalton
LB	Luria-Burtani
MAZ	MYC-associated zinc finger protein
MDBK	Madin-Darby bovine kidney
MEM	Minimal essential medium
MLP	Major late promoter
MOI	Multiplicity of infection
mTOR	Mammalian target of rapamycin
NES	Nuclear export signal
NF	Nuclear factor
NFBP	NFκB-binding protein
NFκB	Nuclear factor kappa-light-chain-enhancer of activated B cells
NLS	Nuclear localization signal
NPC	Nuclear pore complex

NTF2	Nuclear transport factor 2
Nup	Nucleoporin
Oct-1	Octamer-1
ORF	Open reading frame
PAdV	Porcine adenovirus
PAGE	Polyacrylamide gel electrophoresis
PBS	Phosphate buffered saline
PDCD11	Programmed cell death protein 11
PFU	Plaque-forming unit
PI3K	Phosphoinositide-3-OH kinase
PIC	Preinitiation complex
PKR	RNA-dependent protein kinase
Pol	Viral DNA polymerase
pTP	Pre-terminal protein
PVDF	Polyvinylidene fluoride
RanGAP	Ran-specific GTPase activating protein
RanGEF	Ran-specific guanine nucleotide exchange factor
RB	Retinoblastoma
RBP-2N	Recombination signal-binding protein 2N
RGD	Arginine-glycine-aspartic acid
RID	Receptor internalization and degradation
RRL	Rabbit reticulocyte lysate
RS	Arginine-serine
rDNA	Ribosomal DNA
rRNA	Ribosomal RNA
SDS	Sodium dodecyl sulphate
SL1	Selectivity factor 1
snoRNA	Small nucleolar RNA
snoRNP	small nucleolar ribonucleoprotein
SV40	Simian virus 40
TB	Transport buffer

$TCID_{50}$	Tissue culture infectious $dose_{50}$
TNF	Tumor necrosis factor
UBF	Upstream binding factor
USF	Upstream stimulatory factor
VA RNA	Virus-associated RNA
VSV	Vesicular stomatitis virus
WGA	Wheat germ agglutinin
Ycbp80	Yeast cap binding protein 80

1.0 LITERATURE REVIEW

1.1 Adenoviruses

Adenoviruses were first isolated in 1953 by two groups attempting to identify the causative agents of acute respiratory infections (Rowe et al., 1953; Hilleman and Werner, 1954). They were termed adenoviruses based on their initial isolation from adenoid tissues (Enders et al., 1956), and were later associated with acute respiratory infections and a cause of the common cold in the general population.

All adenoviruses have a double-stranded DNA genome, ranging from 26 to 45 kilobases in size (Davison et al., 2003), which is contained in an icosahedral capsid (Berk, 2007). They can replicate in respiratory and gut epithelium, as well as the eye, but tissue tropism varies between serotypes. Although adenoviruses are present in a wide range of species, their replication is generally limited to their host species. However, the occasional presence of neutralizing antibodies to adenoviruses of other species suggests the possibility of asymptomatic infections in species other than the natural host (Shenk, 2001).

1.1.1 Adenovirus taxonomy

Adenoviruses comprise the family *Adenoviridae*. Numerous serotypes infecting a wide range of species have since been identified (Berk, 2007) and are divided into five genera: *Mastadenovirus*, which exclusively infect mammalian species; *Aviadenovirus*, whose members are limited to avian hosts; *Atadenovirus*, which can be found in mammalian, avian, and reptile hosts but have a common phylogenetic ancestor; *Siadenovirus*, which are phylogenetically closest to *Aviadenovirus* but which have been isolated from a wide range of species; and *Ichtadenovirus*, found in fish (Benko et al., 2002; Davison et al., 2003).

The majority of identified adenoviruses belong to the *Mastadenovirus* genus and its members have been the most extensively characterized. Members of the *Mastadenovirus* genus are limited to mammalian species and include all identified human adenoviruses. Their genome size ranges from 30,536 bases for canine adenovirus type 1 to 36,519 bases for simian adenovirus type 25 (Davison et al., 2003). Several proteins present in the E1, E3, and E4 regions of the genome, as well as the capsid protein pV, are unique to members of the *Mastadenovirus* genus (Davison et al., 2003).

The members of the *Aviadenovirus* genus infect birds with varying degrees of pathogenicity. They have the largest genomes in the *Adenoviridae* family at up to 45 kilobases for fowl adenovirus type 8 (Ojkic and Nagy, 2000). Genomes of members of the *Aviadenovirus* genus lack homology to the corresponding E1, E3, and E4 regions of *Mastadenoviruses* (Chiocca et al., 1996; Ojkic and Nagy, 2000), but at least two proteins from chicken embryo lethal orphan virus are able to bind to the cellular retinoblastoma protein and activate E2F-dependent transcription, complementing the function of the *Mastadenovirus* E1A protein (Lehrmann and Cotten, 1999).

Members of the *Atadenovirus* genus have been identified from a wide range of host species, including cattle, birds, sheep, and snakes, but none from humans (Benko and Harrach, 1998; Both, 2004). There is evidence that members of the *Atadenovirus* genus originated in reptilian species (Wellehan et al., 2004). Several features distinguish members of the *Atadenovirus* genus from the other adenovirus genera. Their genomes have a high A/T content (Benko and Harrach, 1998) and they lack homologs of the E1A protein, the E3 region, and the structural proteins V and IX (Xu et al., 2000; Davison et al., 2003; Both, 2004). Members of the *Atadenovirus* genus also encode two unique capsid proteins and several novel open reading frames not found in other adenoviruses. (Both, 2002; Both, 2004; Gorman et al., 2005).

Analysis of members of the *Siadenovirus* genus shows that their closest phylogenetic relationship is to those from *Aviadenovirus* genus (Davison et al., 2000). Three viruses are recognized members of this genus: turkey adenovirus type 3 (also known as turkey hemorrhagic enteritis virus), frog adenovirus type 1, and raptor adenovirus type 1 (Pitcovski et al., 1998; Davison et al., 2000; Kovács and Benko, 2009). However, several other putative members of the *Siadenovirus* genus have been recently identified in a number of bird species as well as from a tortoise (Katoh et al., 2009; Rivera et al., 2009; Wellehan et al., 2009; Kovács et al., 2010). The genomes of frog adenovirus type 1 and turkey adenovirus type 3 are 26,163 and 26,263 bases in length, respectively (Pitcovski et al., 1998; Davison et al., 2000). This is significantly shorter than most other adenoviruses. Homologs of proteins encoded by the E1, E3, and E4 regions of members of the *Mastadenovirus* genus appear to be absent in members of the *Siadenovirus* genus (Davison et al., 2003). However, members of the *Siadenovirus* genus have a protein related to bacterial sialidases (Davison et al., 2000).

A single member of the genus *Ichtadenovirus* has been isolated to date. Partial sequence analysis of white sturgeon adenovirus type 1 has demonstrated that it represents a genus distinct

from the other previously identified genera but shares characteristics of the non-*Mastadenovirus* genera (Benko et al., 2002; Kovács et al., 2003).

1.1.2 Human adenovirus

Human adenovirus (HAdV) was first isolated in the 1950s and identified as the causative agent of acute respiratory disease (Rowe et al., 1953; Hilleman and Werner, 1954). Adenoviruses are responsible for a small percentage of acute respiratory morbidity in the general population, an estimated 5-10% of respiratory illness in children, and mild and self-limiting infection in most immunocompetent adults (Berk, 2007). Adenoviruses can also cause epidemic conjunctivitis and gastroenteritis in children (Mautner et al., 1995; O'Brien et al., 2009). In immunocompromised patients, such as individuals with acquired immunodeficiency syndrome and patients who have received organ or bone marrow transplants, adenoviruses can cause serious and often fatal disease (La Rosa et al., 2001; Kojaoghlanian et al., 2003; Leen and Rooney, 2005). Although a number of HAdVs are found to be oncogenic in hamsters (Trentin et al., 1962), no HAdV has been shown to cause cancer in humans (McLaughlin-Drubin and Munger, 2008).

To date, 51-54 serotypes of HAdVs have been identified (Berk, 2007; Jones et al., 2007; Ishiko et al., 2008; Ishiko and Aoki, 2009; Walsh et al., 2009). Of these, HAdV serotypes 2 and 5 have been the most extensively studied. The identified serotypes are distinguished by their resistance to neutralization by antibodies against other adenovirus serotypes (Berk, 2007). Based on their ability to agglutinate erythrocytes, oncogenicity in animals, and genetic homology, HAdVs are divided into six species, A to F (Berk, 2007). HAdV-52 is proposed to be the only member of a new species, G (Jones et al., 2007).

1.1.2.1 Virus structure and genome organization

Adenoviruses are non-enveloped, consisting of a protein shell encapsidating a DNA-containing core, and have a diameter of approximately 75-90 nanometers (Niiyama et al., 1975; Berk, 2007). The viral capsids are icosahedral, with fiber proteins projecting outward from the icosahedron's vertices. The capsid consists primarily of the hexon protein, of which there are 720 copies per virion. These are grouped in trimers known as hexon capsomers (Vellinga et al., 2005). These hexon capsomers subsequently assemble into groups of nine (GONs), which make up the faces of the icosahedron. At each of the 12 vertices is a penton capsomer, made up of 5

copies of the penton protein. These penton capsomers serve as the base for the fiber protein, which form trimers (Russell, 2009). In addition to these three major capsid proteins, several minor capsid proteins, namely IIIa, VI, VIII, and IX, are also present. An estimated 60 copies of protein IIIa are present in mature virions. It appears to be positioned on the inside of the capsid, between the penton base and its surrounding hexon capsomers (San Martín et al., 2008). A portion of IIIa may also be exposed on the outside of the viral capsid (Vellinga et al., 2005; San Martín et al., 2008). An earlier study suggested that IIIa is, in fact, located entirely on the outside of the capsid (Fabry et al., 2005). Mutations in IIIa prevent the formation of mature viral capsids, suggesting that it has an important role in assembly, and there is also evidence that it interacts with the core protein VII (Vellinga et al., 2005). Protein VI is located on the interior of the capsid beneath the penton base and interacts with the core protein V (Vellinga et al., 2005). Protein VIII appears to be present in the interior of the viral capsid (Fabry et al., 2005; Vellinga et al., 2005). Protein IX is located on the outside of the capsid, and acts to stabilize the groupings of hexons (Vellinga et al., 2005; Fabry et al., 2009). Protein IX is not required for virus replication, but contributes to the thermostability of the capsid, presumably through its interactions with the hexons (Vellinga et al., 2005).

The virus core consists of the highly compacted double-stranded DNA genome and the viral core proteins. Proteins V, VII, and μ are basic, arginine-rich proteins that bind to the viral DNA. Protein VII is the predominant core protein, with over 800 copies per virion (Berk, 2007). The viral DNA is condensed around nucleosome-like cores formed by protein VII (Vayda and Flint, 1987). Protein V binds to protein VI and provides a link between the viral core and the capsid (Everitt et al., 1975; Berk, 2007). Also present in the core are the terminal protein, which is covalently attached to the 5' ends of the viral DNA (Rekosh et al., 1977) and the viral protease, which is involved in virus maturation as well as entry and uncoating (Greber, 1998).

1.1.2.2 Virus entry and release

The early steps of adenovirus infection have been primarily determined from studies of HAdV. The first cellular receptor identified for adenovirus was the coxsackie and adenovirus receptor (CAR) for HAdV-2 and -5 (Bergelson et al., 1997). CAR is a member of the immunoglobulin superfamily and is involved in adhesion between epithelial cells (Arnberg, 2009). Its distribution in human tissues is not completely characterized, but CAR mRNA has

been found in the heart, brain, pancreas, intestine, lung, liver, and kidneys (Zhang and Bergelson, 2005). *In vitro*, CAR acts as a receptor for species A, C, E, and F HAdVs, and some members of species D (Arnberg et al., 2000; Russell, 2009). There is some evidence that CAR may not be the primary receptor *in vivo* (Arnberg, 2009). Adenovirus tropism does not always correlate with expression and distribution of CAR, and ablating the ability to bind CAR does not change adenovirus distribution (Alemany and Curiel, 2001). Species B HAdVs are able to use CD80, CD86, or CD46 (except serotypes 3 and 7) as a receptor (Marttila et al., 2005; Short et al., 2006). Some species D adenoviruses have been shown to use sialic acid as a receptor (Arnberg et al., 2000). HAdV-40 and -41, which belong to species F, express both a long fiber and a short fiber (Favier et al., 2002). The long fiber binds to CAR, but the receptor for the short fiber has not been identified (Roelvink et al., 1998). A number of other host cell proteins or compounds, such as coagulation factors, heparan sulfate proteoglycans, and lactoferrin, have been found to bind adenovirus or promote transduction *in vitro* and could have roles as functional adenovirus receptors (Arnberg, 2009).

After the fiber binds to its host cell receptor, efficient internalization requires a second interaction between the arginine-glycine-aspartic acid (RGD) motif of the penton base and $\alpha_v\beta_3$ and $\alpha_v\beta_5$ integrins on the cell surface (Bai et al., 1993; Wickham et al., 1993). All sequenced HAdVs have this RGD motif with the exception of HAdV-40 and -41, which have a gastrointestinal tropism and show delayed internalization (Albinsson and Kidd, 1999; Zhang and Bergelson, 2005). The fiber protein is released from the viral capsid at the cell surface, a step that is dependent on the penton-integrin interaction (Greber et al., 1993; Nakano et al., 2000).

The binding of the α_v integrins by penton results in the activation of phosphoinositide-3-OH kinase (PI3K), which in turn activates Rho family guanosine triphosphatases and stimulates reorganization of the actin cytoskeleton to promote virus internalization (Li et al., 1998a; Li et al., 1998b). The virus is primarily internalized by receptor-mediated endocytosis in clathrin-coated vesicles (Varga et al., 1991; Wang et al., 1998). After endocytosis, the pH of the vesicle becomes more acidic, creating an early endosome (Gastaldelli et al., 2008). The acidic pH of the endosomal compartment induces the virus capsid to begin dismantling, starting with the dissociation of IIIa, penton, and VIII (Greber et al., 1993; Wiethoff et al., 2005). These conformational changes in the viral capsid expose an amphipathic helix in protein VI (well-conserved among human and non-human adenoviruses) that disrupts the endosomal membrane

and allows the virus to escape into the cytosol (Wiethoff et al., 2005). There, protein IX dissociates from the remains of the viral capsid, but at least some hexon capsomers remain associated with the viral DNA and core proteins (Greber et al., 1993).

After escaping the early endosome, the partially disassembled capsid is translocated to the nucleus along microtubules (Leopold et al., 2000). Hexons still associated with the viral DNA can bind directly to the microtubule motor protein dynein, which allows minus-end directed movement of the viral capsid along the microtubules towards the nucleus (Bremner et al., 2009). Depolarization of microtubules or blocking minus-end transport using anti-dynein antibodies inhibits nuclear localization of adenovirus capsids (Leopold et al., 2000; Bremner et al., 2009).

The capsids localize to nuclear pore complexes (NPCs) after transport along the microtubules by binding to CAN/Nup214, a filament protein on the cytosolic face of the NPC (Trotman et al., 2001). There, several protein-protein interactions promote further disassembly of the viral capsid, such as the binding of histone H1 to hexon. For HAdV-2, it is proposed that histone H1 is then bound by nuclear import factors importin β and importin 7, transporting the histone/hexon complex into the nucleus and making the viral DNA bound by core proteins V and VII accessible for nuclear import (Trotman et al., 2001). Since this interaction is not observed in HAdV-3 it may not be a conserved mechanism of viral entry. The molecular chaperone hsc70 and the nuclear export protein CRM1 may also be involved in capsid disassembly and nuclear import of the viral DNA (Saphire et al., 2000; Strunze et al., 2005). Another nuclear import receptor, transportin, can bind protein V and protein VII and is required for importing the viral DNA/protein V/protein VII complex into the nucleus (Hindley et al., 2007).

Different species of HAdV exhibit patterns of intracellular trafficking that diverge from the "classical" pathway of species C HAdVs such as HAdV-2 (Leopold and Crystal, 2007). HAdV-12, a member of species A, does not escape early endosomes in a subclone of HeLa cells and accumulates in late endosomes and lysosomes (Chardonnet and Dales, 1970). Species B HAdVs that do not use CAR as a receptor also traffic to late endosomes and lysosomes (Miyazawa et al., 2001; Shayakhmetov et al., 2003). After escaping from the lysosomes, which are transported near the nucleus in many cell types, the viral DNA is translocated into the nucleus as with species C HAdVs (Miyazawa et al., 2001; Leopold and Crystal, 2007).

1.1.2.3 Early gene expression

The core protein VII remains associated with the viral DNA after its entry into the nucleus and for several hours post-infection (Johnson et al., 2004; Chen et al., 2007). The binding of protein VII to the viral DNA represses viral transcription during the early stages of infection, possibly as a mechanism to control the level of expression of the early proteins, and is released 10-12 hrs post-infection. Its release is dependent on E1A and transcription of viral genes.

The first region of the viral genome to be transcribed is the E1A region (Nevins et al., 1979). Two major mRNA transcripts are generated from E1A by differential splicing (Perricaudet et al., 1979). In HAdV-2 and HAdV-5, the two major E1A proteins have 289 and 243 amino acid residues and are termed 289R and 243R, respectively. Five conserved regions (CRs) have been identified in E1A: the N-terminus, CR1, CR2, CR3, and CR4 (Avvakumov et al., 2004). In HAdV-5, the 243R protein shares common N- and C-termini with the 289R protein but lacks a 46-amino acid region near the center of the protein (Perricaudet et al., 1979). This gap corresponds to CR3 (Avvakumov et al., 2004). E1A has two primary functions: to induce the host cell to enter S phase, creating a permissive environment for viral replication, and to stimulate expression of other early viral genes.

E1A is a potent transactivator, able to stimulate transcription from a variety of promoters. It does not bind DNA directly, but instead associates with the DNA-binding domains of transcription factors bound to promoters (Liu and Green, 1994). This allows it to activate transcription from a number of viral and cellular promoters. The CR3 domain in the E1A 289R protein contains a zinc finger domain that binds to a subunit of the cellular mediator complex, recruiting RNA polymerase II and stimulating assembly of the preinitiation complex required to begin transcription (Wang and Berk, 2002).

E1A is also involved in stimulating the host cell to enter S phase. The CR1 and CR2 domains of E1A can bind to the cellular retinoblastoma (RB) protein and displace the bound cellular transcription factor E2F (Berk, 2005). Normally, release of E2F is mediated by cyclin-dependent kinases (CDKs) that help regulate entry into the cell cycle; CDK- or E1A-mediated release of E2F activates transcription of cellular genes including genes essential for the cell to enter into S phase. E2F also activates transcription from the viral E2A promoter in cooperation with the viral E4orf6/7 protein (Obert et al., 1994).

The E1A and E1B proteins are necessary and sufficient to transform cells (White, 2001). E1A de-regulates cell cycle checkpoints by forcing the cell into S phase, and this induces apoptosis (White, 2001). E1A binding to cellular proteins such as the retinoblastoma (RB) protein and CREB-binding protein/p300 leads to stabilization of p53, which in turn stimulates apoptosis (Gallimore and Turnell, 2001). The pro-apoptotic effects of E1A are counteracted by the E1B proteins, which is why both E1A and E1B proteins are required for transformation (Gallimore and Turnell, 2001).

The E1B region encodes two proteins, E1B-55K and E1B-19K, that are involved in preventing apoptosis induced by viral infection and the actions of the E1A proteins (Berk, 2005). E1B-55K can bind to p53 and contains a repressor domain that suppresses transcription of p53-activated genes. Since activation of p53 normally leads to transcription of proapoptotic genes, binding of E1B-55K to p53 prevents apoptosis induced by virus infection or by E1A transformation. E1B-55K also interacts with the viral E4orf6 protein and cellular proteins to form a ubiquitin ligase complex that targets p53 for degradation as well as a complex that responds to cellular DNA damage. The E1B-55K/E4orf6 complex is also important for events late in viral infection (discussed in section 1.1.2.6). The E1B-19K protein antagonizes the apoptosis response induced by E1A (Berk, 2005). E1B-19K is homologous to the cellular protein BCL-2 and is able to bind the proapoptotic proteins BAK and BAX and prevent them from forming pores in mitochondria that releases proteins such as cytochrome c and triggers apoptosis (Berk, 2005).

The proteins expressed by the E2 region are involved in viral DNA replication (Berk, 2007). The E2A region encodes the viral DNA-binding protein (DBP), while the E2B region encodes the viral DNA polymerase (Pol) and the pre-terminal protein (pTP) (Berk, 2007).

The E3 region is under the control of an E1A-responsive promoter and encodes proteins mainly involved in suppressing the host immune responses to viral infection (Weeks and Jones, 1985; Wold et al., 1995; Horwitz, 2004). The 19-kilodalton glycoprotein (gp19K) is localized in the endoplasmic reticulum and sequesters class I major histocompatibility complex molecules, preventing them from being transported to the cell surface and potentially activating an immune response against viral infection (Pääbo et al., 1987; Horwitz, 2004). The gp19K protein is also able to sequester ligands recognized by natural killer cells (McSharry et al., 2008). The 14.7K protein inhibits tumor necrosis factor (TNF)-mediated apoptosis by preventing endocytosis of the TNF receptor (Gooding et al., 1988; Schneider-Brachert et al., 2006). The 14.5K and 10.4K

proteins form a receptor internalization and degradation (RID) complex that downregulates surface expression of Fas and TNF receptors involved in apoptosis and stimulates their degradation (Shisler et al., 1997; Tollefson et al., 1998; Chin and Horwitz, 2006). RID also downregulates the epidermal growth factor receptor to stimulate cell metabolism (Tollefson et al., 1991) and inhibits NFκB activation and cytokine production (Horwitz, 2004). The 6.7K protein cooperates with RID to downregulate the receptors for the TNF-related apoptosis-inducing ligand (Benedict et al., 2001). The 11.6K protein differs from the other E3 proteins in that it is expressed at high levels during late times of infection and promotes apoptosis and cell lysis, and will be discussed later.

The E4 region encodes proteins that appear to have a wide variety of functions during virus infection (Weitzman and Ornelles, 2005). It produces transcripts for six proteins, named after their open reading frames (E4orf1, orf2, orf3, orf4, orf6, and orf6/7). E4orf1 and E4orf4 activate the mammalian target of rapamycin that is required for efficient entry into S-phase (O'Shea et al., 2005). The E4orf3 and E4orf6 proteins have functional redundancy and inhibit the cellular DNA damage response to prevent the viral genome from forming concatomers. E4orf3 also disrupts ND10 domains in the nucleus. The E4orf6 protein is highly conserved among HAdVs and forms a complex with the E1B-55K protein that has several important functions during virus infection (previously discussed in this section, p.8). The E4orf6 protein can also inhibit p53 independently of E1B-55K. E4orf6/7, as previously mentioned, enhances binding of E2F to the viral E2 promoter.

Two virus-associated RNA molecules (VA RNA) that also function to counteract host defences are transcribed from HAdV genomes. These two VA RNAs, VAI and VAII, have stable secondary structures and are able to inhibit activation of RNA-dependent protein kinase (PKR) (Mathews and Shenk, 1991). In the absence of VAI, activated PKR phosphorylates eIF2α, preventing translation initiation (O'Malley et al., 1986). VAI is also processed into viral micro RNAs that interact with the cellular complex responsible for RNA silencing and can alter expression of host genes (Andersson et al., 2005; Aparicio et al., 2010).

1.1.2.4 DNA replication

DNA replication begins 5-8 hrs after infection of HeLa cells with HAdV-2 or HAdV-5 at a multiplicity of infection of 10 (Berk, 2007). Three viral proteins encoded by the E2 region are

required for DNA replication: Pol, pTP, and DBP. The inverted terminal repeats (ITRs) located at each end of the linear genome contain origins of DNA replication where a preinitiation complex (PIC) consisting of viral and cellular proteins forms. Within the ITR are the binding sites for pTP and Pol (Temperley and Hay, 1992). Pol and pTP interact to form a heterodimer that binds to the minimal origin of replication (Temperley and Hay, 1992). Downstream of the minimal origin of replication are binding sites for two cellular proteins, the transcription factors nuclear factor I (NFI, also known as CAAT transcription factor) and nuclear factor III (NFIII, also known as Oct-1). NFI and NFIII interact with Pol and pTP, respectively, and stimulate DNA replication by recruiting the Pol/pTP heterodimer to its binding site on the viral DNA, and by stabilizing the protein-DNA interaction (Chen et al., 1990; Mul et al., 1990; Mul and van der Vliet, 1992; Armentero et al., 1994; Coenjaerts et al., 1994).

After the formation of the PIC, DNA replication is initiated using a protein-priming mechanism (de Jong et al., 2003). Pol catalyzes the covalent linkage of a dCMP residue to pTP, followed by the addition of A and T residues to create a pTP-CAT intermediate using residues 4-6 of the 3'-GTAGTA-5' sequence at the terminus of the ITR as a template. The pTP-CAT intermediate then jumps back to residues 1-3 and begins elongation of the new DNA strand from the template (King and van der Vliet, 1994). This jumping back mechanism protects against errors and prevents shortening of the genome (King et al., 1997).

Synthesis of the new viral DNA proceeds 5' to 3', displacing one parental strand and using the other parental strand as a template (Lechner and Kelly, 1977). New rounds of DNA replication can be initiated from the same ITR, creating multiple single-stranded branches from the double-stranded molecule as more strands are displaced by new strand synthesis. This is known as type I DNA replication. When synthesis of the daughter strand is complete, the result is a daughter duplex and a parental single strand. Type II replication occurs when the ITRs of this single strand hybridize, forming a panhandle structure and restoring the double-stranded origin of replication that can be recognized by the PIC. Synthesis of a new daughter strand from the 3' end of the parental strand displaces the 5' ITR hybridized to the 3' ITR, creating a single strand template for synthesis of the daughter strand.

In addition to pTP and Pol, the viral DBP is required for DNA replication. DBP stimulates the initiation of DNA replication by enhancing binding of NFI and Pol to the origin of replication (Stuiver and van der Vliet, 1990; van Breukelen et al., 2003). DBP is also required to unwind the

parental double-stranded helix during elongation. DBP destablizes the double-stranded helix and binds to the single parental strand displaced by DNA replication, protecting it from degradation (Zijderveld and van der Vliet, 1994).

In order for the full viral genome to be replicated, cellular topoisomerase I (also called NFII) is required. In the absence of topoisomerase I, initiation of DNA synthesis is not affected but replication halts approximately a quarter of the way through the genome (Nagata et al., 1983). Presumably, topoisomerase activity is required to relax torsional stress placed on the viral DNA by the replication forks (Schaack et al., 1990).

1.1.2.5 Intermediate and late gene expression

Two viral proteins, IVa2 and pIX, are classified as intermediate or delayed-early since their expression is dependent on viral DNA replication but their transcripts appear earlier than those of the other late proteins (Binger and Flint, 1984). Expression of IVa2 and pIX is suppressed during the early stages of infection by cellular transcriptional repressors. The repressor for IVa2 remains to be identified (Chen et al., 1994; Lin and Flint, 2000; Iftode and Flint, 2004), while the repressor for pIX is the cellular protein RBP-2N (Dou et al., 1994). As new copies of the viral genome are synthesized the availability of binding sites for these repressors increases. This is proposed to titrate out the repressors and relieve the inhibition of IVa2 and pIX transcription (Dou et al., 1994; Lin and Flint, 2000; Iftode and Flint, 2004).

The late genes encode structural proteins that make up the viral capsid (hexon, penton, fiber, IIIa, V, VI, VII, VIII, IX, and μ) and non-structural proteins (52K, 100K, 33K, 22K, and the viral protease). Expression of the late genes is controlled by the major late promoter (MLP). At early times during infection, transcription occurs from the MLP at a low level, producing only transcripts from the L1 region (Shaw and Ziff, 1980). The presence of an additional sequence in the tripartite leader at the 5' end that is not included at late times of infection appears to inhibit translation from these transcripts, which code for the L1 52/55-kilodalton protein (Akusjärvi and Persson, 1981). Transcription from the MLP involves several viral and cellular factors. The TATA box is bound by the transcription factor TFIID (Sawadogo and Roeder, 1985), which recruits other factors that make up the transcription complex, including RNA polymerase II (Deng and Roberts, 2007). The cellular transcription factors MAZ and Sp1 bind to sequences within the MLP (Parks and Shenk, 1997). Both factors interact with E1A, and the presence of

E1A increases transcription activation of the MLP by MAZ and Sp1 by several fold. An inverted CAAT box element is bound by CCAAT-binding factor (CBF) (Reach et al., 1991), while another element is bound by the upstream stimulatory factor (USF; also called major late transcription factor) (Sawadogo and Roeder, 1985). The functions of USF and CBF may be redundant, with both proteins being able to recruit TFIID (Reach et al., 1991). Binding of USF to the MLP is enhanced by DBP (Zijderveld et al., 1994). USF only binds to the MLP after viral DNA replication (Toth et al., 1992), and thus may be important for the timing of MLP activation during viral infection.

Sequences downstream of the transcription initiation site on the MLP are also required for maximum activation during viral infection (Leong et al., 1990). These two downstream enhancer sequences are DE1 and DE2, which is subdivided into DE2a and DE2b (Ali et al., 2007). DE2b is bound by DEF-B, while DE1 and DE2a are bound by DEF-A. DEF-B is a homodimer of the viral protein IVa2 (Tribouley et al., 1994; Lutz and Kedinger, 1996). The identity of DEF-A remains unclear, but was initially believed to be a complex of IVa2 and another viral protein (Lutz and Kedinger, 1996). There is evidence that the L4 33K protein alone constitutes DEF-A (Ali et al., 2007). In addition, the L4 22K protein, but not 33K, enhances binding of IVa2 to the MLP and is required for MLP activation (Ostapchuk et al., 2006; Morris and Leppard, 2009). The 33K and 22K proteins share a common N-terminus and reactivity of any antibodies raised to this sequence complicates analysis of the complexes bound at the MLP.

Transcription from the MLP produces a single RNA transcript, which is then differentially spliced to create mRNA transcripts for the late viral genes (Goldberg et al., 1978; Imperiale et al., 1995). The late mRNA transcripts are grouped into five families in human adenovirus based on common polyadenylation sites (Miller et al., 1980) and all share a common 5' tripartite leader (Chow et al., 1977). Splicing of viral mRNAs is temporally regulated, with some splice sites only being used at later times of infection (Imperiale et al., 1995). The E4orf3, E4orf6, and L4 33K proteins have all been identified as splicing factors during viral infection (Imperiale et al., 1995; Törmänen et al., 2006).

During late times in infection, viral mRNA transcripts are preferentially exported from the nucleus and translated in the cytoplasm over host mRNA transcripts (Babich et al., 1983). Export of cellular mRNAs to the cytoplasm is inhibited by the E1B-55K and E4orf6 proteins (Babich et al., 1983; Blackford and Grand, 2009). E1B-55K and E4orf6 also inhibit phosphorylation of the

translation initiation factor eIF2α by PKR (Spurgeon and Ornelles, 2009). The 100K protein encoded by the L4 region is also involved in the inhibition of cellular translation and promoting translation from viral transcripts by inhibiting the phosphorylation of the eukaryotic initiation factor 4E (Cuesta et al., 2000; Cuesta et al., 2004).

1.1.2.6 Virus assembly and release

When the viral structural proteins have been translated, they are transported to the nucleus where virus assembly occurs. The initiation of capsid assembly may be triggered by the adenovirus protease cleaving a C-terminal peptide of pVI which contains the nuclear localization signal (NLS) and the nuclear export signal (NES) (Wodrich et al., 2003). There is evidence that pVI acts as a shuttle to transport hexon, which lacks an identified NLS and is cytoplasmic when expressed in the absence of other viral proteins or in a mutant that lacks functional pVI, to the nucleus (Kauffman and Ginsberg, 1976; Wodrich et al., 2003). Cleavage of the pVI NLS could stop its shuttling activity and the transport of hexons into the nucleus and initiate virus assembly instead.

The hexon monomers trimerize to form capsomers (Horwitz, 1969), using the 100K protein as a scaffold (Hong et al., 2005). The penton base interacts with fiber trimers, then assembles with the hexon capsomers to form intact capsids (Horwitz et al., 1969). Deletion of the IVa2 protein prevents capsid assembly (Zhang and Imperiale, 2003); this suggests that IVa2 may act as a scaffold protein for capsid formation. It has also been proposed that the formation of empty capsids is reversible or that they are a dead end product, and that capsid assembly in fact occurs around the viral nucleoprotein core (Zhang and Imperiale, 2003). However, there are several lines of evidence to dispute this model. First, pulse-chase experiments demonstrated that the empty capsids are precursors of mature capsids containing viral DNA (Sundquist et al., 1973) and that pVII appears in mature capsids more rapidly than structural proteins such as hexon after a pulse (Horwitz et al., 1969), suggesting that pVII and its associated viral DNA are inserted into already formed capsids. Additionally, intermediate viral particles associated with a portion of the viral genome are precursors of virions containing the complete viral genome, and young virions containing the viral genome but not the core proteins pV and pVII were detected (D'Halluin et al., 1978a); these intermediates would not be predicted to be precursors of virions with the complete genome if capsid assembly occurred around the viral nucleoprotein complex. Empty viral capsids

have also been shown to associate with viral DNA (Tibbetts and Giam, 1979) with an affinity which suggests that the viral DNA binds to the empty capsid and then is inserted. Thus, the current model is that the adenovirus genome is packaged into preformed capsids (Ostapchuk and Hearing, 2005), a mechanism used by several bacteriophages as well as herpesviruses (Rao and Feiss, 2008; Mettenleiter et al., 2009).

Packaging of the adenovirus genome is dependent on sequences present at the left end of the genome. Deletions at the left terminus prevent encapsidation of the viral DNA (Gräble and Hearing, 1990). In HAdV-5, the packaging signal is located between the left ITR and the coding sequence for E1A, between base pairs 200 and 400. Seven AT-rich repeats that are involved in packaging have been identified (Gräble and Hearing, 1992). These repeats are functionally redundant, but they do not direct genome packaging with equal efficiency (Gräble and Hearing, 1990; Schmid and Hearing, 1997). Spacing between the repeats has been shown to be important (Gräble and Hearing, 1992). This could be due to some secondary structure of the DNA required for packaging, or the binding of proteins to different repeats that need to interact to direct packaging. Repeats AI, AII, AV, and AVI have been shown to be the most important (Erturk et al., 2003). Replacing the wild-type packaging domain with a single A repeat permits virus packaging, but at a lower level than wild-type (Gräble and Hearing, 1990; Schmid and Hearing, 1997). However, a dimer of repeats AI and AII, a dimer of repeats AV-AVII, or six copies of repeat AI are necessary and sufficient for packaging at levels comparable to wild-type (Schmid and Hearing, 1997; Ostapchuk and Hearing, 2005). The bipartite motif 5'-TTTG-N_8-CG-3' is required for packaging domain function of the dominant motifs and is conserved between different HAdV serotypes (Schmid and Hearing, 1997).

A complex of cellular and viral proteins forms on the packaging domain and is termed P-complex. The cellular proteins octamer-1 (Oct-1) and chicken ovalbumin upstream promoter transcription factor (COUP-TF) bind to the packaging sequences but do not appear to be required for packaging of the viral DNA (Schmid and Hearing, 1998; Erturk et al., 2003). The cellular CCAAT displacement protein (CDP) is a component of the P-complex and, unlike Oct-1 and COUP-TF, is present in virus particles (Erturk et al., 2003). However, mutations in the packaging signal that disrupted CDP binding produced viable viruses, while a mutation that was still bound by CDP did not permit virus replication, suggesting that the role of CDP in packaging is not essential (Ostapchuk et al., 2005).

Several viral proteins have also been implicated in packaging. The IVa2 protein is part of the P-complex and binds directly to the packaging signal; it is essential for the packaging of the viral DNA (Zhang and Imperiale, 2000; Zhang et al., 2001; Perez-Romero et al., 2005; Tyler et al., 2007). Binding of IVa2 to the A repeats of the packaging signal correlates with their efficiency of directing DNA packaging (Ostapchuk et al., 2005). IVa2 binds to the packaging sequence as a homodimer and as a heterodimer with the viral 22K protein encoded by the L4 region (Perez-Romero et al., 2005; Ewing et al., 2007). IVa2 recognizes the CG base pairs in the packaging motif, while 22K is able to recognize the TTTG sequence, but only in the presence of IVa2 (Ostapchuk et al., 2006; Ewing et al., 2007). The binding of IVa2 to the packaging sequence is also enhanced by 22K. Deletion of 22K prevents the production of infectious virus particles without blocking viral gene expression or DNA replication, suggesting that its function in binding to the packaging domain is essential (Ostapchuk et al., 2006). The third viral protein shown to have an essential role in packaging of the viral DNA is the 52/55-kilodalton protein. While it is not required for capsid assembly, it is essential for encapsidation of the viral DNA and the production of mature virions (Gustin and Imperiale, 1998).

It is unclear precisely how the viral DNA is inserted into the capsid. The viral DNA could be inserted into the preformed capsids in a complex with pVII, which binds to the viral DNA prior to encapsidation (Weber and Philipson, 1984), or pVII could be stripped from the viral DNA by an unknown mechanism as it is translocated into the capsid (Zhang and Arcos, 2005). In bacteriophages with double-stranded DNA genomes, the DNA is inserted into empty, preformed icosahedral capsids with an opening created by a portal protein (Rao and Feiss, 2008). Translocation of the DNA is driven by a motor with ATPase activity. A similar mechanism is observed in herpesviruses (Mettenleiter et al., 2009). IVa2 is able to bind ATP, and mutation of the ATP binding sites renders the protein unable to complement a IVa2-deleted virus (Ostapchuk and Hearing, 2008), indicating that the ability of IVa2 to bind ATP is somehow essential to virus replication. While IVa2 did not demonstrate detectable ATPase activity *in vitro*, which could be due to a low binding affinity or a requirement for other proteins such as 22K or 52K, it raises the possibility that IVa2 acts as a motor similar to those found in bacteriophages and herpesvirus.

Activity of the viral protease is required to generate infectious virus (Weber, 1976). The protease is partially activated inside immature virions by binding to viral DNA, and then fully activated by the C-terminal fragment of pVI (pVIc) cleaved by the protease (Gupta et al., 2004).

DNA binding increases the catalytic activity of the protease by threefold, while pVIc increases it by 350-fold and the presence of both cofactors stimulates a 6000-fold increase (Mangel et al., 1997). Presumably, binding to the viral DNA increases the protease activity sufficiently for it to cleave pVI and generate mature protein VI and the pVIc fragment, which then binds the protease to activate it completely. This mechanism delays protease activation until after viral assembly has begun, when the capsid proteins and DNA are close together. Cleavage of more pVI yields more pVIc and activates more protease molecules, which then cleave a number of viral proteins including pIIIa, pVII, pVIII, and pTP. Protease activity may also be required to release 52K from the virus particle, since 52K can be detected in young virions when there is no active protease (Hasson et al., 1992).

Escape of the virus from the host cell is facilitated by several mechanisms. Actin can act as a cofactor for the viral protease, which cleaves cytokeratin 18 (Brown and Mangel, 2004). Cleavage of cytokeratin 18 prevents it from polymerizing, disrupting the host cell cytoskeleton and facilitating cell lysis and virus release (Chen et al., 1993). The E3 11.6-kDa protein, also known as the adenovirus death protein (ADP) is expressed from the E3 promoter during early stages of infection and at a much higher level from the MLP during late stages (Tollefson et al., 1992). ADP is necessary for efficient lysis of the host cell (Tollefson et al., 1996), and while its mechanism of action is not known it appears to increase apoptosis when overexpressed (Yun et al., 2005). Finally, excess production of fiber during viral infection appears to facilitate virus escape by binding to CAR, thereby disrupting tight junctions and allowing the virus easier access to the apical surface of the epithelium (Walters et al., 2002).

1.1.3 The 52/55-kilodalton protein

The HAdV-5 52/55-kilodalton protein (hereafter referred to as 52K) exists as differentially phosphorylated forms of a 48-kilodalton precursor (Lucher et al., 1986; Hasson et al., 1992). 52K is encoded by the L1 region, and in HAdV-2 can be detected at low levels at around 10 hrs post infection and at higher levels by 15 hrs post infection. As previously discussed (p.11; section 1.1.2.5), the transcript from the L1 region corresponding to 52K is present at early times during infection due to a low level of transcription from the MLP that results in a truncated transcript that includes the coding region for 52K (Shaw and Ziff, 1980). However, the inclusion of an extra region in the spliced tripartite leader appears to inhibit translation (Akusjärvi and Persson,

1981), explaining why 52K is not detected until later in infection despite the early presence of its mRNA. 52K localizes to regions in the nucleus separate from DNA replication centers and is associated with assembling viruses (Hasson et al., 1992). One to two molecules of 52K associate with each assembling virion (Hasson et al., 1992). Analysis of a 52K temperature-sensitive mutant of HAdV-5 revealed that 52K was essential for the production of mature virus particles but did not greatly affect DNA replication or late protein synthesis (Hasson et al., 1989; Gustin and Imperiale, 1998), suggesting that it had a role in viral assembly. It was found to be associated with empty capsids, intermediate particles, or young virions, but not mature capsids (Hasson et al., 1992). Since empty capsids were able to form in its absence, it does not function as a scaffolding protein (Gustin and Imperiale, 1998). The capsids formed in the absence of 52K could be found associated with the left end of the genome, further suggesting that the role of 52K is in DNA encapsidation rather than capsid assembly as a scaffolding protein (Hasson et al., 1989). 52K interacts with the IVa2 protein *in vitro* and in infected cells (Gustin et al., 1996). Chromatin immunoprecipitation and *in vitro* binding studies have demonstrated that 52K can bind the packaging signal, but since purified 52K alone or with purified IVa2 does not complex with the packaging signal this interaction may be indirect or dependent on another protein (Ostapchuk et al., 2005; Perez-Romero et al., 2005). 52K is associated with the packaging signal in a IVa2-deleted virus, further suggesting that its association with the packaging signal can not be solely dependent on its interaction with IVa2. The N-terminal 173 amino acids (out of 416) of 52K are required for its interaction with IVa2 in HAdV-5, while the N-terminal 331 residues are required for it to complement a 52K-deleted virus (Perez-Romero et al., 2006). Interactions between 52K and the core protein pVII and between IVa2 and pVII have also been demonstrated (Zhang and Arcos, 2005).

Despite its potential lack of specificity for the packaging sequence, encapsidation of viral DNA by 52K is serotype specific. Replication of viruses lacking 52K can only be rescued by expression of a 52K protein of the same serotype (Wohl and Hearing, 2008). The serotype specificity was shown to require the N-terminal 191 amino acids in HAdV-5. IVa2 binding to the packaging signal was believed to be serotype specific since expression of IVa2 from HAdV-5 supported replication of a chimeric virus with the ITR and packaging signal of HAdV-5 but the remainder of the genome from HAdV-7 (and therefore, expressing IVa2 from HAdV-7) (Zhang et al., 2001). However, a IVa2-deleted HAdV-5 could be rescued by expression of IVa2 from

HAdV-17, suggesting that the interaction between IVa2 and the packaging sequence may not be serotype specific (Wohl and Hearing, 2008). Growth of a 22K deletion mutant was also complemented by the expression of 22K from another serotype (Wohl and Hearing, 2008). This suggests that it is 52K, and not IVa2 or 22K binding to the packaging sequence, that determines the serotype specificity of DNA packaging by some undetermined mechanism or interaction.

1.1.4 Bovine adenovirus

Bovine adenovirus (BAdV) was first isolated in the 1960s (Darbyshire et al., 1965) and eleven serotypes have since been identified (Lehmkuhl and Hobbs, 2008). Although BAdVs have been associated with respiratory disease or enteric disease in cattle (Lehmkuhl et al., 1975; Smyth et al., 1996), they have also been isolated from apparently healthy animals (Darbyshire et al., 1965). BAdVs can cause sub-clinical to severe symptoms in experimental infections of calves (Lehmkuhl et al., 1975).

1.1.4.1 Classification

Based on phylogenetic sequence analysis, the identified serotypes of bovine adenoviruses are grouped in either the *Mastadenovirus* genus (BAdV-1, -2, -3, -9, and -10) or the *Atadenovirus* genus (BAdV-4, -5, -6, -7, -8, and strain Rus) (Harrach, 2000; Lehmkuhl and Hobbs, 2008). The *Mastadenovirus* serotypes are more closely related to adenoviruses of other host species, particularly ovine adenoviruses, than they are to each other, and each is classified as their own species. The *Atadenovirus* serotypes are more closely related to each other, particularly BAdV-4, -5, and -8.

1.1.4.2 Bovine adenovirus type 3

The strain of BAdV-3 was isolated from the eye of an apparently healthy cow (Darbyshire et al., 1965). Experimental infections of cattle can produce sub-clinical infections with the production of neutralizing antibodies (Mittal et al., 1999) or mild respiratory disease (Lehmkuhl et al., 1975).

1.1.4.2.1 Genome structure and organization

The genome of BAdV-3 has been completely sequenced and is 34,446 base pairs long (Reddy et al., 1998). The G/C content of the genome is 54%, similar to that of HAdVs (Chroboczek et al., 1992; Reddy et al., 1998). The BAdV-3 genome has predicted open reading frames encoding 33 proteins (Reddy et al., 1998; Reddy et al., 1999a; Kulshreshtha, 2009). The ITRs of BAdV-3 are 195 bases in length, longer than many other adenoviruses, and have an unusually high G/C content (Shinagawa et al., 1987; Reddy et al., 1998). The packaging signal is present at the left end of the genome as in other adenoviruses, but it is unique in that portions of the E1A open reading frame appear to be required for packaging (Xing et al., 2003; Xing and Tikoo, 2007). BAdV-3 mutants deleted from the end of the ITR to approximately 40 nucleotides upstream of the E1A region are still able to package viral DNA, although at reduced levels. Deletion of sequences within the E1A open reading frame are required to render the virus non-viable. BAdV-3 also lacks TATA or CAAT boxes between the inverted terminal repeat and upstream of the E1A start codon. However, evidence suggests that the E1A promoter is actually located within the ITR (Xing and Tikoo, 2006).

The transcription map of BAdV-3 is shown in figure 1.1. Nine mRNA transcripts are produced from the E1 region, all sharing 5' and 3' termini (Reddy et al., 1999a). The longest of these transcripts is unspliced, representing the primary transcript. Unlike in HAdV, where the transcription units for E1A and E1B have independent promoters and polyadenylation sites, BAdV-3 E1A and E1B are expressed from the same transcription unit. The six transcripts produced from the E1A region are translated into three proteins of 211, 115, and 100 amino acids that share a common N-terminus. The C-terminal 22 residues of 115R are not present in the other two E1A proteins. Three of the transcripts detected have the same open reading frame for the 211R E1A protein but have alternate splicing downstream. Similarly, two transcripts with the same open reading frame for the 115R protein have different splicing downstream. The 100R protein is detected beginning at 12 hrs post infection and until 36 hrs post infection, while the 115R and 211R proteins were observed starting at 24 hrs after infection. The critical residues in the CR3 region responsible for transactivation in HAdV E1A are conserved in BAdV-3 E1A. BAdV-3 E1A is able to transactivate HAdV-5 genes, showing that it has functional as well as

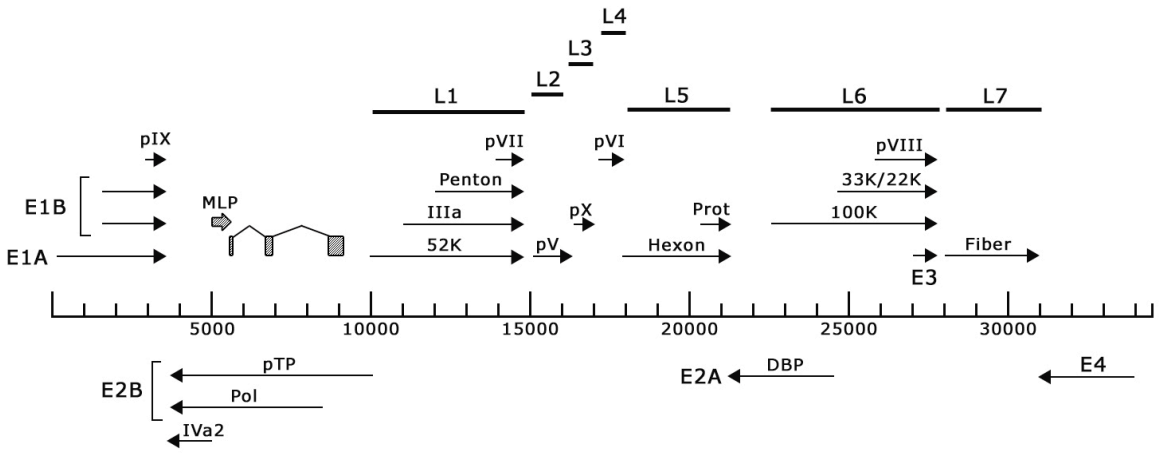

Figure 1.1 Transcription map of BAdV-3. Location and direction of transcripts are indicated by arrows. Scale in nucleotides. (Adapted from Reddy et al., 1998).

sequence homology (Zheng et al., 1994). Two transcripts from the E1B region are produced and code for proteins of 420 ($E1B^{large}$) and 157 amino acids ($E1B^{small}$) with overlapping reading frames (Reddy et al., 1999a). Deletion analysis suggests that while E1A and $E1B^{large}$ are essential for replication, $E1B^{small}$ is dispensable in some cell types (Zhou et al., 2001b).

The E2 region coding for proteins involved in DNA replication is located on the complementary strand (Reddy et al., 1998). E2A codes for the DNA binding protein, which is 432 amino acids long. This is shorter than the DBPs of some HAdVs but longer than some other adenoviruses, and the DBP of BAdV-3 shares homologies ranging from 38 to 47% with the DBPs of other members of the *Mastadenovirus* genus. The C-terminus of DBP required for many of its functions is conserved, as are zinc binding sites essential for DBP function. DBP is detected 6-12 hrs post-infection and immunohistochemical detection of DBP can be used to quantify BAdV-3 titers in infected cells (Zhou et al., 2001a). The E2B region codes for the viral DNA polymerase (Pol) and the preterminal protein (pTP). Pol and pTP share 59-62% and 58-60% sequence identity, respectively, with their homologs in other members of the *Mastadenovirus* genus (Reddy et al., 1998). The Pol protein of BAdV-3 is 1,023 amino acids long. The zinc finger motifs of Pol are conserved with that of Pol proteins from other members of the *Mastadenovirus* genus except for a single histidine residue in each motif that is not essential for DNA replication (Baxi et al., 1998). The pTP protein is 649 amino acids long in BAdV-3 (Baxi et al., 1998). It contains a YSRLVYR motif similar to a conserved YSRLRYT motif in the pTP of other adenoviruses and which has been shown to be essential for protein priming of DNA replication initiation. The serine 580 residue of HAdV pTP to which dCMP is covalently attached by DNA Pol to initiate DNA replication is also conserved in BAdV-3 pTP, but the flanking sequences are not. Two of the three recognition sites for cleavage of pTP by the adenovirus protease are conserved in BAdV-3 pTP, as is the nuclear localization signal.

The E3 region is located between the coding sequences for pVIII and the fiber protein as it is in HAdV (Reddy et al., 1998; Idamakanti et al., 1999). It is 1.5 kilobases long, about half the size of the E3 region of HAdV-2 and -5 (Mittal et al., 1992). Like HAdV, the E3 region is not essential for BAdV-3 replication in cultured cells (Zakhartchouk et al., 1998). Five transcripts are generated from the E3 region that contain open reading frames for four proteins of 284, 121, 86, or 82 amino acids (Idamakanti et al., 1999). The 284R protein is glycosylated but is not homologous to the 19K glycoprotein of HAdV and may be unique to BAdV-3 (Idamakanti et al.,

1999). The 121R protein shares some homology with the 14.7K protein of HAdV and has been shown to protect mouse cells from TNF-mediated cell lysis (Zakhartchouk et al., 2001).

The E4 region is positioned near the right end of the genome as it is in HAdV (Reddy et al., 1998). Seven 5'- and 3'-coterminal mRNA transcripts are produced from the complementary strand and encode five unique open reading frames (Baxi et al., 1999). Two of these, ORF3 and ORF5, encode proteins of 268 and 219 amino acids respectively and share homology with the E4orf6 protein of HAdV. ORF1, ORF2, and ORF4 encode proteins 143, 69, and 143 amino acids in length respectively and may be unique to BAdV-3 as they lack identified homologs in other adenoviruses. The E4 proteins are not required for BAdV-3 replication in cultured cells (Baxi et al., 2001).

In HAdVs, sequences for the VA RNAs are located between the E2B region encoding pTP and the L1 region encoding 52K. In BAdV-3, VA RNAs have not yet been identified (Reddy et al., 1998). Since in BAdV-3 pTP and 52K are situated close together, if the VA RNA sequences are present in the same location in BAdV-3 as in HAdV they must overlap the open reading frames for pTP and/or 52K. It is also possible that VA RNAs are present in a different region of the BAdV-3 genome or that BAdV-3 does not encode VA RNAs.

The intermediate proteins pIX and IVa2 have approximately the same positions in BAdV-3 as in HAdV (Reddy et al., 1998). The pIX transcription unit is located downstream of the coding regions for E1A and E1B, while the IVa2 transcription unit is on the complementary strand downstream of the E2B region encoding pTP and Pol (Baxi et al., 1998; Zheng et al., 1999). The pIX transcription unit is 3' co-terminal with the E1A and E1B regions (Zheng et al., 1999). The BAdV-3 pIX protein is 125 amino acids long and has sequence identity with pIX proteins from other members of the *Mastadenovirus* genus ranging from 16 to 28%. Its expression is detected 24 hrs after infection and, like HAdV, it is present in the viral capsid (Reddy et al., 1999b) An RGD motif fused to the C-terminus of pIX enhances the ability of BAdV-3 to infect integrin-expressing cells and a fluorescent protein fused to the C-terminus of pIX can be detected on the surface of the capsid, indicating that the C-terminus of pIX is exposed on the surface of the viral capsid (Zakhartchouk et al., 2004). The IVa2 protein of BAdV-3 is 376 amino acids long, shorter than that of other adenoviruses (Reddy et al., 1998). It shares 64-70% sequence identity with the IVa2 proteins from other members of the *Mastadenovirus* genus. The IVa2 transcript has a

polyadenylation signal unique from that of pTP and DNA Pol, while in HAdV all three are 3' co-terminal.

The organization of the major late promoter (MLP) and late genes of BAdV-3 is similar to that seen in HAdV. The MLP is located at 16.2 map units, with the late genes positioned downstream in distinct transcription units continuing to the right terminus of the genome (Reddy et al., 1998). Like the MLP of HAdV, the MLP of BAdV-3 contains a TATA box, an inverted CAAT box, a binding site for USF, and an initiator element. The downstream enhancer elements DE1 and DE2 are also conserved in BAdV-3. The tripartite leader of BAdV-3 is 205 nucleotides in length and has a similar organization to that of HAdV, which is 201 nucleotides long. The three parts of the leader are located near the MLP (40 nucleotides), within the DNA Pol gene on the non-coding strand (78 nucleotides), and in the pTP gene on the non-coding strand (87 nucleotides).

A significant difference between the late regions of HAdV and BAdV-3 is that the late transcripts of BAdV-3 are divided into seven families (L1 to L7) based on common 3' polyadenylation sites, while HAdV late genes are grouped into five families (L1 to L5) (Reddy et al., 1998). The L1 region of BAdV-3 encodes four proteins: 52K, IIIa, penton, and pVII. In HAdV, penton and pVII are in the L2 region. The BAdV-3 52K protein was predicted to be 331 amino acids long (Reddy et al., 1998). The pIIIa protein is 568 amino acids long and shares 52-57% sequence identity with the pIIIa proteins from other members of the *Mastadenovirus* genus (Reddy et al., 1998). A putative site for cleavage by the viral protease is located 19 residues from the C-terminus of pIIIa. The penton protein of BAdV-3 is 482 amino acids long and shares 63-65% sequence identity with penton proteins from other members of the *Mastadenovirus* genus (Reddy et al., 1998). A significant difference in the BAdV-3 penton is that it lacks the conserved RGD motif required for $\alpha_v\beta_3$ and $\alpha_v\beta_5$ integrin binding. It also lacks a leucine-aspartic acid-valine motif that could bind $\alpha_4\beta_1$ integrins, although a methionine-aspartic acid-valine motif is present. The penton proteins of canine adenovirus (CAdV)-1 and -2 also lack an RGD motif (Reddy et al., 1998; Soudais et al., 2000). The penton of CAdV-1 has a deletion in the middle of the coding region where the RGD motif is localized and is very similar to that seen in the BAdV-3 penton (Reddy et al., 1998). The region of the penton protein that interacts with the fiber protein is conserved in BAdV-3. The core protein pVII of BAdV-3 is 171 amino acids long and has 44-53% sequence identity with pVII proteins of other members of the *Mastadenovirus* genus (Reddy et al., 1998). Like pVII from other members of the *Mastadenovirus* genus, and consistent

with a DNA-binding function, BAdV-3 pVII is highly basic (43 basic residues out of 171). The consensus cleavage site for the adenovirus protease is MYGG↓A and is located 19 nucleotides from the N-terminus of the protein, In HAdV-2, cleavage occurs 24 nucleotides from the N-terminus at the recognition site MSGG↓A (Webster et al., 1989).

The L2 region of BAdV-3 codes for a single transcript encoding the core protein pV, whereas in HAdV L2 codes for penton, pVII, and pV (Reddy et al., 1998). The pV protein of BAdV-3 is 410 amino acids long and shares 28-41% sequence identity with pV proteins of other members of the *Mastadenovirus* genus. Like pVII and the pV proteins of other adenoviruses, BAdV-3 pV has a high content of basic amino acids (77 out of 410 residues). A sequence similar to the nuclear localization signal found in pV of HAdVs is present in BAdV-3 pV.

The L3 region of BAdV-3 also produces only one transcript which encodes the μ protein, also known as pX (Reddy et al., 1998). In HAdV, μ is located in the L2 region. The μ protein of BAdV-3 is 80 amino acids long and shares 53-64% sequence identity with the μ proteins of other members of the *Mastadenovirus* genus. Like the other viral DNA-binding proteins, BAdV-3 μ contains a high proportion of basic amino acids (18 out of 80 residues). In HAdV, μ is cleaved by the adenovirus protease after residues 31 and 50, leaving a highly basic peptide of 19 amino acids in length (Anderson et al., 1989). Cleavage sites on BAdV-3 μ are predicted after residues 30 and 50 to generate a basic product of 20 amino acids (Reddy et al., 1998). The nuclear localization signal of μ also appears to be conserved in BAdV-3.

The L4 region produces a transcript coding for pVI, which is located in the L3 region in HAdV (Reddy et al., 1998). The BAdV-3 pVI protein is 263 amino acids in length and shares 32-39% sequence identity with the pVI proteins of other members of the *Mastadenovirus* genus. Consensus cleavage sites for the viral protease are located in the N-terminus after residue 33 and in the C-terminus after residue 252. In HAdV, pVI cleavage occurs after residues 33 and 239 (Weber, 1995). The 11 amino acid C-terminal peptide predicted by protease cleavage in BAdV-3 has high sequence identity with the C-terminal peptide of the same size produced by cleavage of HAdV pVI (7 out of 11 residues), indicating that it should function as a cofactor for activation of the viral protease.

The coding sequences for hexon and the viral protease are located in the L5 region of BAdV-3 (Reddy et al., 1998). In HAdV, hexon and the protease are expressed from the L3 region along with pVI. The hexon protein of BAdV-3 is 910 amino acids long and has a high degree of

sequence identity with the hexon proteins of other members of the *Mastadenovirus* genus (66-71%). Three regions in the protein sequence of BAdV-3 hexon show significant differences from that of HAdV-2, but these regions correspond to loops exposed on the surface of the virion (Hu et al., 1984; Crawford-Miksza and Schnurr, 1996). Two of these loops contain the hypervariable regions that contribute to differences between adenovirus serotypes. The hexon protein of BAdV-3 is therefore predicted to have the same general structure as that of HAdV (Reddy et al., 1998). The BAdV-3 protease is 204 amino acids long and shows 65% sequence identity with the proteases of other members of the *Mastadenovirus* genus (Reddy et al., 1998). The active site of the HAdV-2 protease is formed by residues His54, Glu71, and Cys122 (Ding et al., 1996). The histidine and cysteine residues are present in BAdV-3 protease, but there is an aspartic acid residue in place of the Glu71 of the HAdV-2 protease. The region involved in binding pVIc is fairly well conserved between BAdV-3 and HAdV-2, as are most of the residues implicated in the binding of the protease to DNA (Gupta et al., 2004).

The L6 region of BAdV-3 encodes the 100K, 33K, 22K, and pVIII proteins, which in HAdV are located in the L4 region (Reddy et al., 1998; Kulshreshtha, 2009). The 100K protein of BAdV-3 is 850 amino acids long, the largest 100K protein yet identified in members of the *Mastadenovirus* genus, and has 50-52% sequence identity with the 100K protein of other members of the *Mastadenovirus* genus. In HAdV-5, the 33K and 22K proteins are generated by differential splicing (Ostapchuk et al., 2006). The open reading frame of 22K is present in the unspliced mRNA and contains splice acceptor and donor sites for an intron within the open reading frame; when this intron is spliced out, an alternate reading frame sharing the N-terminus of 22K is generated that codes for 33K. In BAdV-3 the 22K protein is 274 amino acids long and the 33K protein is 279 amino acids long (Reddy et al., 1998; Kulshreshtha, 2009), both significantly larger than the 22K and 33K proteins of HAdV. BAdV-3 mutants with a stop codon inserted at amino acid 97 of 33K/22K are deficient in assembly of virus capsids, suggesting that one or both proteins are essential for capsid assembly (Kulshreshtha et al., 2004). Insertion of a stop codon at the seventh residue decreases the production of mature virus particles but is not lethal, suggesting that the C-terminus of either 33K or 22K is important for virus assembly (Kulshreshtha et al., 2004). The 33K protein of BAdV-3 interacts with the viral 100K and pV proteins (Kulshreshtha and Tikoo, 2008) and is able to transactivate the MLP (Kulshreshtha, 2009).

The minor capsid protein pVIII of BAdV-3 is 216 amino acids long (Reddy et al., 1998). It shares 51-56% sequence identity with pVIII proteins in other members of the *Mastadenovirus* genus and has two consensus sites for cleavage by the adenovirus protease.

The fiber protein is encoded by the L7 region of BAdV-3 and the L5 region in HAdV (Reddy et al., 1998). The BAdV-3 fiber is 976 amino acids long and has relatively low sequence identity with the fiber proteins of other members of the *Mastadenovirus* genus (22-27%) but retains the conserved sequence known to interact with the penton base and the sequence conserved at the beginning of the fiber head domain. The fiber shaft of BAdV-3 is quite long and has an usual structure with several bends (Ruigrok et al., 1994). The knob of the BAdV-3 fiber can be replaced with the fiber knob from HAdV-5, altering the virus tropism (Wu and Tikoo, 2004). Like the fiber protein of HAdV-2, the fiber protein of BAdV-3 contains an NLS at its N-terminus (Wu et al., 2004). Mutant BAdV-3 with the fiber NLS removed shows significantly impaired growth (Wu et al., 2004).

1.1.4.2.2 Replication cycle

BAdV-3 appears to enter cells by CAR- and integrin-independent mechanisms (Bangari et al., 2005). A recent report suggests that BAdV-3 is able to use sialic acid as a receptor for cell entry (Li et al., 2009). Removing sialic acid residues or blocking it with a lectin inhibits infection of Madin-Darby bovine kidney (MDBK) cells by BAdV-3, as does removal of carbohydrates or glycoproteins containing sialic acid. This suggests that the BAdV-3 receptor has protein and carbohydrate components and expresses sialic acid that is recognized by the virus. Proteins of 97 and 34 kilodaltons have been described as potential candidates for a BAdV-3 receptor but have not yet been identified or characterized (Li et al., 2009). Several human adenovirus serotypes have also been shown to use sialic acid as a receptor (Arnberg et al., 2000).

The replication cycle of BAdV-3 in MDBK cells appears to be slower than for HAdV. The early proteins such as E1A are not detected until 12 hours post-infection (Reddy et al., 1999a) and DNA replication also appears to occur later in BAdV-3 than in HAdV (Zhou et al., 2001b). In HAdV, the early phase of infection lasts 5 to 6 hours before the onset of DNA replication and the beginning of the late phase of infection (Berk, 2007).

As previously discussed, the packaging signal of BAdV-3 is similar to that of HAdV in that it contains functionally redundant repeats located on the left end of the genome, but appears to

extend into the E1A open reading frame (Xing et al., 2003; Xing and Tikoo, 2007). The consensus packaging sequence determined from studies of HAdV-5 does not appear to be well conserved in non-human adenoviruses. CAdV-2 has at least four redundant but not functionally equivalent packaging domains and only one instance of the HAdV-5 consensus sequence which does not appear to be very efficient at directing packaging (Soudais et al., 2001). Instead, mutation of TTTG/A sequences caused decreases in the efficiency of packaging; whether this sequence is bound directly or may be involved in the formation of secondary structures in the DNA required for packaging is unknown. Porcine adenovirus type 3 (PAdV-3) has a packaging domain localized within nucleotides 212 and 531 (Xing and Tikoo, 2003). There are six identified packaging domains identified in PAdV-3 that appear to be functionally redundant, but it has only one consensus sequence in common with CAdV-2 and none with HAdV-5 (Xing and Tikoo, 2004). Instead, continuous A/T regions flanked by G/C-rich regions are observed, with the A/T region having greater importance than the G/C-rich sequences. The BAdV-3 packaging domain does not contain any consensus packaging sequences with HAdV-5, CAdV-2, or PAdV-3, but does have a number of A/T-rich motifs. The viral or cellular components that may bind to the BAdV-3 packaging signal have not been characterized.

BAdV-3 replication is blocked in human cells (Wu and Tikoo, 2004). Transduction of many human cell lines by BAdV-3 is poor, but a chimeric fiber with the knob of HAdV-5 increases transduction efficiency. Inside the cell, BAdV-3 is able to express early and late proteins but infectious virus is not produced, suggesting that there is a species-specific block of replication, possibly at a late stage of infection. BAdV-3 is able to efficiently transduce 293 cells, but capsid assembly does not occur (Patel and Tikoo, 2006). Unlike in HeLa, Hep-2, and A549 cells, production of late proteins was not detected in 293 cells, which express the E1 proteins of HAdV-5. BAdV-3 DNA replication is inhibited in 293 cells, but this defect can be compensated for by expression of the simian virus 40 (SV40) T antigen and allows for virus replication, although titres are slightly lower compared to MDBK cells and replication appears to be slower (Patel and Tikoo, 2006).

1.2 Nuclear transport in Eukaryotes

In the cell, transcription of DNA into RNA and translation of RNA into protein are sequestered in the nuclear and cytoplasmic compartments, respectively. While water, ions, and other small molecules can exchange freely, the exchange of larger molecules is regulated.

1.2.1 Nuclear pore complexes

Access to the nucleus is controlled by nuclear pore complexes (NPCs) inserted in the nuclear envelope. In vertebrates, the NPC has a molecular weight of approximately 120 MDa and is composed of over 30 unique proteins called nucleoporins (Nups) (Lim et al., 2008). Proliferating human cells have 2,000-5,000 NPCs per nucleus.

The structure for the NPC has been determined and is well conserved (Lim et al., 2008). It consists of a cylinder with eight-fold symmetry inserted where the outer and inner nuclear membranes are fused to form a pore in the membrane. Eight filaments extend outward into the cytoplasm, and a "nuclear basket" made up of eight filaments joined by a distal ring extends inward to the nucleus (figure 1.2). The NPC is approximately 150 nm long and has an outer diameter of 125 nm. The pore formed by the NPC has a diameter of 60-70 nm at the cytoplasmic and nuclear faces, but narrows to 45 nm in the middle. There are also small channels 8 nm in diameter around the periphery of the NPC that may be involved in the diffusion of ions and small molecules between the nucleus and the cytoplasm. Proteins with a molecular mass greater than approximately 40 kDa are unable to cross the NPC unaided and require cellular transport factors in order to traverse the pore.

The nucleoporins that make up the NPC are present in at least eight copies per NPC and can be divided into three main classes (Tran and Wente, 2006; Lim et al., 2008). The first class consists of transmembrane proteins that contain α-helices and are involved in anchoring the NPC to the nuclear membranes. The second class consists of Nups which are proteins with β propeller folds, which are made up of β folds arranged around a central axis and are involved in protein-protein interactions, and α solenoid folds, which contain a curved pattern of α-helices. These form the core of the NPC. The third class consists of FG Nups, so named because they contain multiple domains of phenylalanine-glycine repeats that are important in transporting proteins across the NPC. The FG Nups account for one-third of the nucleoporins and have coiled-coil, β propeller, and β sandwich domains which may allow them to interact with the β propeller/α

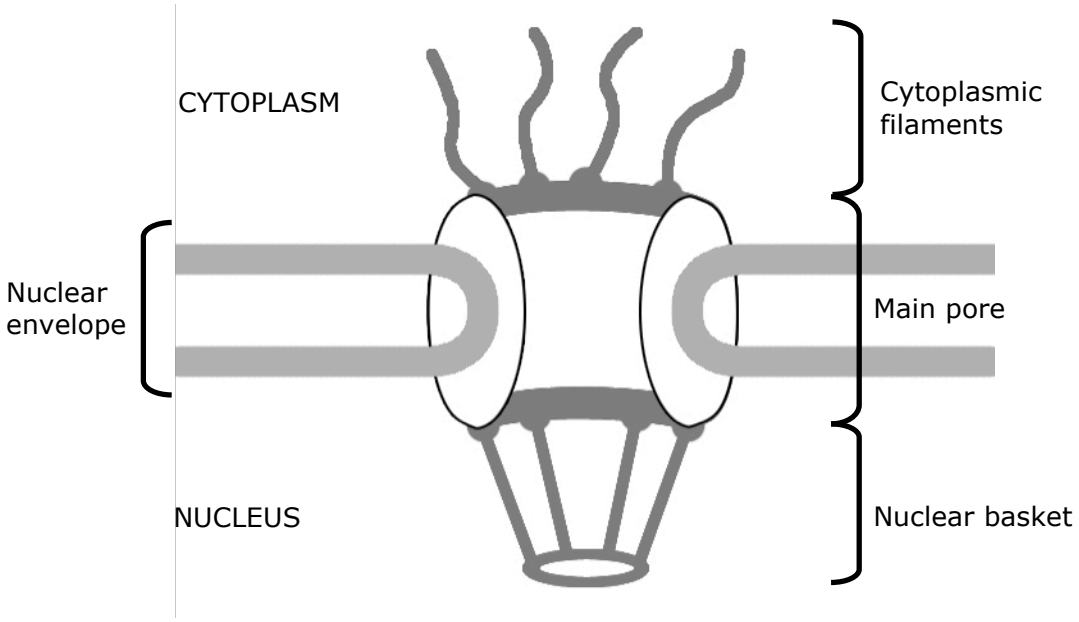

Figure 1.2 Schematic diagram of NPC structure.

solenoid proteins in the core. The FG repeats, particularly the ring of phenylalanine, interact with hydrophobic residues on transport receptors such as importin β. While the precise mechanism by which the transport receptor/cargo complexes use the FG repeats to traverse the NPC is unclear (Lim 2008), it is proposed that sequential binding by the receptor to FG repeats throughout the pore allow the complex to "step" its way through the pore and exit into the nucleus. Other models suggest that the FG repeats block entry to the NPC until they are bound by a transport receptor.

1.2.2 Ran-dependent nuclear transport

The majority of transport into and out of the nucleus is dependent on the cellular GTPase Ran. Directional transport of cargos bound by soluble transport receptors is maintained due to differing levels of RanGTP and RanGDP between the cytoplasm and the nucleus, and specific interactions of RanGTP or RanGDP with transport receptors.

1.2.2.1 Importins

Transport of proteins to the nucleus is mediated by specific transport receptors called karyopherins or importins that recognize nuclear localization signals (NLSs) of cargo proteins and translocate them across the NPC through interactions with FG nucleoporins. Most transport is mediated by karyopherins belonging to the importin β family, of which there are over 20 types in higher eukaryotes (Fried and Kutay, 2003). All importin β-related proteins contain a RanGTP binding domain and have a common structural organization. The best characterized members of this family are importin β and transportin. Some cargo proteins are bound by importin β or transportin directly for transport to the nucleus, but there are also adaptor proteins that bind to importin β and to a cargo protein to direct nuclear import.

The importin α family of proteins act as adaptors for importin β-directed nuclear import. There are six variants of importin α in humans that differ in their expression patterns in various tissues and can be bound by cargo proteins with varying specificity (Köhler et al., 1999). The members of the importin α family share a common domain organization (Herold et al., 1998; Goldfarb et al., 2004). Importin α interacts with importin β through its importin β binding (IBB) domain, a basic region near the N-terminus of the protein (Görlich et al., 1996a). The IBB domain is essential and sufficient for transport of importin α to the nucleus. Near the end of the IBB domain is an autoinhibitory signal, followed by ten hydrophobic armadillo (ARM) repeats, arranged in

tandem, each consisting of three α-helices connected by loops (Fontes et al., 2000). The ARM repeats form a concave, twisted structure of α-helices with a long groove. Two NLS binding sites in this groove have been identified that interact with monopartite and bipartite NLSs. The binding site for the nuclear export protein CAS (cellular apoptosis susceptibility) is located on one of the ARM repeats near the C-terminus of importin α and overlaps with part of the NLS binding site (Herold et al., 1998).

The autoinhibitory signal located on the flexible IBB domain can also bind to the NLS-binding groove (Kobe, 1999). In the absence of importin β sequestering the IBB domain, importin α has less affinity for NLS binding since the flexible IBB domain blocks the NLS binding pocket.

Importin β contains 19 HEAT repeats (named after the proteins in which they were first identified: huntingtin, elongation factor 3, the A subunit of protein phosphatase A, and Tor1 kinase), each consisting of two α-helices in a hairpin structure (Bayliss et al., 2000). The HEAT repeats are linked together by loops or other α-helices and are similar to the ARM repeats of importin α. The HEAT repeats are coiled into a crescent-like structure. Ran and IBB binding occurs on the concave side (Cingolani et al., 1999; Vetter et al., 1999), while interaction with FxFG motifs on nucleoporins is mediated by HEAT repeats on the convex surface of importin β (Bayliss et al., 2000).

Other members of the importin β family, such as transportins 1, 2, SR1, and SR2, and importins 4, 5, and 7, have been identified that are involved in nuclear import of cellular proteins such as mRNA binding proteins, ribosomal proteins, and histones (Fried and Kutay, 2003). These transport receptors bind directly to their cargo and transport them into the nucleus similarly to importin β/importin α-mediated nuclear import.

1.2.2.2 Nuclear localization signals

Nuclear localization signals that direct import of proteins into the nucleus are diverse, but in general consist of a region of basic amino acids. There are two types of "classical" NLSs recognized by importin α that have been well characterized: the monopartite NLS of the SV40 T antigen (PKKKRKV) (Kalderon et al., 1984) and the bipartite NLS of nucleoplasmin (KRPAATKKAGQAKKKK) (Robbins et al., 1991). These types of basic NLSs can be identified in a number of proteins. The monopartite SV40 NLS can bind to two different sites in the NLS-

binding pocket of importin α (Fontes et al., 2000). The same two sites are bound by the essential residues of the bipartite NLS of nucleoplasmin (Fontes et al., 2000).

NLSs can also exist that use the importin α/importin β pathway but do not match the convential monopartite or bipartite NLSs, suggesting that a variety of protein sequences can drive nuclear import (Christophe et al., 2000). In support of this observation, generation of random peptides yields a surprisingly high number of functional nuclear localization signals, over half of which do not appear to have a classical basic NLS. Some proteins lack a classical NLS in their primary sequence but can display an NLS motif when properly folded, such as the cellular retinoic acid binding protein-II (Sessler and Noy, 2005). The Vpx protein of simian immunodeficiency virus has an α-helix whose integrity is essential for nuclear localization (Rajendra Kumar et al., 2003). The influenza A virus nucleoprotein contains both a bipartite NLS and an NLS that is non-conventional, and it is the non-convential NLS that appears to be dominant (Wang et al., 1997; Wu and Pante, 2009). The non-conventional NLS is essential for nuclear localization of the nucleoprotein, and its selective exposure regulates the intracellular localization of nucleoprotein during virus infection (Wu and Pante, 2009).

Proteins such as the human immunodeficiency virus (HIV)-1 Tat and Rev proteins (Truant and Cullen, 1999) and the Rex protein of human T-cell leukemia virus type 1 (Palmeri and Malim, 1999) have been identified that contain arginine-rich NLSs that can bind directly to importin β. Nuclear import of these proteins can be blocked by an IBB domain peptide (Palmeri and Malim, 1999; Truant and Cullen, 1999), suggesting that these arginine-rich NLSs bind to importin β in the same manner as the IBB domain of importin α.

The ribosomal protein rpL23a contains a beta-like import receptor binding (BIB) domain that can bind to receptors of the importin β family and act as a nuclear localization signal (Jäkel and Görlich, 1998). Binding of the BIB domain to importin β is distinct from importin α binding, as well as independent of M9 NLS binding to transportin. Similarly, the Stat1 protein uses importin α/importin β for nuclear import, but it binds importin α on its C-terminus in a region distinct from SV40 NLS binding (Sekimoto et al., 1997). The nucleoprotein of influenza virus A is also able to bind to importin α at a site distinct from that used by the SV40 NLS through its non-conventional NLS (Wang et al., 1997; Melen et al., 2003).

The heterologous nuclear ribonucleoprotein A1 contains a nuclear localization signal that has been termed an M9 NLS (Pollard et al., 1996). Transport of M9 NLSs is mediated by transportin,

a member of the importin β family. The M9 NLS is approximately 40 amino acids long and has an overall positive charge (Siomi and Dreyfuss, 1995; Cook et al., 2007). Transportin is primarily involved in the nuclear import of mRNA-binding proteins and ribosomal proteins (Fried and Kutay, 2003). Serine/arginine-rich proteins involved in splicing of pre-mRNA contain phosphorylated RS domains (arginine/serine repeats) that are recognized and transported to the nucleus by transportin-SR2 (Lai et al., 2001).

1.2.2.3 Nuclear import cycle

Directional import of NLS-containing proteins from the cytoplasm into the nucleus is maintained by the levels of RanGTP in the nucleus and RanGDP in the cytoplasm, and the affinity of import receptors and export receptors for RanGTP or RanGDP (Fried and Kutay, 2003). A schematic of Ran-dependent nuclear import is shown in figure 1.3.

In the cytoplasm, the cargo protein NLS is bound by importin α/importin β. The importin β/importin α/cargo complex is transported across the NPC into the nucleus by importin β interactions with FG Nups. Once inside the nucleus, RanGTP binds to importin β and causes it to release importin α and its bound cargo (Görlich et al., 1996c). When the IBB domain of importin α is no longer interacting with importin β, it folds back into the NLS-binding pocket of importin α, releasing the cargo protein into the nucleus (Kobe, 1999). The RanGTP/importin β complex is exported to the cytoplasm, while importin α is bound by the export factor CAS (Kutay et al., 1997). The interaction of CAS with importin α requires RanGTP and is mutually exclusive with NLS binding to importin α (Herold et al., 1998; Fried and Kutay, 2003). This exclusivity prevents cargo proteins from being exported back out of the nucleus. The RanGTP/CAS/importin α complex is exported to the cytoplasm along with RanGTP/importin β (Kutay et al., 1997; Fried and Kutay, 2003). There, Ran hydrolyzes GTP and RanGDP releases bound importin β and CAS, which in turn releases importin α. The transport receptors are now able to bind a new cargo and begin the cycle again.

Maintaining high levels of Ran-GDP in the cytoplasm and Ran-GTP in the nucleus is critical for this directional transport (Fried and Kutay, 2003). Ran hydrolysis of GTP is normally very slow, with a half life of several hours. In the cytoplasm, the Ran-specific GTPase activating protein (RanGAP) increases the rate of hydrolysis by a factor of 10^5, maintaining low levels of

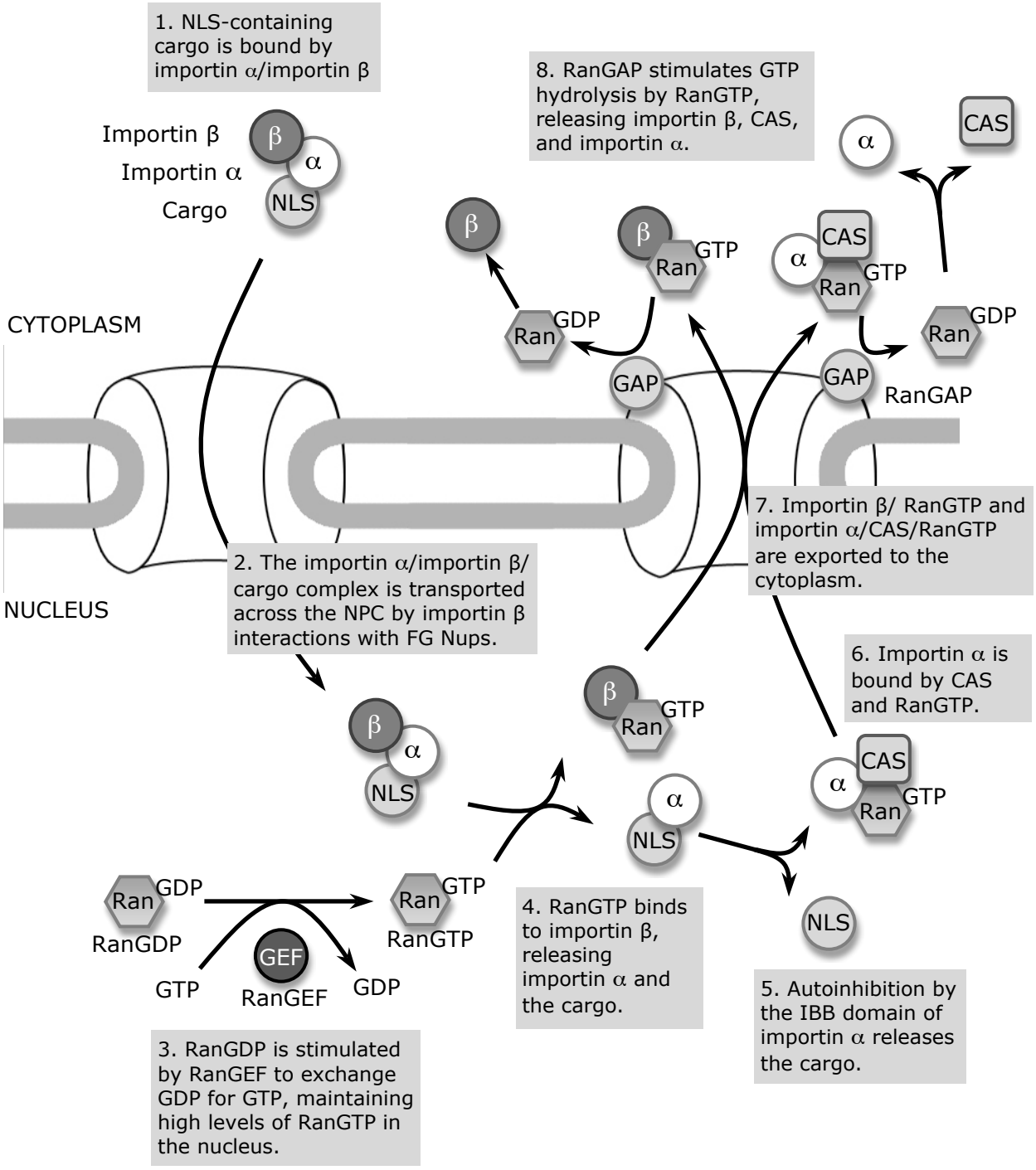

Figure 1.3 Ran-dependent nuclear import by importin α/importin β.

cytoplasmic RanGTP (Klebe et al., 1995). RanGAP is localized on the cytoplasmic side of the NPC. A means of returning exported Ran to the nucleus is also required to maintain nuclear levels of RanGTP. Cytoplasmic RanGDP is transported to the nucleus by nuclear transport factor 2 (NTF2), where the Ran-specific guanine nucleotide exchange factor (RanGEF) stimulates the exchange of GDP for GTP by a factor of 10^5 and triggers dissociation of NTF2 and RanGDP (Klebe et al., 1995; Fried and Kutay, 2003). RanGEF can bind to chromatin (Nemergut et al., 2001) or to nucleoporins on the nuclear face of the NPC (Fontoura et al., 2000), restricting its localization to the nucleus so that cytoplasmic RanGEF does not result in an increase of cytoplasmic RanGTP.

1.2.3 Ran-independent nuclear transport

Alternative transport pathways to the nucleus that are independent of Ran have been described, but are poorly characterized and lack a consensus (Stochaj and Rother, 1999). In general, transport receptors (such as importin β, transportin 1, CRM1, and exportin-t) can enter the nucleus without the need for other soluble factors such as Ran (Kose et al., 1997; Kutay et al., 1998; Nakielny and Dreyfuss, 1998; Zhang et al., 2003). Numerous proteins not involved in nuclear transport have also been shown to be capable of entering the nucleus without the use of importin α/importin β and Ran.

Some proteins appear to direct nuclear import by binding directly to nucleoporins, localizing to the nucleus without a requirement for additional soluble factors such as Ran or importin β. The import of heterogenous ribonucleoprotein K is independent of soluble factors and may shuttle in and out of the nucleus by binding directly to nucleoporins (Michael et al., 1997). The Tax protein of human T cell lymphotropic virus type 1 can bind directly to p62, a nucleoporin also shown to interact with importin β, and is imported into the nucleus independently of soluble factors (Tsuji et al., 2007). The nuclear import of IκBα, involved in the regulation of the NFκB family of transcription factors, and the Vpr protein of HIV-1 may also be mediated by direct binding to nucleoporins (Jenkins et al., 1998; Sachdev et al., 2000).

Nuclear import of the SV40 NLS can be mediated by the cellular protein calmodulin in a calcium-dependent, GTP-independent manner (Sweitzer and Hanover, 1996). The release of calcium into the cytoplasm triggered by cell signaling events may induce calmodulin-dependent nuclear import of proteins such as the SOX family transcription factors and thus may represent a

method of inducible nuclear import in the cell (Hanover et al., 2009). An importin β-like protein may also be involved in calmodulin-mediated import, but it is independent of Ran.

Accumulation of proteins in the nucleus can also be assisted by (or dependent on) binding to nuclear components. The respiratory syncytial virus matrix protein and the integrase protein of HIV-1 can be imported into the nucleus by Ran-dependent pathways, but can also accumulate in the nucleus at lower levels in the absence of soluble factors by binding to nuclear components (Ghildyal et al., 2005; Hearps and Jans, 2006). The HIV-1 Tat protein is also able to accumulate in the nucleus by binding to nuclear components, but unlike the integrase protein its import is not increased by the presence of soluble factors (Efthymiadis et al., 1998).

1.2.4 Nuclear transport of adenovirus proteins

The mechanisms of nuclear transport of some adenovirus proteins have been described for events during cell entry, which has been previously discussed (section 1.1.2.3), and for nuclear transport of viral proteins synthesized during infection. In general, the nuclear localization signals of some viral proteins have been identified but the import pathways used during viral infection are often uncharacterized.

The viral capsid is able to bind to CAN/Nup214 on the NPC, and histone H1 binds to hexon (Trotman et al., 2001). A proposed model suggests that an importin β/importin 7 heterodimer directs nuclear import of the histone H1/hexon complex into the nucleus, disassembling the viral capsid and exposing the viral DNA core. The core proteins V and VII bound to the viral DNA are recognized by transportin, which directs import of the viral DNA into the nucleus (Hindley et al., 2007). The M9 NLS, also recognized by transportin, is able to block nuclear accumulation of the viral DNA, while the SV40 NLS that uses the importin α/importin β pathway is not.

Viral proteins synthesized in the cytoplasm that exert their effects in the nucleus or proteins that are required for virus assembly must be transported back to the nucleus after translation. The E1A protein contains a short NLS at its C-terminus (KRPRP) and is transported to the nucleus by importin α/importin β (Lyons et al., 1987; Kohler et al., 2001). While several isoforms of importin α can support the import of E1A, it has the strongest preference for importin α3 (Kohler et al., 2001). The E1B-55K/E4orf6 complex shuttles between the nucleus, and each protein appears to contain an NLS as well as a nuclear export signal (NES) (Dobbelstein et al., 1997; Grand et al., 1999; Querido et al., 2001). E4orf6 also has an arginine-rich α-helix that acts as a

nuclear retention signal by masking the NES in the absence of E1B-55K (Querido et al., 2001). The E4orf6/7 protein has an arginine-rich NLS and relocalizes the E2F-4 transcription factor to the nucleus during infection (Schaley et al., 2005).

The hexon protein that makes up the majority of the viral capsid does not have an identified NLS and is cytoplasmic when expressed in the absence of other viral proteins (Wodrich et al., 2003). The pVI protein contains both an NLS and an NES in its C-terminus, which allows it to shuttle between the nucleus and the cytoplasm and helps to direct the hexon protein to the nucleus (Wodrich et al., 2003). A virus mutant with a temperature-sensitive mutation in pVI is defective for capsid assembly and does not transport hexon to the nucleus (Kauffman and Ginsberg, 1976). The NLS/NES of pVI is removed by the viral protease late in infection, retaining VI in the nucleus for capsid assembly (Wodrich et al., 2003).

Protein VII contains three NLS domains and can bind *in vitro* to importin α, importin β, importin 7, and transportin (Wodrich et al., 2006). The mature form of VII found in virus capsids appears to have a preference for transportin, while the premature pVII produced during viral infection primarily uses the importin α/importin β pathway for nuclear import (Hindley et al., 2007).

The 100K protein contains a nuclear localization signal in a glycine-arginine-rich domain that is located near its C-terminus and a nuclear export signal in the middle of the protein. The 100K protein is localized in both the cytoplasm and the nucleus during virus infection (Cuesta et al., 2004; Koyuncu and Dobner, 2009). There is some evidence that the 100K protein plays a role in the nuclear localization of hexon (Hong et al., 2005).

The NLS of the fiber protein is located in its N-terminus (Hong and Engler, 1991). The sequence ^{1}M<u>KRAR</u>PSEDTF^{11} was shown to be sufficient for nuclear targeting of fiber in HAdV-2, while the deletion of the underlined KRAR sequence abolished nuclear localization. The sequence ^{1}MTKRVRL^{7} from HAdV-7 fiber was able to complement the deletion of the essential KRAR sequence. In BAdV-3, the fiber protein NLS is located slightly further away from the N-terminus, with residues ^{16}KAKR^{19} being essential for nuclear import (Wu et al., 2004). Residues 12-22, however, were not sufficient for nuclear localization of fiber.

1.3 Ribosomal RNA processing

Eukaryotic ribosomes are made up of a small 40S subunit and a large 60S subunit. In humans, the 40S subunit contains an 18S ribosomal RNA (rRNA) 1,870 nucleotides in length and 30 to 50 ribosomal proteins (Nazar, 2004). The 60S subunit consists of three rRNA molecules: 5S (121 nucleotides), 5.8S (156 nucleotides) and 28S rRNA (5,070 nucleotides). The 60S subunit also contains 40-50 ribosomal proteins (Nazar, 2004). The synthesis of rRNA and ribosome assembly is closely associated with the nucleolus.

1.3.1 Ribosomal RNA processing in eukaryotes

The 5.8S, 18S, and 28S rRNAs are derived from a single pre-rRNA transcribed by RNA polymerase I (Nazar, 2004). The 5S rRNA gene is transcribed separately by RNA polymerase III, while genes encoding ribosomal-associated proteins are transcribed by RNA polymerase II (Cavanaugh et al., 2004). In mammals, there are 150-200 copies of rRNA genes (rDNA) present on different chromosomes, arranged in tandem and separated by untranscribed spacers (Cavanaugh et al., 2004). Transcription of rDNA accounts for 40-60% of all transcription in the cell. In mammals, the rDNA promoter has a core promoter element, an upstream promoter element and has two identified transactivators. Selectivity factor 1 (SL1) is required for rDNA transcription and is analogous to the TFIID protein for RNA polymerase II in that it acts to recruit the preinitiation complex and the TATA-binding protein to the promoter. Upstream binding factor (UBF) enhances rDNA transcription but is not essential. Transcription of rDNA can be regulated in a number of ways (Cavanaugh et al., 2004; Lempiäinen and Shore, 2009). Cell cycle-dependent kinases can modify SL1 and UBF activity by phosphorylation. The mammalian target of rapamycin kinase that is responsive to nutrient availability can also affect factors involved in rDNA transcription. The UBF protein can also be sequestered by the RB protein, inhibiting rDNA transcription.

The pre-rRNA transcript is processed by covalent modification and cleaved into mature rRNA species (Nazar, 2004) (figure 1.4). In HeLa cells, the 45S pre-rRNA transcript has several transcribed spacers surrounding the rRNA sequences (Hadjiolova et al., 1993). A 5’ external transcribed spacer (ETS) is located upstream of the 18S rRNA sequence. Two internal transcribed spacers (ITS) lie between the 18S and 5.8S rRNA sequences (ITS1), and between the 5.8S and 28S rRNA sequences (ITS2). A 3’ETS lies downstream of the 28S rRNA sequence.

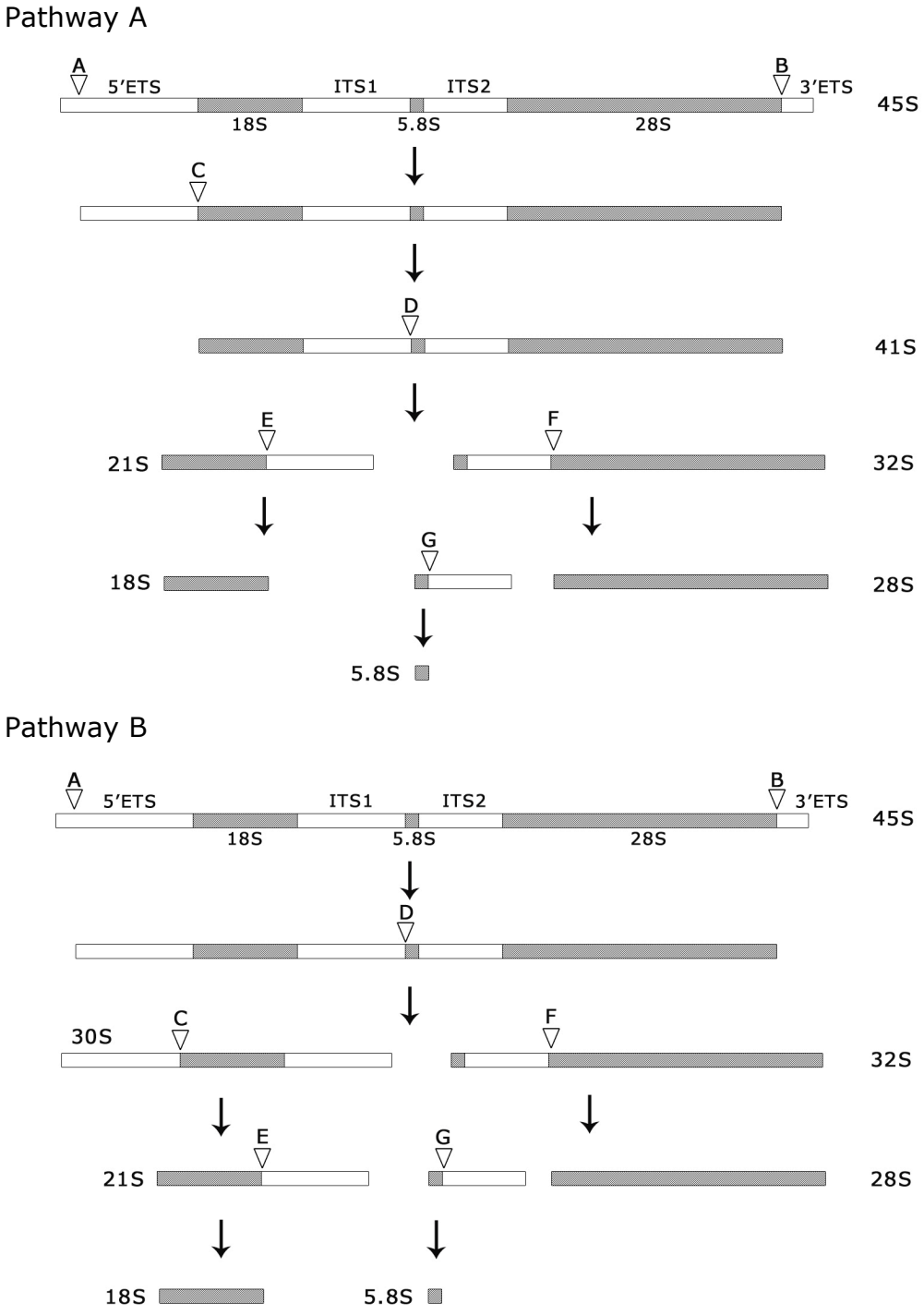

Figure 1.4 Ribosomal RNA processing in HeLa cells. The processing of pre-ribosomal 45S rRNA to 18S, 5.8S, and 28S rRNA in HeLa cells. Cleavages are indicated A-G. Processing can occur by one of two pathways depending on the order of cleavages C and D. (Adapted from Hadjiolova et al., 1993.).

The first cleavage steps remove part of the 5'ETS and the entire 3'ETS. Two pathways of processing can then occur, dependent on the order of the next two cleavage events. In the first pathway, the next cleavage step removes the remainder of the 5'ETS, followed by cleavage at the end of ITS1. The 21S product of this cleavage contains the 18S rRNA sequence and ITS1; cleavage of ITS1 generates 18S rRNA. The 32S product contains the 5.8S and 28S rRNA sequences separated by ITS2. Cleavage at the end of ITS2 generates 28S rRNA and a 12S product containing the 5.8S rRNA sequence and ITS2, which is then cleaved to generate 5.8S rRNA. In the second pathway, cleavage at the end of ITS1 occurs prior to the removal of the 5'ETS, generating a 30S product containing the 5'ETS, the 18S rRNA sequence, and ITS1, and the same 32S product composed of 5.8S, ITS2, and 28S generated in the first pathway after cleavage at ITS1. The 32S product is processed in the same manner as in the first pathway. Removal of the 5'ETS from the 30S subunit generates the 21S product containing 18S and ITS1; ITS1 is then removed to produce 18S rRNA as in the first pathway.

During or shortly after the pre-rRNA precursor is transcribed, covalent modifications such as methylation and pseudouridine synthesis take place within the 18S, 5.8S, and 28S regions (Gerbi and Borovjagin, 2004). Small nucleolar RNA molecules (snoRNAs) complementary to the modification sites bind and recruit small nucleolar ribonucleoprotein (snoRNP) complexes that modify the pre-rRNA molecule. The U3 snoRNA that makes up part of the U3 snoRNP base pairs to complementary sequences within the 5'ETS with the assistance of nucleolin. Binding of U3 snoRNA to the ETS and other sites within the rRNA is required for several of the first cleavage steps in rRNA processing, while binding of U8 snoRNA to other sequences is required for other processing steps, particularly the generation of 28S rRNA. In addition to binding of snoRNAs and snoRNPs, the pre-rRNA associates with ribosomal and non-ribosomal proteins to form a pre-ribosomal particle (90S in yeast, 80S in mammals) (Cavanaugh et al., 2004; Gerbi and Borovjagin, 2004; Henras et al., 2008). The 80S/90S pre-ribosome is processed into the 40S and 60S subunits, then transported to the cytoplasm where the final processing steps occur and additional ribosomal proteins are added to generate mature, functional ribosomes (Henras et al., 2008).

1.3.2 Inhibition of ribosomal RNA processing during adenovirus infection

In cells infected with HAdV-2, it was observed that production of new ribosomes decreased during infection to 20% of the level seen in uninfected cells (Raskas et al., 1970). In HAdV-12-infected cells, there is a decrease in the amount of new 28S, 18S, and 5.8S rRNAs in the cytoplasm and a new rRNA species not observed in uninfected cells appears (Ledinko, 1972; Lawler et al., 1989). The amount of 28S and 18S rRNA produced in HAdV-5 infected cells shows a dramatic decrease as the infection progresses (Castiglia and Flint, 1983). The amount of 28S rRNA produced at 12 hrs post infection was only 10% of the level in uninfected cells and less than 1% at 24 hrs. The production of 18S rRNA showed a less severe inhibition, falling to approximately 40% of control cell levels at 12 hrs post infection and less than 10% at 24 hrs. It was also demonstrated that while synthesis of ribosomal proteins is suppressed in adenovirus-infected cells, they are not downregulated more than other cellular proteins. This appears to be due to the generalized inhibition of host cell translation during infection. If the decreased levels of 28S and 18S were due to the virus interfering with host cell translation and inhibiting proteins required for their production, it would be expected that their inhibition would lag behind that of host cell proteins. The inhibition of 28S and 18S rRNA production reached 50% at an average of 9.7 and 15 hrs post infection, respectively, while inhibition of host cell protein synthesis was 50% at an average of 12.3 hrs. The levels of other pre-rRNA species decreased during infection, but the 45S pre-rRNA did not, suggesting that the decrease in mature rRNA species is due to inhibition of pre-rRNA processing rather than rRNA synthesis by RNA polymerase I. It is possible that the virus also interferes with transport of the rRNA to the cytoplasm, since the levels of 28S rRNA decreased much more rapidly in the cytoplasm than in the nucleus.

In HAdV-2-infected cells, the UBF protein involved in activation of rDNA transcription is recruited to centers of viral DNA replication, but this does not appear to affect the localization of RNA polymerase I, the rate of pre-rRNA synthesis, or, in contradiction with results of Castiglia and Flint (1983), rRNA processing (Lawrence et al., 2006). Several viral proteins including IVa2, pV, pVII, and μ have been shown to localize to the nucleolus (Lutz et al., 1996; Matthews, 2001; Lee et al., 2003; Lee et al., 2004b). Redistribution of nucleolar proteins such as nucleolin and B23 by pV has been shown (Matthews, 2001). Other nucleolar proteins are also relocalized during adenovirus infection (Lam et al., 2010). However, inhibition of rRNA processing has not yet been linked to a viral protein.

1.3.3 Inhibition of ribosomal RNA processing by viruses

Several other viruses have been shown to inhibit rRNA metabolism during infection, either by interfering with rRNA synthesis, rRNA processing, or both. The mechanisms by which these viruses interfere with rRNA synthesis and processing are often not well characterized, particularly with respect to inhibition of rRNA processing. Interactions with nucleolar proteins and disruption of nucleoli by many viruses could be important due to the close relationship of rRNA processing with nucleolar proteins and structures (Hiscox, 2002).

1.3.3.1 Poliovirus

Poliovirus is a member of the *Picornaviridae* family and has a single-stranded, positive-sense RNA genome (Banerjee et al., 2005). Poliovirus infection disrupts normal rRNA processing, since the levels of several minor rRNA species are increased in infected cells (Weinberg et al., 1967). The viral protease is also able to cleave SL1 and decrease the levels of UBF, inhibiting transcription from the rDNA promoter and downregulating pre-rRNA production (Banerjee et al., 2005).

1.3.3.2 Vesicular stomatitis virus

Vesicular stomatitis virus (VSV) is a member of the *Rhabdoviridae* family and has a single-stranded, negative-sense RNA genome (Lyles and Rupprecht, 2007). VSV is able to inhibit both synthesis and processing of rRNA (Zan et al., 1990; Ahmed and Lyles, 1998). The VSV matrix protein can inhibit RNA polymerase I-dependent transcription of 45S pre-rRNA. The processing of the 45S precursor is also inhibited by a distinct but unidentified viral protein.

1.3.3.3 Poxviruses

Members of the *Poxviridae* family are large, enveloped viruses that contain a double-stranded DNA genome and replicate entirely in the cytoplasm of infected cells (Moss, 2007). Members of the *Poxviridae* family such as vaccinia virus and Shope fibroma virus have been shown to inhibit the production of mature rRNA during infection (Salzman et al., 1964; Ewton and Hodes, 1967). The mechanisms by which this occurs have not been well characterized, but inhibition appears to occur by downregulating RNA synthesis as well as inhibition of either transport of rRNA to the cytoplasm or rRNA processing.

1.3.3.4 Herpes simplex virus

Members of the family *Herpesviridae* such as herpes simplex virus (HSV) are enveloped viruses with a double-stranded DNA genome (Pellett and Roizman, 2007). During HSV infection, synthesis of 45S pre-rRNA and processing of the precursor into 28S and 18S rRNA decrease (Wagner and Roizman, 1969). As the levels of 28S and 18S decline, heavier species accumulate, indicating a defect in processing. The production of 45S rRNA drops to 30% of the level observed in uninfected cells, while the levels of 28S and 18S rRNA are 10% or less of the amount from control cells. HSV also alters the intracellular distribution of rRNA, recruiting it to virus-induced regions in the nucleus where viral DNA replication, transcription, and assembly occur (Besse and Puvion-Dutilleul, 1996).

1.3.3.5 Human immunodeficiency virus

HIV-1 belongs to the family *Retroviridae* , a family of enveloped viruses with single-stranded, positive-sense RNA genome that is reverse transcribed into double-stranded DNA that can integrate into host cell chromosomal DNA (Goff, 2007). The HIV-1 Tat protein inhibits the processing of rRNA (Ponti et al., 2008). Probes specific for the 5'ETS and two sites in ITS1 detected increased levels of various rRNA precursors in *Drosophila* flies expressing the Tat protein, indicating a defect of rRNA processing. Tat interacts with fibrillarin and U3 snoRNA and can bind to the region of rRNA between the 5'ETS and 18S where an early cleavage step occurs. Since both fibrillarin and U3 snoRNA are involved in early steps of processing pre-rRNA, it is likely that their interaction with Tat somehow disrupts these processing steps.

2.0 HYPOTHESIS AND OBJECTIVES

2.1 Hypothesis

Non-human adenoviruses such as bovine adenovirus (BAdV)-3 are being studied for use as expression vectors for vaccine delivery and gene therapy (Reddy et al., 1999b). A number of differences between human adenoviruses (HAdVs) and BAdV-3 have been observed. Differences in cell entry (Bangari et al., 2005), transcriptional organization of the genome (Reddy et al., 1998), and the packaging signal located at the left end of the genome (Xing and Tikoo, 2003; Xing and Tikoo, 2007) have been observed in BAdV-3 compared to HAdVs. In addition, several proteins unique to BAdV-3 are present in the E3 and E4 regions (Reddy et al., 1998; Idamakanti et al., 1999) and the virus-associated RNAs present in HAdVs appear to be absent in BAdV-3 (Reddy et al., 1998). Because of these differences between HAdVs and BAdV-3, it is important to characterize the structure and function of BAdV-3 proteins.

Interactions between viral proteins and between viral and cellular proteins are important for adenovirus replication. For example, interactions between structural proteins are critical for the formation of the adenoviral capsid (Vellinga et al., 2005), while interactions between early viral proteins and cellular proteins such as the retinoblastoma protein and p53 are essential for the virus to push the cell into S phase and prevent apoptosis induced by virus replication (Berk, 2005).

All sequenced adenoviruses contain a non-structural protein termed 52K (Davison et al., 2003). In HAdV, 52K has been shown to be essential for encapsidation of the viral genome (Hasson et al., 1989; Gustin and Imperiale, 1998) and interacts with the viral pVII and IVa2 proteins (Gustin et al., 1996; Zhang and Arcos, 2005). We propose to study the 52K protein of BAdV-3 and hypothesize that the BAdV-3 52K protein interacts with additional viral and cellular proteins during BAdV-3 infection of bovine cells.

2.2 Objectives

The overall objective of this work is to characterize the 52K protein of BAdV-3, as a step towards developing BAdV-3 as an expression vector.

The specific objectives of this work are:

(i) To raise specific antibodies against the BAdV-3 52K protein and characterize its open reading frame, its expression during BAdV-3 infection, and its intracellular localization;

(ii) To identify viral and cellular proteins interacting with BAdV-3 52K;

(iii) To identify if possible the biological functions of detected interactions.

3.0 CHARACTERIZATION OF 52K PROTEIN OF BAdV-3

3.1 Introduction

Adenoviruses are non-enveloped, icosahedral viruses containing a double-stranded DNA genome. The virus enters the cells by endocytosis, escapes the pre-lysosomal compartment, and travels to the nuclear envelope where it releases the viral DNA into the nucleus. Expression of viral genes is divided into early, intermediate, and late phase of viral infection. The early and intermediate genes are transcribed after the viral DNA enters the nucleus and prior to the onset of DNA replication. In contrast, the late genes are transcribed after the onset of viral DNA replication and are grouped into different families based on usage of polyadenylation signals.

Bovine adenovirus (BAdV)-3, a member of the *Mastadenovirus* genus, is being developed as a vector for vaccination of animals and humans (Rasmussen et al., 1999; Zakhartchouk et al., 1999). Earlier, determination of the genome sequence and transcriptional map (Reddy et al., 1998) suggested that the BAdV-3 genome is also organized into early, intermediate, and late regions. The late genes are all expressed from the major late promoter (MLP) and are grouped into seven families (L1 to L7) based on usage of polyadenylation sites. Although the genome organization appears to be similar to human adenovirus (HAdV)-5, recent studies have identified distinct features of BAdV-3 (Reddy et al., 1998; Idamakanti et al., 1999; Xing and Tikoo, 2003; Bangari et al., 2005; Xing and Tikoo, 2006; Xing and Tikoo, 2007).

The L1 region of HAdV-5 encodes a nonstructural protein named 52/55K (Lucher et al., 1986), which is expressed as two differentially phosphorylated forms of a 48-kDa precursor (Lucher et al., 1986; Hasson et al., 1992). The 52K protein is involved in packaging of adenovirus DNA (Hasson et al., 1989; Gustin and Imperiale, 1998). The N-terminal half of the 52K protein mediates serotype specificity for packaging of the viral genome into the capsid (Wohl and Hearing, 2008). Although the 52K protein is predominantly localized in the nucleus of infected cells (Lucher et al., 1986; Hasson et al., 1992), the molecular mechanism involved in nuclear localization is not known.

Protein entry into the nucleus is regulated by the nuclear pore complexes (NPCs), which are embedded in the nuclear membrane and form a channel through which regulated transport in and out of the nucleus can occur (Lim et al., 2008). Proteins larger than ~40 kDa cross the NPC (Lim et al., 2008) only after interaction of a nuclear localization signal (NLS) with one or more soluble

transport receptors (Kalderon et al., 1984; Robbins et al., 1991). Classical NLSs contain one or two clusters of basic amino acids, however a growing number of non-classical NLSs that do not fit this consensus have been identified (Christophe et al., 2000).

The majority of protein trafficking into and out of the nucleus is dependent on the cellular GTPase Ran and soluble transport receptors such as importin α and importin β (Fried and Kutay, 2003). However, some proteins can bind to importin β without importin α (Palmeri and Malim, 1999; Truant and Cullen, 1999) or to receptors such as transportin (Pollard et al., 1996) for nuclear import. While these mechanisms are still Ran-dependent, Ran-independent nuclear import mechanisms such as calcium-dependent calmodulin-mediated (Hanover et al., 2009) or nucleoporin-mediated (Michael et al., 1997; Tsuji et al., 2007) have also been reported.

Homologs of 52K have been identified in other members of the *Mastadenovirus* genus including BAdV-3 (Reddy et al., 1998; Davison et al., 2003). The L1 region of the late transcription unit of BAdV-3 encodes the 52K protein (Reddy et al., 1998), which is collinear with 52K of HAdV-5. Since BAdV-3 52K shows 56.8% to 61.6% sequence identity to 52K proteins of other *Mastadenoviruses* (Reddy et al., 1998), we sought to characterize this protein. Here, we report its characterization and identification of pathway(s) mediating nuclear localization of the BAdV-3 52K protein.

3.2 Materials and Methods

3.2.1 Cell lines and viruses

Madin Darby bovine kidney (MDBK) cells were propagated in minimal essential medium (MEM; Invitrogen) supplemented with 10% heat-inactivated fetal bovine serum (FBS; SeraCare Life Sciences, Inc.). COS7 cells (Gluzman, 1981) were propagated in Dulbecco's modified Eagle's medium (DMEM; Invitrogen) supplemented with 10% FBS. Wild-type BAdV-3 (WBR-1 strain) was propagated in MDBK cells in MEM supplemented with 2% FBS and purified by cesium chloride density-gradient centrifugation (Reddy et al., 1999a). The virus titer was determined by plaque assay (Mittal et al., 1995) to be 5×10^8 plaque-forming units (pfu)/mL.

3.2.2 Sequence analysis

Sequence alignment of BAdV-3 52K with the sequences of 52K proteins of other *Mastadenoviruses* was performed with Clone Manager (Sci Ed Software) using a BLOSUM 62 scoring matrix.

3.2.3 GST fusion protein

A 312-bp *Hinc*II/*Eag*I fragment of 52K corresponding to amino acids 29 to 133 (nucleotides 10072 to 10384 of the BAdV-3 genome, Genbank AF03014) was cloned into *Sma*I-*Eag*I-digested plasmid pGEX-5x-2 (GE Healthcare) downstream and in frame with glutathione-S-transferase (GST) to create plasmid pGEX-52K(N). The translation frame of the fusion protein was verified by DNA sequencing. The plasmid pGEX-52K(N) DNA was transformed into *E. coli* BL21 cells. An aliquot of an overnight culture was added to 12 mL 2xTY broth [16g/L tryptone, 10 g/L yeast extract, 5 g/L sodium chloride] containing 100 µg/mL ampicillin and grown at 37˚C with shaking to an OD_{600} of approximately 0.6. Fusion protein expression was induced by the addition of 0.1mM isopropyl-β-D-thiogalactopyranoside (IPTG). After incubation of 2-3 hrs, the cells were harvested by centrifugation (6,000x*g* for 15 min), resuspended in 0.1 M phosphate buffered saline (PBS), and lysed by the addition of lysozyme (0.1 mg/mL) for 5 minutes at room temperature followed by ten freeze/thaw cycles. The lysate was cleared by centrifugation (10,000x*g* for 10 min) and GST-52K(N) fusion protein was purified using glutathione sepharose columns (GE Healthcare) as per manufacturer's instructions. The purity of the eluted protein was confirmed by sodium dodecyl sulphate (SDS) - polyacrylamide gel electrophoresis (PAGE). The proteins were separated by 10% SDS-PAGE and the gel was stained for 15 minutes with Coomassie Blue. Finally, the gel was destained with destaining solution [10% acetic acid, 40% methanol] to visualize protein bands.

3.2.4 Immunization

Antibodies against the GST-52K(N) protein were raised by subcutaneous immunization of rabbits with 500 µg of purified GST-52K(N) emulsified in Freund's complete adjuvant (Sigma-Aldrich). Three boosts of 300 µg GST-52K(N) emulsified in Freund's incomplete adjuvant (Sigma-Aldrich) were given at 21, 42, and 63 days post immunization. Finally, serum was collected at day 74 of primary immunization, aliquoted, and stored at –20˚C.

3.2.5 Western blotting

MDBK cells were grown in 6-well plates to 80-90% confluency and infected with wild-type BAdV-3 at a multiplicity of infection (MOI) of 4 plaque forming units (pfu)/cell. At indicated times post infection, infected cells were harvested by centrifugation at 3,000 rpm (950x*g*) for 5 minutes and lysed by addition of RIPA buffer [0.15 M NaCl, 50 mM Tris-HCl (pH 8.0), 1% NP-40, 1% deoxycholate, 0.1% SDS] containing 1 µg/mL each aprotinin, leupeptin, and pepstatin A. Proteins from lysates of infected cells were separated by 10% SDS-PAGE and transferred to a nitrocellulose membrane (Bio-Rad). The membrane was blocked with 1% bovine serum albumin (BSA) in TBST [Tris-buffered saline (pH 8.0), 0.05% tween 20] overnight at 4˚C and probed with anti-52K serum diluted 1:100 in TBST containing 0.1% BSA for 1 hour at room temperature. After three TBST washes, the membranes were probed with alkaline phosphatase (AP)-conjugated goat anti-rabbit IgG (Jackson Immunoresearch) diluted 1:10,000 in TBST containing 0.1% BSA for 1 hr at room temperature. The membranes were washed three times in TBST and developed using a colorimetric kit.

3.2.6 Immunofluorescence microscopy

MDBK cells seeded in 2-well glass slides were infected with wild-type BAdV-3 at an MOI of 4. COS7 cells seeded on 4-well glass slides were transfected with 1µg of plasmid DNA as indicated in the text and figures using ExGen transfection reagent (Fermentas) as per the manufacturer's instructions. Twenty-four hrs post infection or post transfection, the cells were fixed in 100% methanol for 20 minutes at -20˚C. After three washes in PBS, cells were blocked with 2% goat serum in PBS for 30 minutes, then probed with anti-52K serum (diluted 1:50) and a mouse anti-nucleolin monoclonal antibody (Stressgen; diluted to 1 µg/mL) in PBS containing 1% goat serum for 1 hr at room temperature. After three washes in PBS, Cy2-conjugated goat anti-rabbit IgG (Jackson Immunoresearch; diluted 1:400) and Cy3-conjugated goat anti-mouse IgG (Jackson Immunoresearch; diluted 1:800) in PBS containing 1% goat serum were added for 1 hr at room temperature. Cells were washed three times in PBS and stained with 2 µg/mL 4',6-diamino-2-phenylindole (DAPI), then mounted in Citifluor mounting reagent (Citifluor, Ltd., Leicester, U.K.) and visualized on an Axiovert UV microscope using Zeiss AxioVision software.

Cells transfected with plasmids expressing enhanced yellow fluorescent protein (EYFP) fusion proteins were fixed 24 hrs post transfection with 3.7% paraformaldehyde in PBS for 15 min,

washed three times in PBS and stained with 2 μg/mL DAPI. Finally, the cells were analyzed using Axiovert UV Microscope and Zeiss AxioVision software.

3.2.7 Plasmid construction

(a) Construction of pcDNA.52K. A 1,124-bp fragment containing the 52K open reading frame was amplified by PCR using primers CP1 and CP2 (table 3.1), and plasmid pTG5435 (containing the full-length BAdV-3 genome) (Rasmussen et al., 1999) DNA as a template. The PCR product was digested with *Eco*RI-*Bam*HI and ligated to *Eco*RI–*Bam*HI digested pcDNA3.1(-) (Invitrogen) creating plasmid pcDNA.52K (figure 3.1).

(b) Construction of pEY.52K. The 1,124-bp PCR fragment containing 52K described in section 3.2.7 (a) was blunt-end ligated to *Eco*RV-digested plasmid Litmus28i (New England Biolabs). A clone with 52K inserted in the same orientation as the Litmus28i LacZ ORF was selected and named L28i.52K. A 1.1 kb *Sna*BI-*Sal*I fragment was isolated from plasmid L28i.52K and ligated to *Afe*I-*Xho*I-digested plasmid pEYFPN1 (Clontech), creating plasmid pEY.52K (figure 3.1).

(c) Construction of 52K deletion mutants. Sequential deletions in the 52K ORF were created as previously described (Lee et al., 2004a). A schematic of the overlap PCR strategy is shown in figure 3.2. All deletions were confirmed by restriction enzyme analysis and sequencing.

(i) Construction of pEY.52KΔ1. A 984-bp fragment amplified by PCR using primers Δ1F and CP2 (table 3.1), and plasmid pcDNA.52K DNA as a template was ligated to *Srf*I-digested plasmid PCR-Script Amp (Stratagene). A clone with the mutant 52K ORF inserted in the same orientation as the plasmid PCR-Script Amp T7 promoter was selected and named pScript-Δ1. A 1kb *Eco*RV-*Sal*I fragment was isolated from plasmid pScript-Δ1 and ligated to *Afe*I-*Xho*I digested plasmid pEYFPN1 creating plasmid pEY.52KΔ1 (figure 3.1).

(ii) Construction of pEY.52KΔ2. A 141-bp fragment was amplified by PCR using primers CP1 and Δ2R (table 3.1), and plasmid pcDNA.52K DNA as a template. Similarly, a 851-bp fragment was amplified by PCR using primers Δ2F and CP2 (table 3.1), and plasmid pcDNA.52K DNA as a template. The two PCR fragments were mixed, annealed, and amplified by PCR using primers CP1 and CP2. This 974-bp PCR product was ligated to *Srf*I-digested plasmid PCR-Script Amp. A clone with the mutant 52K ORF inserted in the same orientation as the PCR-Script Amp T7 promoter was selected and named pScript-Δ2. A 990-bp *EcoRV-SalI* fragment was isolated from

Table 3.1 Primers used for PCR.

Primer name	Sequence
CP1	5′-GAATTC***ATG***CATCCCGCTTTACGGCAAATG-3′
CP2	5′-GGATCCAC***TCA***TTCGTCGACTTCAT-3′
Δ1F	5′-AGAATTC***ATG***CTGTACGCGCACCCGGACAC-3′
Δ2F	5′-**TGCGGCGAGAAGGCCGGT**CGG-3′
Δ2R	3′-CCACAGCTC**ACGCCGCTCTTCCGGCCA**-5′
Δ3F	5′-**GGGAGCCGAGTGCGGGCT**TACGAGCAAAC-3′
Δ3R	3′-CTTGGGCTT**CCCTCGGCTCACGCCCGA**-5′
Δ4F	5′-**GCCCACATGGGCAGCAAG**ACCCTTACG-3′
Δ4R	3′-GAGTCGGTTT**CGGGTGTACCCGTCGTTC**-5′
Δ5F	5′-**GCATACGCGCAGTCCATT**GTGGTGCAAGAG-3′
Δ5R	3′-GAAACGCCTC**CGTATGCGCGTCAGGTAA**-5′
Δ6F	5′-**GAGGGACGATTTGTGCCG**CTTGACAAGGAG-3′
Δ6R	3′-GTATCGTCTCGGG**CTCCCTGCTAAACACGGC**-5′
Δ7F	5′-**GCCCGCAAGGCGGAGCTGC**TGTTCAACC-3′
Δ7R	3′-GTTTGTAATA**CGGGCGTTCACTGTGCACA**-5′
Δ8R	5′-TCTCCCGACGCCTGCCTATGC-3′
Δ3.1F	5′-**GAGGAACCCGCCGGAATG**CCCCGAAAGCG-3′
Δ3.1R	3′-CTGGCGTCGCCC**CTCCTTGGGCGGCCTTAC**-5′
Δ3.2F	5′-**TTGCGCGCCGAAGGGGAC**TTTGAGGTGGAT-3′
Δ3.2R	3′-CGGCCAGCTGTC**AACGCGCGGCTTCCCCTG**-5′
Δ3.3F	5′-**GGCATCAGCCGGGCGTAC**GAGCAAACGGTG-3′
Δ3.3R	3′-CCTACTCGCGTGA**CCGTAGTCGGCCCGCATG**-5′
CP3	5′-ATTCGTCGACTTCATCGTCC-3′
NLSmF	5′-TGCCCGAAGAGGAGGTGCTGACCGAAGGGGACTTTGAGG-3′
NLSmR	3′-CAGCCGTCAACGCGCGGCCGTACGGGCTTCTCCTCCACG-5′
CP4	5′-ATGGCTAGCGGCATGCCCCGAAAGCGGGTGCTGACCAAAGGAGAAGA ACTCTTCACTGGAGTTGTCCCAATTC-3′
CP5	5′-AGCACGTGTCTTGTAGTTGCCGTCATC-3′

Overlapping regions to create deletions are shown in bold. Restriction enzyme sites are underlined. Start and stop codons for the 52K open reading frame are indicated in bold italics.

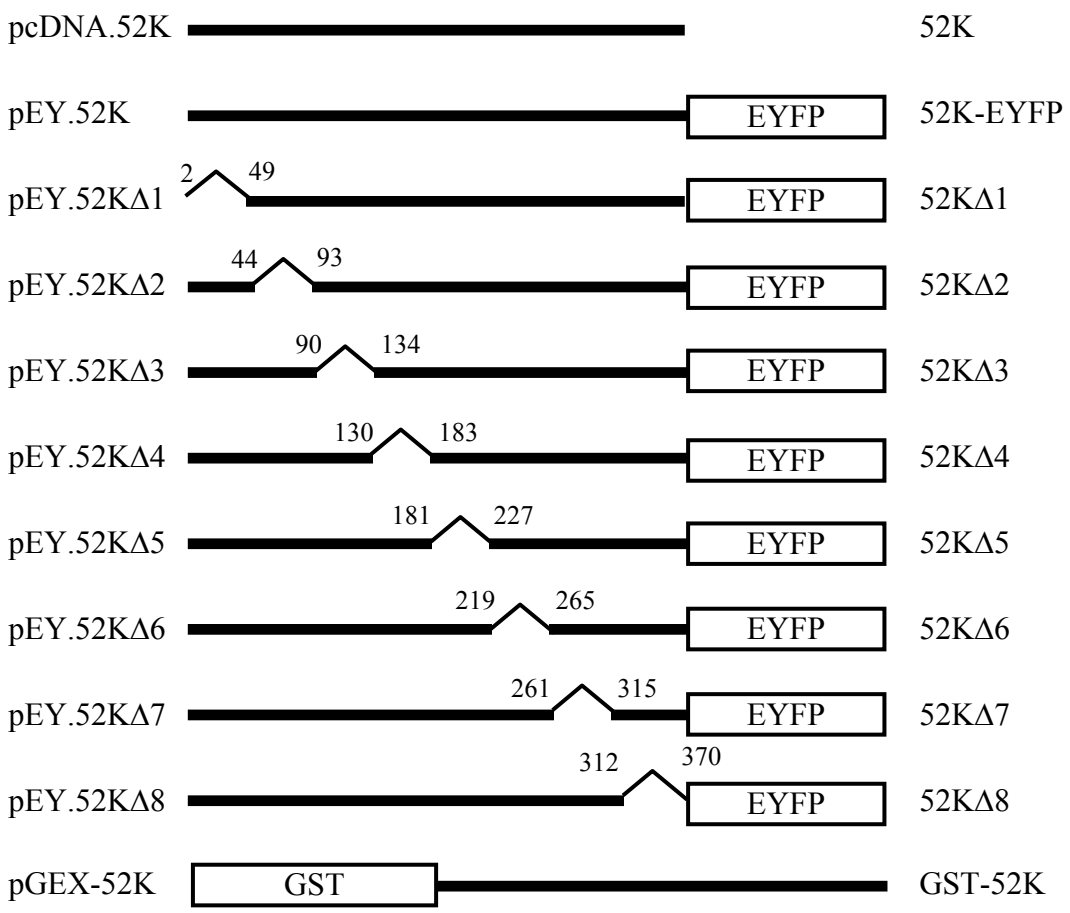

Figure 3.1. Schematic representation of 52K constructs and mutants. Amino acids deleted by PCR mutagenesis are indicated. Plasmid names are indicated on the left; proteins expressed from these plasmids are indicated on the right.

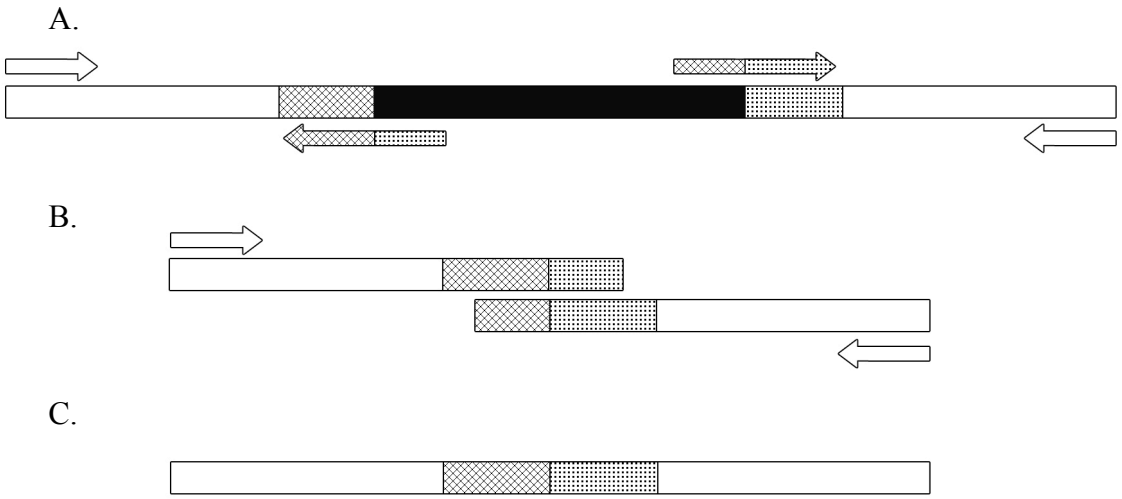

Figure 3.2 Schematic of deletion mutagenesis by overlap PCR. A. Amplification of upstream and downstream sequences. Forward and reverse primers are designed complementary to sequences flanking the region to be deleted (in black) and contain a sequence complementary to the other primer in the pair (filled arrows). Two separate PCR reactions amplify the regions upstream and downstream of the area to be deleted, using forward and reverse primers complementary to the ends of the gene (open arrows). **B.** Overlap PCR. The products of the two PCR reactions are mixed and amplified using the non-chimeric primers. **C.** PCR product. The product of the final PCR reaction contains the desired deletion. (Adapted from Lee et al., 2004a)

plasmid pScript-Δ2 and ligated to *Afe*I-*Xho*I digested plasmid pEYFPN1 creating plasmid pEY.52KΔ2 (figure 3.1).

(iii) Construction of pEY.52KΔ3. A 279-bp fragment was amplified by PCR using primers CP1 and Δ3R (table 3.1), and plasmid pcDNA.52K DNA as a template. Similarly, a 728-bp fragment was amplified by PCR using primers Δ3F and CP2 (table 3.1), and plasmid pcDNA.52K DNA as a template. The two PCR fragments were mixed, annealed, and amplified by PCR using primers CP1 and CP2. This 989-bp PCR product was ligated to *Srf*I-digested plasmid PCR-Script Amp. A clone with the mutant 52K ORF inserted in the same orientation as the PCR-Script Amp T7 promoter was selected and named pScript-Δ3. A 1,005-bp *Eco*RV-*Sal*I fragment was isolated from plasmid pScript-Δ3 and ligated to *Afe*I-*Xho*I digested plasmid pEYFPN1 creating plasmid pEY.52KΔ3 (figure 3.1).

(iv) Construction of pEY.52KΔ4. A 399-bp fragment was amplified by PCR using primers CP1 and Δ4R (table 3.1), and plasmid pcDNA.52K DNA as a template. Similarly, a 581-bp fragment was amplified by PCR using primers Δ4F and CP2 (table 3.1), and plasmid pcDNA.52K DNA as a template. The two PCR fragments were mixed, annealed, and amplified by PCR using primers CP1 and CP2. This 962-bp PCR product was ligated to *Srf*I-digested plasmid PCR-Script Amp. A clone with the mutant 52K ORF inserted in the same orientation as the PCR-Script Amp T7 promoter was selected and named pScript-Δ4. A 978-bp *EcoR*V-*Sal*I fragment was isolated from plasmid pScript-Δ4 and ligated to *Afe*I-*Xho*I digested plasmid pEYFPN1 creating plasmid pEY.52KΔ4 (figure 3.1).

(v) Construction of pEY.52KΔ5. A 552-bp fragment was amplified by PCR using primers CP1 and Δ5R (table 3.1), and plasmid pcDNA.52K DNA as a template. Similarly, a 449-bp fragment was amplified by PCR using primers Δ5F and CP2 (table 3.1), and plasmid pcDNA.52K DNA as a template. The two PCR fragments were mixed, annealed, and amplified by PCR using primers CP1 and CP2. This 983-bp PCR product was ligated to *Srf*I digested plasmid PCR-Script Amp. A clone with the mutant 52K ORF inserted in the same orientation as the PCR-Script Amp T7 promoter was selected and named pScript-Δ5. A 999-bp *EcoR*V-*Sal*I fragment was isolated from plasmid pScript-Δ5 and ligated to *Afe*I-*Xho*I digested plasmid pEYFPN1 creating plasmid pEY.52KΔ5 (figure 3.1).

(vi) Construction of pEY.52KΔ6. A 666-bp fragment was amplified by PCR using primers CP1 and Δ6R (table 3.1), and plasmid pcDNA.52K DNA as a template. Similarly, a 335-bp fragment

was amplified by PCR using primers Δ6F and CP2 (table 3.1), and plasmid pcDNA.52K DNA as a template. The two PCR fragments were mixed, annealed, and amplified by PCR using primers CP1 and CP2. This 983-bp PCR product was ligated to *Srf*I-digested plasmid PCR-Script Amp. A clone with the mutant 52K ORF inserted in the same orientation as the PCR-Script Amp T7 promoter was selected and named pScript-Δ6. A 999-bp *Eco*RV-*Sal*I fragment was isolated from plasmid pScript-Δ6 and ligated to *Afe*I-*Xho*I digested plasmid pEYFPN1 creating plasmid pEY.52KΔ6 (figure 3.1).

(vii) Construction of pEY.52KΔ7. A 792-bp fragment was amplified by PCR using primers CP1 and Δ7R (table 3.1), and plasmid pcDNA.52K DNA as a template. Similarly, a 185-bp fragment was amplified by PCR using primers Δ7F and CP2 (table 3.1), and plasmid pcDNA.52K DNA as a template. The two PCR fragments were mixed, annealed, and amplified by PCR using primers CP1 and CP2. This 959-bp PCR product was ligated to *Srf*I-digested plasmid PCR-Script Amp. A clone with the mutant 52K ORF inserted in the same orientation as the PCR-Script Amp T7 promoter was selected and named pScript-Δ7. A 975-bp *Eco*RV-*Sal*I fragment was isolated from plasmid pScript-Δ7 and ligated to *Afe*I-*Xho*I digested plasmid pEYFPN1 creating plasmid pEY.52KΔ7 (figure 3.1).

(viii) Construction of pEY.52KΔ8. A 940-bp fragment amplified by PCR using primers CP1 and Δ8R (table 3.1), and plasmid pcDNA.52K DNA as a template was ligated to *Srf*I-digested plasmid PCR-Script Amp. A clone with the mutant 52K ORF inserted in the same orientation as the PCR-Script Amp T7 promoter was selected and named pScript-Δ8. A 1,002-bp *Eco*RV-*Sac*I fragment isolated from plasmid pScriptΔ8 was ligated to *Afe*I-*Sac*I digested plasmid pEYFPN1 creating plasmid pEY.52KΔ8 (figure 3.1).

(ix) Construction of pEY.52KΔ3.1. A 267-bp fragment was amplified by PCR using primers CP1 and Δ3.1R (table 3.1), and plasmid pcDNA.52K DNA as a template. Similarly, a 830-bp fragment was amplified by PCR using primers Δ3.1F and CP2 (table 3.1), plasmid pcDNA.52K DNA as a template. The two PCR fragments were mixed, annealed, and amplified by PCR using primers CP1 and CP2. This 1,043-bp PCR product was ligated to *Srf*I-digested plasmid PCR-Script Amp. A clone with the mutant 52K ORF inserted in the same orientation as the PCR-Script Amp T7 promoter was selected and named pScript-Δ3.1. A 1,059-bp *Eco*RV-*Sal*I fragment was isolated from plasmid pScript-Δ3.1 and ligated to *Afe*I-*Xho*I digested plasmid pEYFPN1 creating plasmid pEY.52KΔ3.1 (figure 3.3).

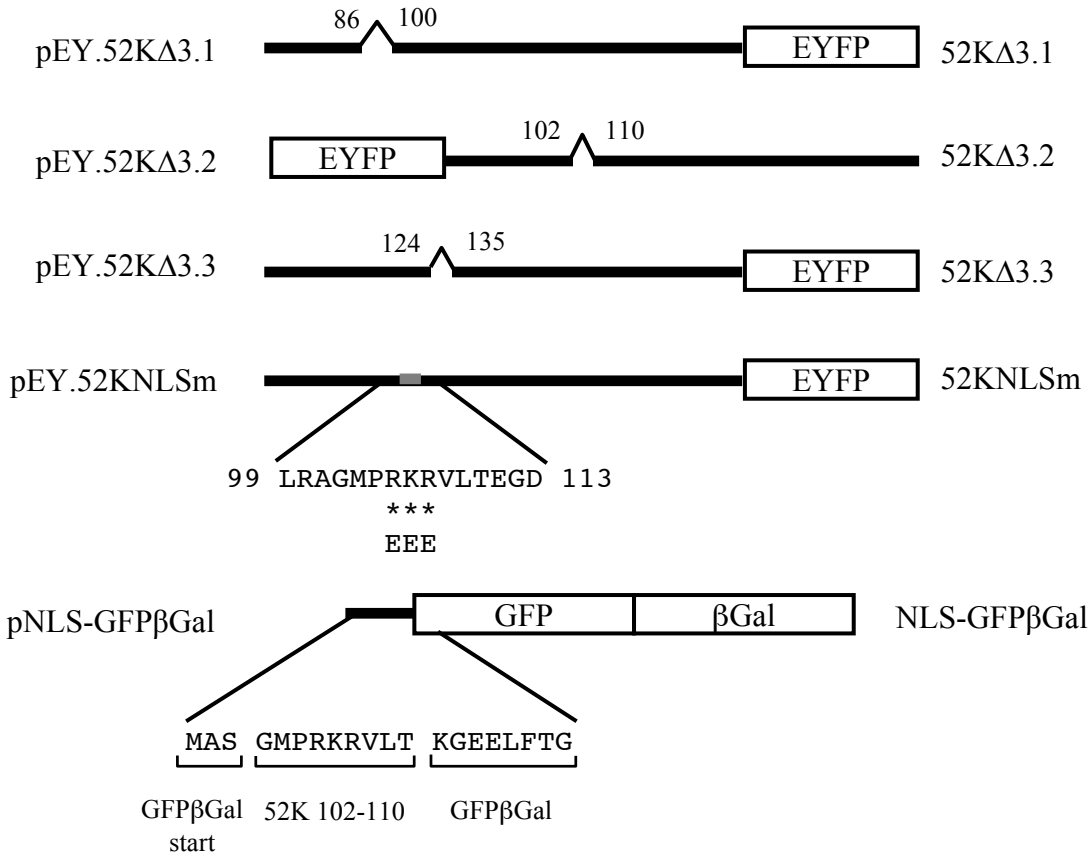

Figure 3.3. Schematic representation of 52K mutants and NLS-GFPβGal fusion. Amino acids deleted by PCR mutagenesis are indicated. Plasmid names are indicated on the left; proteins expressed from these plasmids are indicated on the right. The mutations introduced by PCR in pEY.52KNLSm are indicated. The sequence of the putative 52K NLS (amino acids 102-110) fused to GFPβGal is indicated.

(x) Construction of pEY.52KΔ3.2. A 315-bp fragment was amplified by PCR using primers CP1 and Δ3.2R (table 3.1), and plasmid pcDNA.52K DNA as a template. Similarly, a 800-bp fragment was amplified by PCR using primers Δ3.2R and CP3 (table 3.1), and plasmid pcDNA.52K DNA as a template. The two PCR fragments were mixed, annealed, and amplified by PCR using primers CP1 and CP3. This 1,087-bp PCR product was ligated to *Eco*RV-digested plasmid Litmus28i. A clone with the mutant 52K ORF inserted in the same orientation as the Litmus28i LacZ ORF was selected and named L28iΔ3.2. A 1,112-bp *Xho*I-*Bam*HI fragment was isolated from plasmid L28iΔ3.2 and ligated to *Xho*I-*Bam*HI digested plasmid pEYFPC1 (Clontech) creating plasmid pEY.52KΔ3.2 (figure 3.3).

(xi) Construction of pEY.52KΔ3.3. A 381-bp fragment was amplified by PCR using primers CP1 and Δ3.3R (table 3.1), and plasmid pcDNA.52K DNA as a template. Similarly, a 725-bp fragment was amplified by PCR using primers Δ3.3F and CP2 (table 3.1), and plasmid pcDNA.52K DNA as a template. The two PCR fragments were mixed, annealed, and amplified by PCR using primers CP1 and CP2. This 1,088-bp PCR product was ligated to *Srf*I digested plasmid PCR-Script Amp. A clone with the mutant 52K ORF inserted in the same orientation as the PCR-Script Amp T7 promoter was selected and named pScript-Δ3.3. A 1,104-bp *Eco*RV-*Sal*I fragment isolated from plasmid pScript-Δ3.3 was ligated to *Afe*I-*Xho*I digested plasmid pEYFPN1 creating plasmid pEY.52KΔ3.3 (figure 3.3).

*(d) Construction of pEY.52KNLSm.*A 318-bp fragment was amplified by PCR using primers CP1 and NLSmR (table 3.1), and plasmid pcDNA.52K DNA as a template. Similarly, a 814-bp fragment was amplified by PCR using primers NLSmF and CP2 (table 3.1), and plasmid pcDNA.52K DNA as a template. The two PCR fragments were mixed, annealed, and amplified by PCR using primers CP1 and CP2. This 1,124-base pair PCR product was ligated to *Eco*RV-digested Litmus28i. A clone with the mutant 52K inserted in the opposite orientation of the Litmus28i LacZ ORF was selected and named L28i.NLSm. A 1,149 *Xba*I-*Sal*I fragment was isolated from plasmid L28i.NLSm and ligated to *Nhe*I-*Xho*I digested plasmid pEYFPN1 creating plasmid pEY.52KNLSm (figure 3.3).

(e) Construction of pNLS-GFPβGal. The putative NLS of 52K was fused to the N-terminus of a green fluorescent protein-beta galactosidase (GFPβGal) fusion protein in the plasmid pGFP/βGal (Wu et al., 2004). Briefly, a 360-bp fragment was amplified by PCR using primers CP4 and CP5 (table 3.1), and plasmid pGFP/βGal DNA as a template. The PCR product was digested with

*Nhe*I-*Pml*I and ligated to *Nhe*I–*Pml*I digested plasmid pGFP/βGal creating plasmid pNLS-GFPβGal (figure 3.3).

(f) Construction of pGEX-52K. A 1.1 kb *Eco*RI-*Sal*I fragment was isolated from plasmid pcDNA.52K and ligated to *Eco*RI–*Xho*I digested plasmid pGEX-5x1 (GE Healthcare) creating plasmid pGEX-52K (figure 3.1).

3.2.8 Proteins and peptides for nuclear import assays

Plasmids encoding a fusion protein of glutathione-S-transferase, the nuclear localization signal of the simian virus 40 (SV40) T antigen, and green fluorescent protein (GST-NLS-GFP) and a dominant negative mutant of Ran fused to GST (GST-RanQ69L) were provided by Y. Yoneda (Yokoya et al., 1999; Tachibana et al., 2000). The plasmids were transformed into *E. coli* BL21 cells and expressed and purified as previously described (Imamoto et al., 1995). The transformed BL21 cells were grown overnight in Luria-Burtani (LB) broth with 100 µg/mL ampicillin (LB-AMP) at 37˚C with shaking. An aliquot of the overnight cultures was added to 500 mL of LB-AMP and grown at 37˚C to an OD_{550} of 1.2. Protein expression was induced by the addition of 1 mM IPTG and incubation for 14 hours at room temperature with shaking. The plasmid pGEX-52K was transformed into *E. coli* BL21 cells for expression. The BL21 cells were grown overnight in LB-AMP at 37˚C with shaking. An aliquot of the overnight culture was added to 500 mL of LB-AMP and grown to an OD_{600} of 0.5-0.6. Protein expression was induced by the addition of 0.1 mM IPTG and the culture was incubated for 3 hours at 37˚C.

The cells were harvested by centrifugation at 6,000x*g* for 15 min and resuspended in 25 mL of GST purification buffer [50 mM Tris-HCl (pH 8.3), 1 mM ethylenediamine-tetraacetic acid (EDTA), 2 mM dithiothreitol (DTT), 500 mM NaCl, 1 µg/mL each leupeptin and aprotinin] and lysed by two freeze-thaw cycles followed by sonication (4 x 30 seconds). After centrifugation of the lysate (20,000x*g* for 30 min), the supernatant was collected, mixed with 200 µL washed glutathione-sepharose beads (GE Healthcare), and incubated overnight at 4˚C on a nutator. Beads were washed four times in GST purification buffer before purified proteins were eluted by two 15 minute incubations with GST elution buffer [50 mM Tris-HCl (pH 8.3), 1 mM EDTA, 2 mM DTT, 100 mM NaCl, 10 mM reduced glutathione]. The eluted protein was dialyzed against three changes of dialysis buffer [20 mM HEPES (pH 7.3), 100 mM potassium acetate, 2 mM DTT, 1 µg/mL each aprotinin and leupeptin] for 6-8 hours.

To confirm expression and purity of the bacterially expressed proteins, eluted protein was analyzed by SDS-PAGE and Western blot. Eluted proteins were separated by 10% SDS-PAGE. The gel was stained with Coomassie blue for 15 minutes then incubated with several changes of destaining solution to visualize total protein. In addition, proteins were analyzed by Western blot using goat anti-GST antibody (GE Healthcare) and AP-conjugated rabbit anti-goat IgG (Jackson Immunoresearch).

The nuclear import inhibitory peptides corresponding to amino acids 1-30 (MFNRKRRGDF DEDENYRDFRPRMPKRQRIP) of the protein Ycbp80 (Görlich et al., 1996b) or amino acids 10-51 (RMRKFKNKGKDTAELRRRRVEVSVELRKAKKDEQILKRRNVC) of importin α (Görlich et al., 1996a) were synthesized using a Pioneer Peptide Synthesis system (Perkin Elmer).

3.2.9 *In vitro* nuclear import assays

In vitro nuclear import assays were carried out based on the protocol of Adam *et al*. (1990). MDBK cells (70-80% confluent) seeded onto glass coverslips were washed in ice-cold transport buffer (TB) [20 mM HEPES (pH 7.3), 110 mM potassium acetate, 5 mM sodium acetate, 2 mM magnesium acetate, 1 mM ethylene bis-(β-aminoethylether)-N,N,N',N-tetra-acetic acid (EGTA), 2 mM DTT, and 1 μg/mL each of aprotinin and leupeptin] for 5 min on ice before permeabilizing with 40 μg/mL digitonin (Calbiochem) in TB for 5 min on ice. Cells were washed three times for 5 min each in TB on ice to remove soluble cytoplasmic factors. Coverslips were inverted on 20 μL complete transport solution [ATP-regenerating system (1 mM adenosine triphosphate (ATP), 5 mM creatine phosphate, 20 units/mL creatine phosphokinase), 20 μM cargo protein (GST-52K or GST-NLS-GFP), 50% rabbit reticulocyte lysate (Promega) in TB] and incubated at 30˚C in a humidified chamber for 20 min to allow nuclear import to occur. In some cells, wheat germ agglutinin (WGA) was added at 0.4 mg/mL in TB for 10 min prior to incubation with complete transport solution. The dominant negative mutant RanQ69L was pre-loaded with 2 mM guanosine triphosphate (GTP) for 1 hour at 4˚C and added to complete transport solution at a concentration of 25 μM. Inhibitory peptides were added to complete transport solution at a concentration of 1 mM (50-fold molar excess). After incubation with the complete transport solution, cells were fixed in 3.7% paraformaldehyde in PBS for 15 min at room temperature and washed three times in PBS. Cells incubated with complete transport solution containing GST-

NLS-GFP were counterstained with 2 μg/mL DAPI for 5 min, washed in PBS, then mounted on slides in Citifluor mounting reagent and visualized on an Axiovert UV microscope using Zeiss AxioVision software. Cells incubated with complete transport solution containing GST-52K were permeabilized using 0.5% Triton-X-100 in PBS for 5 min, then stained with anti-52K serum and Cy2-conjugated goat anti-rabbit IgG as described in section 3.2.6.

3.2.10 Purification of nuclear import receptors

Plasmids encoding GST fusions of importin α1, importin α3, importin α5, importin α7, or importin β were a gift from M. Köhler and have been previously described (Depping et al., 2008). The plasmid pGEX-5x1 encoding GST was purchased from GE Healthcare. The plasmids were individually transformed into *E. coli* M15 (pRep4) cells (plasmids encoding GST fused to importin α1, α3, α5, or α7) or BL21 cells (plasmids encoding GST alone or GST fused to importin β) for expression. An aliquot of an overnight culture was added to 50 mL LB-AMP and grown at 37˚C to an OD_{600} of approximately 0.3. Protein expression was induced by the addition of IPTG at a concentration of 0.6 mM and incubated for 3.5 hrs at 37˚C. Cells were harvested by centrifugation (6,000x*g* for 15 minutes) and resuspended in 5 mL GST purification buffer. Cells were lysed by two freeze-thaw cycles and sonication (4 x 30 sec) and the lysate was cleared by centrifugation (20,000x*g* for 30 min). The supernatant was added to 50 μL washed glutathione-sepharose beads and allowed to bind overnight at 4˚C on a nutator. Beads were washed four times in GST purification buffer and eluted by two 15 min incubations with GST elution buffer. Protein expression and purity was confirmed by SDS-PAGE and Western blotting as described in section 3.2.8.

3.2.11 *In vitro* binding assay

GST or GST fusions of importin α1, importin α3, importin α5, importin α7, or importin β (16μg per binding reaction) were individually bound to 25 μL of washed glutathione sepharose beads in IP buffer [20 mM HEPES (pH 7.5), 100 mM potassium acetate, 0.5 mM EGTA, 5 mM magnesium acetate, 250 mM sucrose] for 6 hrs at 4˚C on a nutator. Radiolabeled 52K was synthesized by *in vitro* transcription and translation of plasmid pcDNA.52K in the presence of [^{35}S]-methionine (Perkin Elmer) using a TNT T7 Coupled Reticulocyte Lysate System (Promega). Fifteen μL of the radiolabeled translation mixture was added to GST or individual

GST-importin fusion proteins on glutathione sepharose beads and incubated overnight at 4˚C on a nutator. Beads were washed four times in IP buffer. The bead bound proteins were separated by 10% SDS-PAGE. The gel was fixed in destain solution containing 5% glycerol for 30 min and dried onto filter paper. The gel was exposed to a phosphor screen (Kodak) overnight and visualized on a Bio-Rad Molecular Imager FX using Quantity One software (Bio-Rad).

3.3 Results

3.3.1 Identification of 52K open reading frame

Earlier, it was reported that the BAdV-3 52K ORF was predicted to span nucleotides 9988 to 10983 and encode a protein of 331 amino acids (Reddy et al., 1998) (Genbank accession no. AF030154). However, resequencing of the region of the BAdV-3 genome containing the 52K ORF revealed an error in the published sequence with a missing base at position 10918 compared to the published sequence of 52K. The published sequence $_{10915}$CGTTCG$_{10921}$ should actually read $_{10915}$CGTCG$_{10920}$. Removal of the additional base causes a shift in the 52K ORF (figure 3.4). The new open reading frame ends at $_{11098}$*ATGA*GT$_{11103}$ (underlined bases, numbering based on the uncorrected Genbank sequence), overlaps with the start codon of the open reading frame for IIIa (italicized), and encodes a protein 370 amino acids long. This error in the published sequence explains why Reddy *et al.* (1998) noted that the predicted BAdV-3 52K protein had a large C-terminal deletion compared to the 52K proteins of other adenoviruses.

The revised BAdV-3 52K protein is similar in length to the 52K proteins of other *Mastadenoviruses* (table 3.2). Sequence alignment shows that it also shares a high degree of sequence identity (50% to 60%) with the 52K proteins of other *Mastadenoviruses* (table 3.2).

3.3.2 52K-specific antibodies

To test the antibodies raised against a GST fusion protein expressing a fragment of the N-terminus of 52K (amino acids 29-133), proteins from BAdV-3 infected cell lysate and uninfected MDBK cell lysate were separated by SDS-PAGE, transferred to a nitrocellulose membrane, and probed in Western blot with the anti-52K serum. As shown in figure 3.5, the anti-52K serum recognized a protein with a molecular weight of 40 kDa in the BAdV-3 infected lysate (lane 2).

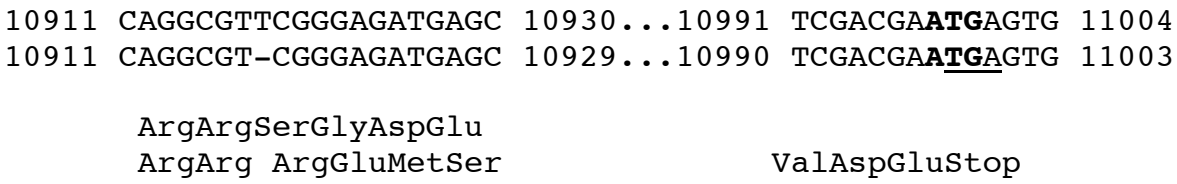

Figure 3.4 Identification of 52K open reading frame. The sequencing error that was found in the published 52K sequence shifts its open reading frame. The GenBank sequence (AF030145) and its predicted protein translation are listed on the top lines; the actual sequences of the DNA and protein translation are listed underneath. The new stop codon for 52K is underlined; start codon for IIIa protein is indicated in bold. Base numbering is based on the GenBank sequence.

Table 3.2 Sequence identity of BAdV-3 52K protein with other 52K proteins.

	Length	% Sequence identity
BAdV-3	370	--
HAdV-2	415	55%
HAdV-5	415	56%
HAdV-12	373	59%
HAdV-11	388	58%
HAdV-17	374	60%
HAdV-4	390	58%
HAdV-40	380	59%
CAdV-1	389	50%
CAdV-2	388	50%
PAdV-3	345	50%
PAdV-5	354	58%
BAdV-1	348	55%

Percent sequence identity indicates identical residues based on sequence alignment with BAdV-3 52K. HAdV, human adenovirus; CAdV, canine adenovirus; PAdV, porcine adenovirus.

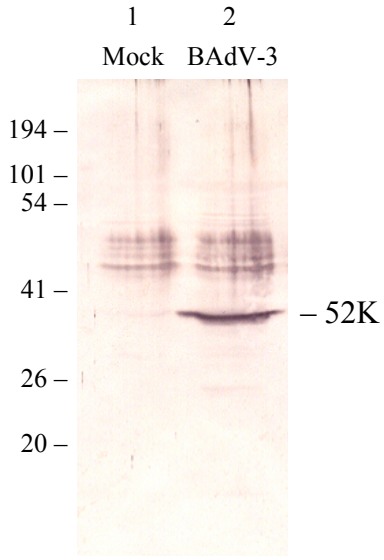

Figure 3.5 Testing 52K antibodies. Mock infected or BAdV-3 infected MDBK cells were harvested 48 hours after infection and lysates were examined by Western Blot using anti-52K serum. The anti-52K serum recognizes a virus-specific protein that corresponds to the predicted size of 52K. Molecular weight standards are indicated in kDa.

No such protein could be detected in uninfected cells (lane 1). The protein could be detected between 24-72 hrs post-infection but not at 12 hrs post-infection (figure 3.6).

3.3.3 Subcellular localization of 52K protein

To determine the localization of the BAdV-3 52K protein, MDBK cells were infected with BAdV-3 and analyzed by indirect imunofluorescence using rabbit anti-52K serum and Cy2 labeled goat anti-rabbit IgG. As seen in figure 3.7, BAdV-3 52K predominantly localized in the nucleus of infected cells. Moreover, dual-label imunofluorescence using Cy2 labeled 52K-specific serum and Cy3 labeled nucleolin-specific serum suggested that 52K does not localize to the nucleolus of infected cells.

Since 52K was shown to localize in the nucleus during BAdV-3 infection, we wished to determine if this localization was dependent on any other viral protein. To this end, we cloned the 52K gene into the eukaryotic expression vector pcDNA and transfected COS7 cells. Like BAdV-3 infected cells, dual immunoflorescence staining suggested that 52K localized in the nucleus, but not in the nucleolus of transfected cells (figure 3.8). The accumulation of 52K in the nucleus in transfected cells indicates that the nuclear localization of 52K is not dependent on any other viral protein.

As the small size of 52K (~40 kDa) could potentially allow it to cross the nuclear pore complex by passive diffusion without the assistance of soluble transport receptors (Lim et al., 2008), we constructed a plasmid expressing 52K fused in frame to the N-terminus of EYFP (pEY.52K). The expected size of this protein (~70 kDa) should prevent diffusion into the nucleus, and therefore any nuclear accumulation should be due to active transport by soluble receptors such as importin α/importin β. As seen in figure 3.9, while EYFP expressed alone is dispersed throughout the cell (panel C), the 52K-EYFP fusion protein localizes in the nucleus of transfected cells (panel F). The results suggest that 52K contains an NLS that mediates its active transport into the nucleus.

3.3.4 Identification of the 52K nuclear localization signal

To identify the location of the 52K NLS, a series of internal deletions covering the entire 52K ORF were generated (figure 3.1). These deletions were cloned into pEYFPN1 to be expressed as 52K-EYFP fusion proteins. These deletions were confirmed by restriction enzyme analysis and

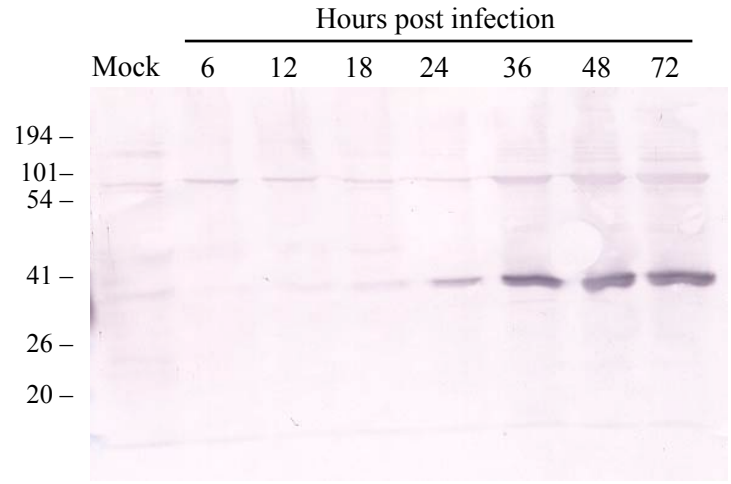

Figure 3.6 Expression of 52K during BAdV-3 infection in bovine cells. MDBK cells were infected with BAdV-3 and harvested at various times post infection. Expression of 52K is detected 24 hours post infection and continues out to 72 hours post infection. Mock-infected MDBK cells were used as a control. Molecular weight standards are indicated in kDa.

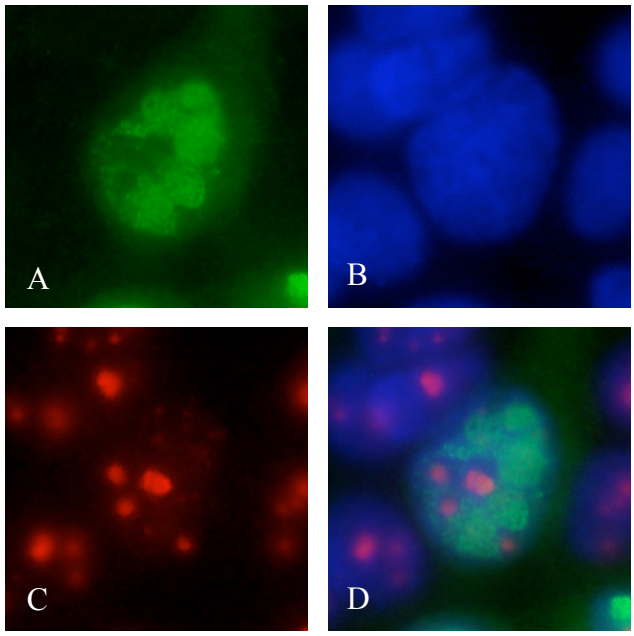

Figure 3.7 Intracellular localization of 52K during BAdV-3 infection. MDBK cells were infected with BAdV-3 and fixed 24 hours post-infection. The intracellular localization of 52K was determined by immunostaining with anti-52K antisera and Cy2-conjugated goat anti-rabbit IgG (panel A) as described in Materials & Methods. Nuclei were stained with DAPI (panel B) and nucleoli were visualized by immunostaining with an anti-nucleolin antibody and Cy3-conjugated goat anti-mouse IgG (panel C). A merge of the images is shown in panel D.

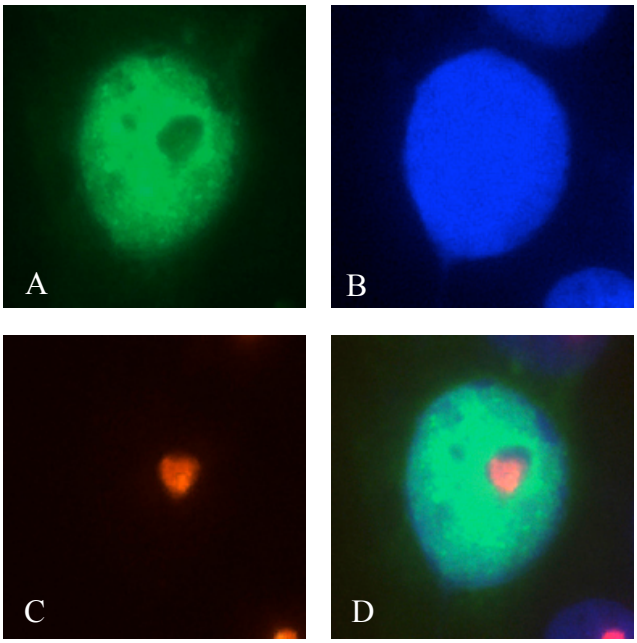

Figure 3.8 Intracellular localization of 52K in transfected cells. COS7 cells were transfected with pcDNA.52K to observe the intracellular distribution of 52K in the absence of other viral proteins. 52K was visualized using 52K antisera and Cy2 conjugated goat anti-rabbit IgG (panel A). Nuclei were stained with DAPI (panel B) and nucleoli were stained with a mouse anti-nucleolin antibody and Cy3 conjugated goat anti-mouse IgG (panel C). A merge of the Cy2, DAPI, and Cy3 images (panel D) shows that 52K is localized in the nucleus but excluded from nucleoli.

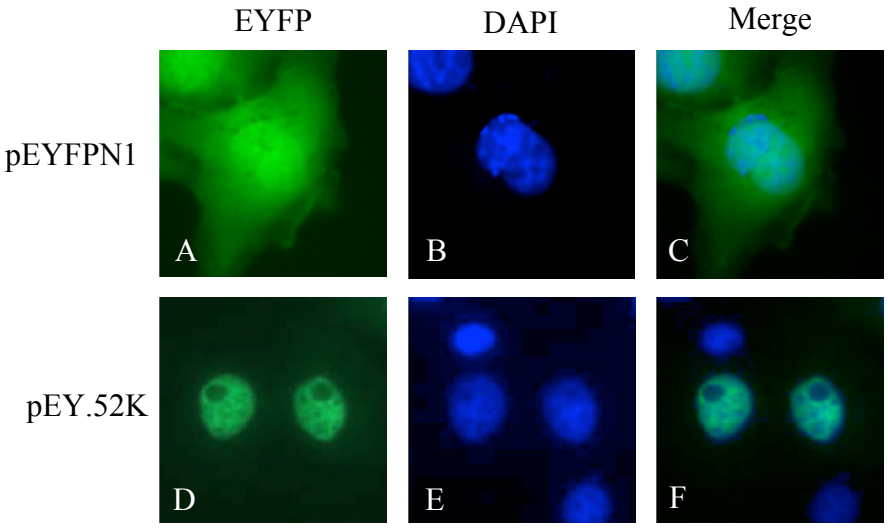

Figure 3.9 Intracellular localization of a 52K-EYFP fusion protein. COS7 cells were transfected with plasmid pEYFPN1 (panels A-C) or pEY.52K (panels D-F). EYFP was visualized directly (panels A, D) and nuclei were stained with DAPI (panels B, E). A merge of the EYFP and DAPI images shows that while EYFP is distributed throughout the cell (panel C), the 52K-EYFP fusion accumulates in the nucleus (panel F).

sequencing of mutant plasmid DNA. COS7 cells were transfected with individual plasmid DNAs. At 24 hrs post transfection, the cells were stained with DAPI and analyzed by fluorescent microscopy. As seen in figure 3.10, all mutant 52K proteins except 52KΔ3 localized predominantly in the nucleus of transfected cells. The punctate staining observed in 52KΔ3 appears to be an artifact of the fixation process since in unfixed cells, 52KΔ3 can be observed diffused throughout the cytoplasm. These results suggested that the 52K NLS is localized between amino acids 90-134.

To further identify the 52K NLS, we constructed mutant 52Ks containing three smaller deletions within amino acids 90-134 that targeted two predicted α-helices and a cluster of three basic amino acids (figure 3.3). Deletion of the predicted α-helices (52KΔ3.1 and 52KΔ3.3) did not alter the intracellular localization (figure 3.11). A nine amino acid deletion that included three basic residues (52KΔ3.2), however, disrupted the nuclear localization (figure 3.11). This suggests that the essential residues for the 52K NLS are contained within the sequence ^{102}GMPRKRVLT^{110}. Since basic residues are often critical to NLS function, we constructed a mutant 52K in which the basic arginine and lysine residues were mutated to glutamic acid (R105E, K106E, R107E; 52KNLSm) (figure 3.3). As seen in figure 3.12, mutation of the amino acids ^{105}RKR^{107} to ^{105}EEE^{107} prevented nuclear accumulation of the 52KNLSm protein. This demonstrates that amino acids 102-110 of 52K acts as an NLS and that the basic residues at positions 105, 106, and 107 are essential for its function.

To determine if amino acids 102-110 are sufficient to direct nuclear import, the sequence ^{102}GMPRKRVLT^{110} was fused in frame to the N-terminus of a green fluorescent protein-beta galactosidase (GFPβGal) fusion protein (Wu et al., 2004) (figure 3.3). The GFPβGal protein does not contain an NLS and is localized in the cytoplasm of transfected cells (figure 3.13). The NLS-GFPβGal fusion protein containing the putative 52K NLS also localizes in the cytoplasm (figure 3.13). These results suggest that while the sequence ^{102}GMPRKRVLT^{110} including ^{105}RKR^{107} residues is essential for nuclear import of 52K, it is not sufficient to direct nuclear import of a cytoplasmic protein.

3.3.5 *In vitro* nuclear import of 52K

To investigate the pathway by which 52K is imported into the nucleus, we used an *in vitro* nuclear import assay (Adam et al., 1990). Cells were seeded onto glass coverslips and treated

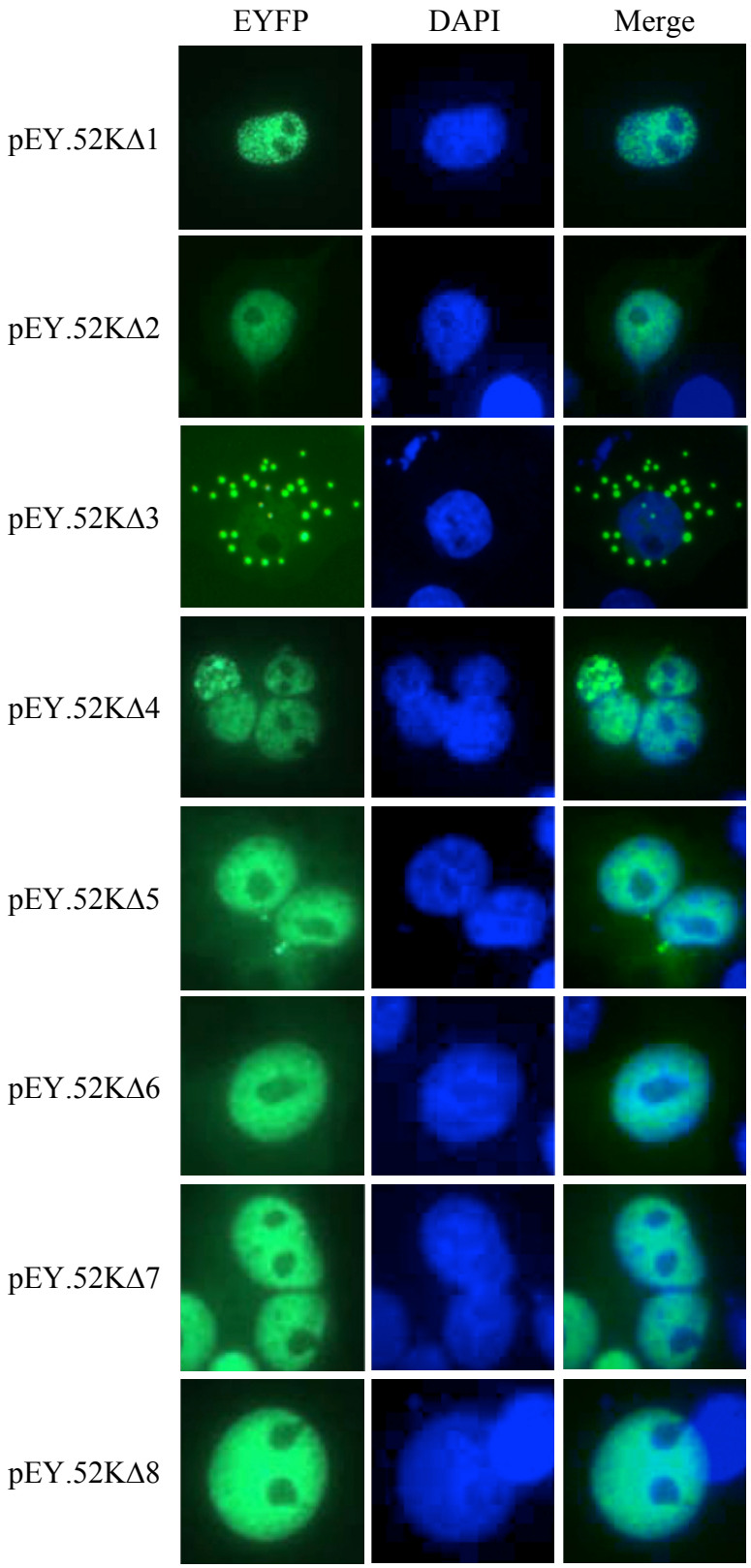

Figure 3.10 Intracellular localization of 52K-EYFP deletion constructs. Plasmids expressing 52K mutants fused to EYFP were transfected into COS7 cells and visualized directly under a fluorescent microscope.

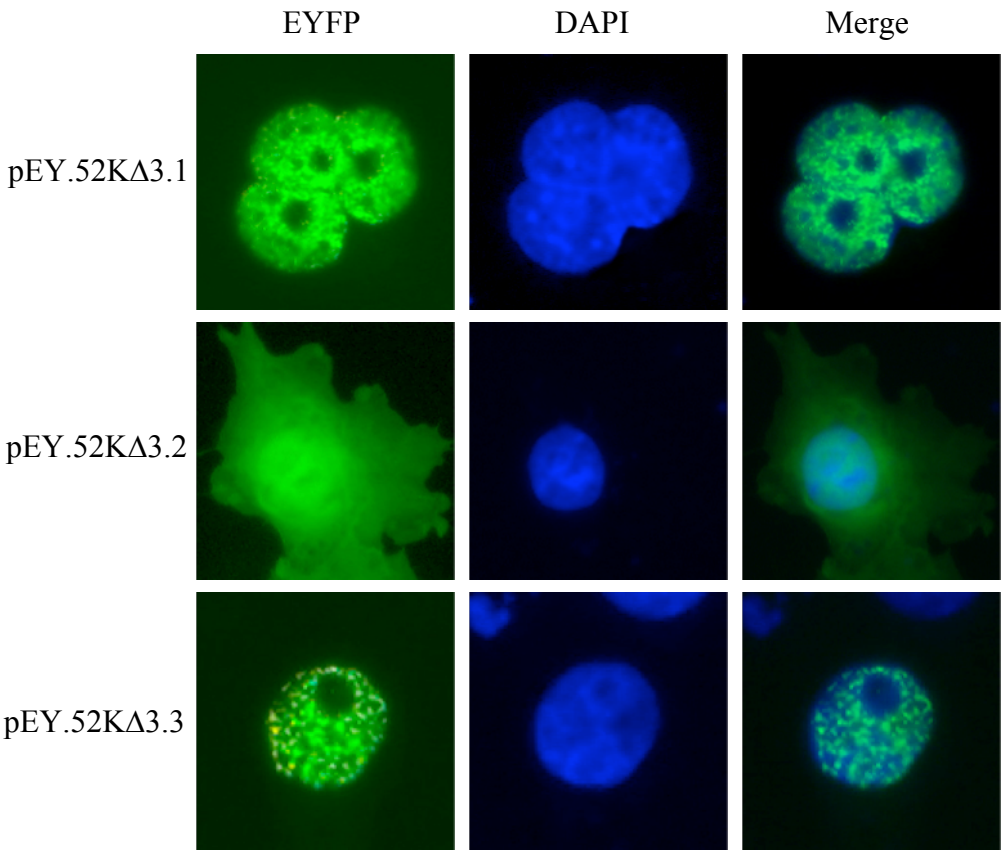

Figure 3.11 Identification of 52K NLS. Plasmids expressing deletion constructs were transfected into COS7 cells and visualized. The 52KΔ3.1 and 52KΔ3.3 proteins, which have deletions in predicted α-helices, were nuclear, while the 52KΔ3.2 construct that lacks a cluster of basic residues was distributed throughout the cell.

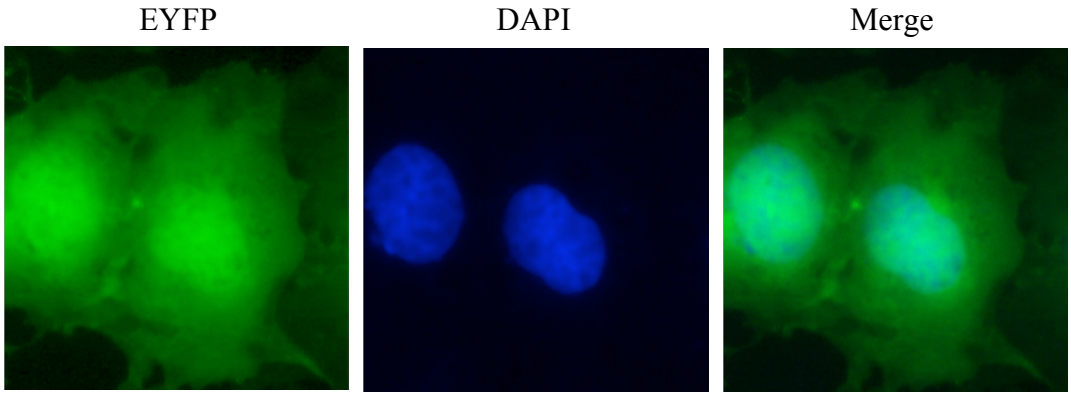

Figure 3.12 Mutation of the putative 52K NLS. COS7 cells were transfected with pEY.52KNLSm and visualized by fluorescent microscopy. The 52KNLSm protein does not accumulate in the nucleus.

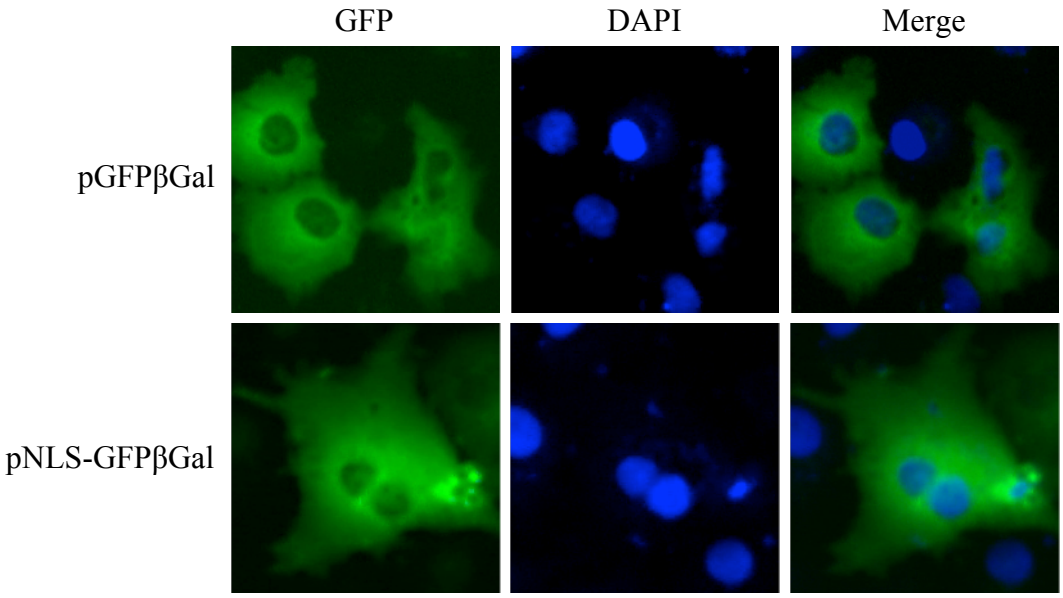

Figure 3.13 Fusion of putative 52K NLS to GFPβGal. Expression of pGFPβGal and pNLS-GFPβGal in transfected COS7 cells. GFPβGal was visualized directly and cells were counterstained with DAPI. The GFPβGal protein alone localizes in the cytoplasm. Fusion of the residues 102-110 of 52K is not sufficient to direct the nuclear import of the NLS-GFPβGal fusion protein.

with digitonin, which permeabilized the cell membrane but left the nuclear envelope intact. Cells were washed to remove soluble cytosolic factors, then incubated with a transport mixture containing the cargo protein of interest, an ATP-regenerating system, and a source of cytosolic factors.

Since the nuclear import of the simian virus 40 (SV40) NLS has been well characterized, the *in vitro* nuclear import assay was established using a GST-NLS-GFP fusion protein (containing GST, the NLS of the SV40 T antigen, and green fluorescent protein) (figure 3.14 A). The nuclear import of GST-NLS-GFP was dependent on cytosolic factors, since omitting the rabbit reticulocyte lysate abolished nuclear import (figure 3.14 B). Moreover, absence of the ATP regenerating system (figure 3.14 C) or carrying out the import reaction at 4˚C (figure 3.14 G) also inhibited nuclear import of GST-NLS-GFP, showing that the import is temperature- and energy-dependent. Addition of wheat germ agglutinin (WGA), which binds to the nuclear pores and blocks protein transport through the NPC, prevented fusion protein GST-NLS-GFP from entering the nucleus (figure 3.14 H). A dominant-negative mutant of Ran that is unable to hydrolyze GTP to GDP (RanQ69L) also blocked nuclear import of GST-NLS-GFP (figure 3.14 I).

Next, we examined the nuclear import of the GST-52K fusion protein. Purified GST-52K accumulates in the nucleus in the *in vitro* assay (figure 3.14 D). Its nuclear import is significantly reduced but not completely inhibited in the absence of cytosolic factors (figure 3.14 E), suggesting that some nuclear accumulation of GST-52K can occur independently of soluble transport receptors. The absence of the ATP regenerating system slightly inhibited nuclear accumulation of GST-52K (figure 3.14 F), although it should be noted that there could be ATP present in the rabbit reticulocyte lysate used as a source of cytosolic factors. Performing the import reaction at 4˚C slightly inhibited nuclear accumulation of GST-52K (figure 3.14 J), whereas nuclear accumulation of GST-NLS-GFP is almost completely inhibited at 4˚C (figure 3.14 G). The addition of wheat germ agglutinin appears to block the nuclear import of GST-52K (figure 3.14 K), indicating that 52K utilizes the nuclear pores to enter the nucleus. The presence of RanQ69L does not appear to have any inhibitory effect on GST-52K nuclear import (figure 3.14 L).

Specific peptide inhibitors known to block nuclear import using the importin-α-importin-β import pathway were used to further characterize the nuclear import pathway of 52K. A 41-amino acid peptide from the N-terminus of importin α that corresponds to its importin β binding

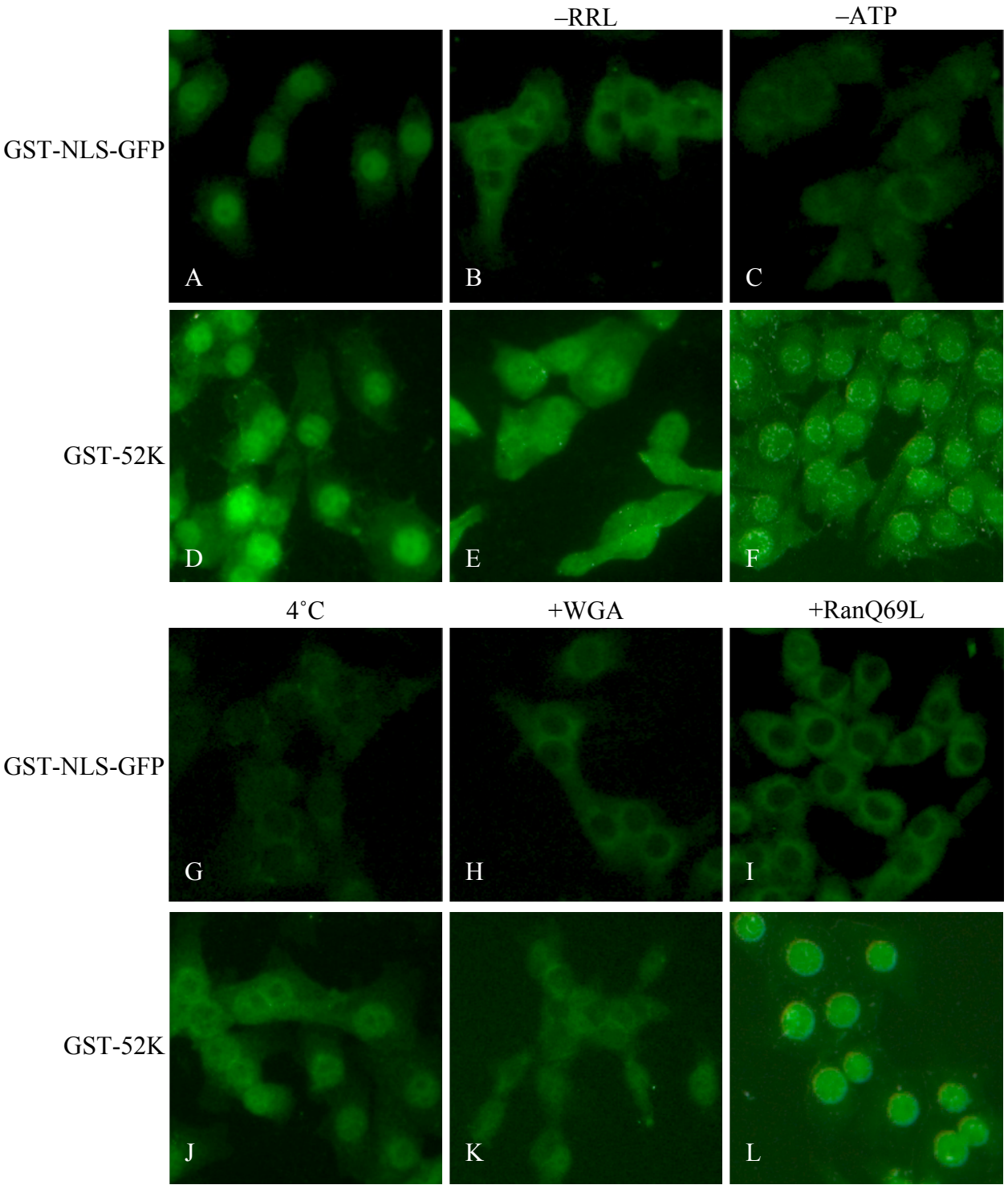

Figure 3.14 *In vitro* nuclear import assays. MDBK cells were permeabilized with digitonin and incubated with complete transport mixture containing GST-NLS-GFP or GST-52K. Import reactions were carried out in the absence of cytoplasmic factors (-RRL), ATP and an ATP-regenerating system (-ATP), at 4˚C, after incubation with wheat germ agglutinin (WGA), or in the presence of the dominant negative mutant RanQ69L.

(IBB) domain (Görlich et al., 1996a) competes for binding to importin β, and thus should inhibit importin α/importin β-mediated nuclear import. Addition of the IBB peptide to the *in vitro* nuclear import reaction significantly inhibited nuclear import of GST-NLS-GFP (figure 3.15 A) and GST-52K (figure 3.15 C). A peptide corresponding to the importin α-binding domain of the yeast cap binding protein 80 (Ycbp80) was used to compete for importin α binding (Görlich et al., 1996b). While the Ycbp80 peptide was able to completely inhibit nuclear import of GST-NLS-GFP (figure 3.15 B), nuclear import of GST-52K was only partially inhibited in the presence of Ycbp80 (figure 3.15 D).

Several proteins have been identified that are able to diffuse passively across the nuclear pore and accumulate in the nucleus by binding to nuclear components (Efthymiadis et al., 1998; Ghildyal et al., 2005; Hearps and Jans, 2006). To determine if 52K is capable of accumulating in the nucleus by binding to nuclear components, a nuclear import assay was performed without soluble factors or an ATP regenerating system in the presence or absence of 0.5% Triton-X-100 to permeabilize the nuclear envelope. Under these conditions, with free diffusion between the nucleus and the cytoplasm, GST-52K should only be able to accumulate in the nucleus if it binds to nuclear components. In the absence of Triton-X-100, no nuclear accumulation of GST-52K was observed (figure 3.16 A). When Triton-X-100 was added to permeabilize the nuclear envelope, GST-52K is able to accumulate in the nucleus (figure 3.16 B). This suggests that GST-52K was able to accumulate in the nucleus independently of soluble transport factors by binding to nuclear components.

3.3.6 Interaction of 52K with transport receptors *in vitro*

Since the nuclear import of 52K appears to be largely dependent on active transport mediated by importin α/importin β, we wished to determine if it was able to bind to transport receptors *in vitro*. GST fusions of importin α1, importin α3, importin α5, importin α7, and importin β were expressed in bacteria and purified for use in a binding assay. The GST-importin fusions were allowed to bind to *in vitro* translated radiolabeled 52K, then precipitated using glutathione sepharose beads, separated by SDS-PAGE, and visualized by autoradiography. GST alone was used as a negative control. As seen in figure 3.17, GST-importin α3 was able to bind radiolabeled 52K (lane 4). No such binding was observed when GST fusions of importin α1, importin α5, importin α7 or importin β were used to pull down radiolabeled 52K (figure 3.17, lanes 3, 5, 6,

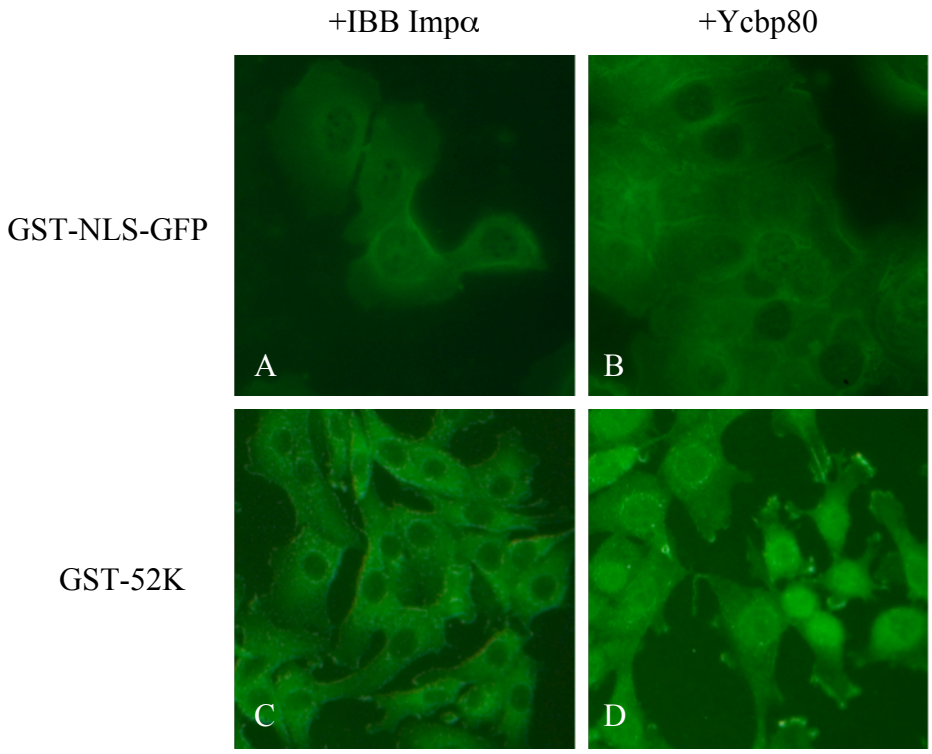

Figure 3.15 Inhibition of nuclear import by specific peptides. Peptides corresponding to the importin β-binding domain of importin α (IBB Impα) or the nuclear localization signal of the yeast cap binding protein 80 (Ycbp80) were added to the nuclear import assay at 50-fold molar excess. The IBB Impα peptide blocks the import of both GST-NLS-GFP (A) and GST-52K (C), while the Ycbp80 NLS completely blocks GST-NLS-GFP (B) but only partially inhibits the nuclear import of GST-52K (D).

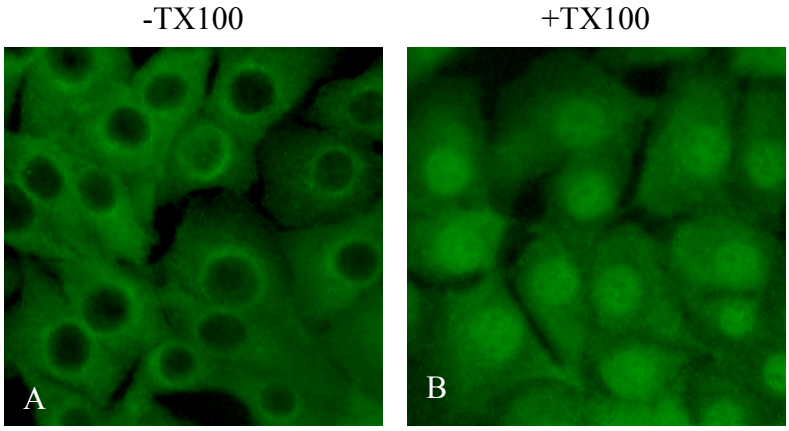

Figure 3.16 Nuclear accumulation of GST-52K in the presence of permeabilizing detergent. A nuclear import assay using GST-52K without soluble cytosolic factors or ATP was carried out in the absence (-TX100; panel A) or presence (+TX100; panel B) of 0.5% Triton-X-100 to permeabilize the nuclear envelope.

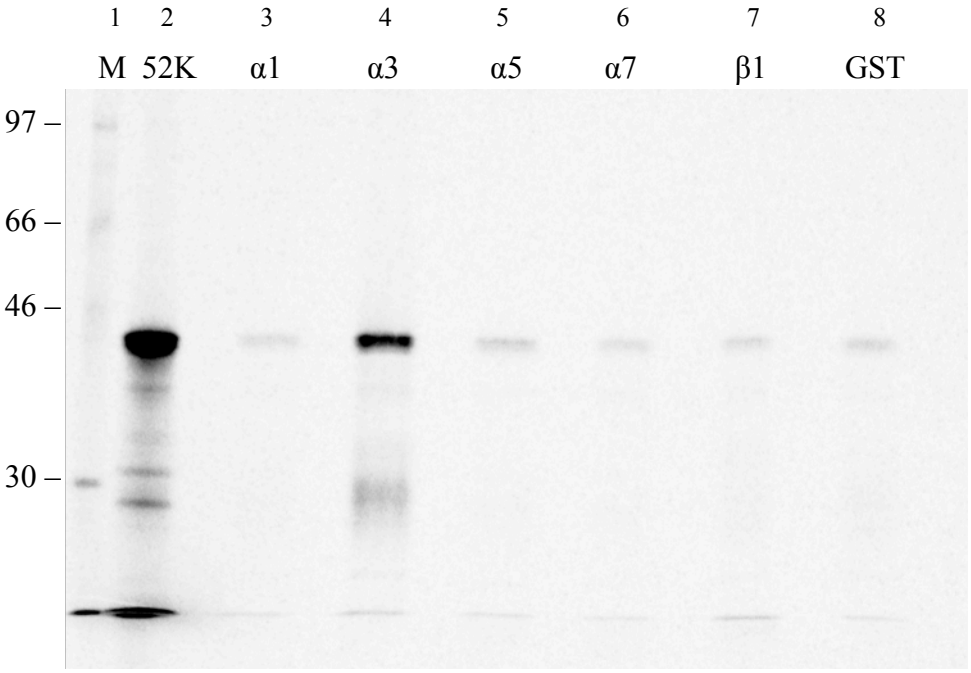

Figure 3.17 *In vitro* interaction of 52K with transport receptors. GST fusions of importin α1, α3, α5, α7, and importin β along with GST alone were incubated with *in vitro* translated, [^{35}S]-labeled 52K and pulled down with glutathione sepharose beads. Samples were separated by 10% SDS-PAGE and visualized using a phosphor screen. 10% of the input [^{35}S]-52K was run as a control (lane 2). Molecular weight standards are indicated in kDa (lane 1).

and 7). This suggests that 52K is imported by the importin α/importin β pathway, with specificity for importin α3.

3.4 Discussion

Members of all adenovirus genera encode a positional homolog of 52K (Davison et al., 2003), suggesting that this protein has an essential function in adenovirus replication. Mutant adenoviruses containing a deletion of the 52K gene form only capsids which are devoid of full length genomic DNA, suggesting 52K is involved in the packaging of the adenovirus genome (Gustin and Imperiale, 1998). However, the exact mechanism regarding the involvement of 52K in this process is not clear. Although the 52K proteins encoded by different adenoviruses including BAdV-3 share 50-60% sequence identity, the 52K protein has been suggested to determine the serotype specificity of adenovirus DNA packaging (Wohl and Hearing, 2008). The experiments presented in this study were designed to characterize the protein and determine the nuclear localization mechanism of 52K of BAdV-3.

An earlier report suggested that mRNA of the BAdV-3 52K protein is predicted to encode a protein of 331 amino acids. However, a sequencing error discovered in the published BAdV-3 sequence (Reddy et al., 1998) revealed that the 52K open reading frame actually encodes a protein of 370 amino acids. A protein of 40 kDa is detected in BAdV-3 infected cells which is consistent with the calculated mass (40.8 kDa) of the 52K protein. The 52K protein is localized predominantly in the nucleus of BAdV-3 infected cells.

While water, ions, and small proteins (less than 40kDa) can diffuse freely between the nucleus and the cytoplasm through NPCs (Lim et al., 2008), the transport of larger molecules is primarily energy-dependent and regulated by the NPCs (Lim et al., 2008). Proteins to be transported into the nucleus may contain classical nuclear localization signals (NLSs), which consists of a single stretch of basic amino acids (e.g SV40 T antigen) or a bipartite NLS consisting of two clusters of basic amino acids (e.g. nucleoplasmin) separated by a linker of ten amino acids (Kalderon et al., 1984; Robbins et al., 1991), or non-classical NLSs that do not fit these consensus sequences (Christophe et al., 2000). It is clear that active transport of proteins to the nucleus requires an NLS. The nuclear localization of 52K in the absence of other viral proteins suggested that the protein contains an NLS(s).

Analysis of mutant BAdV-3 52K proteins suggested that amino acids ^{102}GMPRKRVLT^{110} contain a potential NLS. Interestingly, mutation of three basic residues (^{105}RKR^{107}) to acidic residues (^{105}EEE^{107}) abolished nuclear import, indicating that these residues are essential for nuclear localization of 52K. However, residues ^{102}GMPRKRVLT^{110} were not sufficient to direct nuclear import of a predominantly cytoplasmic fusion protein (GFPβGal). It is possible that residues upstream or downstream of this motif are required for efficient nuclear import of protein. Although deletion of the C-terminal 8 residues containing a cluster of basic amino acids abolishes the nuclear import of DNA helicase Q1 (Seki et al., 1997), upstream sequences are required for it to be bound by importin α3 (Miyamoto et al., 1997). It is also possible that the conformation of the NLS within 52K is important. It has been shown that protein context can modulate NLS specificity. For example, exchanging the NLSs of RCC1 and nucleoplasmin (which bind preferentially to importin α3 and several different importins, respectively) does not confer importin-binding specificity (Friedrich et al., 2006).

An *in vitro* nuclear import assay showed that 52K nuclear import could be reconstituted. The absence of soluble cytoplasmic factors, an ATP regenerating system, and performing the nuclear import reaction at 4˚C inhibited the nuclear accumulation of GST-52K to varying degrees but did not block it completely. This suggests that some nuclear import of 52K can occur independently of soluble factors and energy. Several proteins such as β-catenin (Fagotto et al., 1998) and the Tax protein of human T cell lymphotropic virus type 1 (Tsuji et al., 2007) have been identified that are able to enter the nucleus by binding directly to nucleoporins and do not require soluble factors for nuclear import. Nuclear import of both β-catenin (Yokoya et al., 1999) and Tax (Tsuji et al., 2007) is energy-independent but inhibited when the import reaction is performed on ice. Since 52K, unlike β-catenin and Tax, is partially inhibited in the absence of cytosolic factors or ATP, this suggests that it is unlikely that 52K nuclear import is mediated by binding to nucleoporins.

A dominant negative mutant of Ran was not able to block nuclear import of 52K, suggesting that 52K can be imported into the nucleus in a Ran-independent manner. However, addition of a peptide containing the IBB domain of importin α prevented nuclear accumulation of 52K. If GST-52K is capable of entering the nucleus in a Ran-independent manner, it should also be able to do so independently of importin α/importin β. It is possible that even though the RanQ69L mutant was pre-loaded with GTP that it somehow was insufficient to inhibit Ran-dependent

import of GST-52K. It is also possible that the IBB peptide successfully competed for binding to importin β but that 52K remained bound to importin α, preventing it from entering the nucleus independently of soluble factors as it did under other assay conditions.

Addition of a peptide containing the nuclear localization signal of Ycbp80 was able to partially inhibit nuclear import of GST-52K, suggesting that the peptide was competing with 52K for binding to importin α. The Ycbp80 peptide corresponds to the domain required for binding to the yeast importin α homolog SRP1p, and may act as a nuclear localization signal (Görlich et al., 1996b). Since different nuclear localization signals have varying affinities for transport receptors (Köhler et al., 1999), it is possible that the 52K NLS can bind to importin(s) with a higher affinity than the Ycbp80 peptide. This would explain why the Ycbp80 peptide was able to completely inhibit nuclear import of the GST-NLS-GFP protein but only partially block nuclear import of GST-52K.

Taken together, these results suggest that nuclear import of 52K is largely mediated by a classical importin α/importin β-dependent pathway, in spite of the inability of the RanQ69L mutant to inhibit nuclear import of GST-52K. An *in vitro* binding assay detected an interaction between 52K and importin α3.

Permeabilization of the nuclear envelope with detergent permitted 52K to accumulate in the nucleus. This suggests that 52K is able to enter the nucleus independently of soluble factors or ATP by diffusing through the nuclear pore and binding to nuclear components. The size of 52K is close to the threshold for diffusion across the nuclear pore (Lim et al., 2008). It therefore appears that nuclear import of 52K can be mediated by recognition of its NLS by importin α3 and a classical importin α/importin β import pathway, but that 52K can also accumulate in the nucleus by passive diffusion and binding to nuclear components. This is similar to the nuclear import of the matrix protein of respiratory syncytial virus (Ghildyal et al., 2005) and the integrase protein of HIV-1 (Hearps and Jans, 2006), which both use importin α/importin β import pathways but are capable of accumulating in the nucleus independently of soluble factors.

4.0 INTERACTION OF BAdV-3 52K WITH VIRAL AND CELLULAR PROTEINS

4.1 Introduction

Adenoviruses are non-enveloped viruses containing a double-stranded DNA genome and are found in a wide range of mammalian and non-mammalian species.

Protein-protein interactions are important for efficient replication of adenoviruses. Interactions among adenoviral proteins including structural proteins (hexon, penton, fiber, VI, IIIa, and IX) (Vellinga et al., 2005), viral DNA polymerase and the pre-terminal protein (Temperley and Hay, 1992), E1B-55K and E4orf6 proteins (Blackford and Grand, 2009), L4-22K and IVa2 protein (Ostapchuk et al., 2006), IVa2 and pVIII (Singh et al., 2005), pVII, IVa2 and 52K proteins (Zhang and Arcos, 2005), and 33K with 100K and pV (Kulshreshtha and Tikoo, 2008) have been reported. Similarly, interactions between adenoviral proteins and cellular proteins including E1A and cellular transcription factors (Berk, 2005), E1B-55K and p53 protein (Berk, 2005), E1B-19K protein and BAX/BAK proteins (Berk, 2005), E1B-55K/E4orf6 proteins and host cell factors (Blackford and Grand, 2009), E3-19K glycoprotein and class I MHC molecules (Horwitz, 2004), 100K protein and eIF4G (Cuesta et al., 2000), and 33K protein and bovine presenilin-1-associated protein (PSAP) (Kulshreshtha, 2009) have been reported.

The 52/55-kDa ("52K") protein encoded by the L1 region of human adenovirus (HAdV)-5 has been shown to be essential for encapsidation of the viral DNA (Hasson et al., 1989; Gustin and Imperiale, 1998) and interacts with the viral IVa2 and pVII proteins during HAdV-5 infection (Gustin et al., 1996; Ostapchuk et al., 2005; Zhang and Arcos, 2005). The L1 region of the late transcription unit of bovine adenovirus (BAdV)-3 encodes the 52K protein (Reddy et al., 1998), which is collinear with 52K of HAdV-5. Although 52K proteins encoded by different adenoviruses including BAdV-3 share 50-60% sequence identity, the 52K protein has been suggested to determine the serotype specificity of adenovirus DNA packaging (Wohl and Hearing, 2008). This suggests that the adenovirus 52K protein may interact with specific viral/cellular proteins, thereby contributing to serotype specificity of DNA packaging. Here, we report the interaction of BAdV-3 52K with other viral/cellular proteins.

4.2 Materials and Methods

4.2.1 Cell lines and virus

Madin-Darby bovine kidney (MDBK) cells were propagated in minimal essential medium (MEM; Invitrogen) supplemented with 10% fetal bovine serum (FBS; SeraCare Life Sciences). COS7 cells were propagated in Dulbecco's modified Eagle's medium (DMEM; Invitrogen) supplemented with 10% FBS. Wild type BAdV-3 (WBR-1 strain) was grown in MDBK cells in MEM supplemented with 2% FBS (Reddy et al., 1999a). The virus was purified and titered as described in section 3.2.1.

4.2.2 Plasmids

(a) Yeast expression plasmids. Plasmids expressing BAdV-3 genes in the yeast expression plasmid pGADT7 (Clontech) have been previously described (Kulshreshtha and Tikoo, 2008). A 1.1kb *Eco*RI-*Bam*HI fragment was isolated from plasmid pcDNA.52K (section 3.2.7) and ligated to *Eco*RI-*Bam*HI digested pGBKT7 (Clontech) to create the plasmid pGBK.52K.

(b) Deletions in 52K ORF. Sequential deletions in the 52K ORF were created by PCR as previously described (section 3.2.7).

(i) Construction of pc.52KΔ1. The 984-bp PCR product (section 3.2.7 (c) (i)) was digested with *Eco*RI-*Bam*HI and ligated to *Eco*RI-*Bam*HI digested plasmid pcDNA 3.1(-) (Invitrogen) to create plasmid pc.52KΔ1.

(ii) Construction of pc.52KΔ2. The 974-bp PCR product created by two-step overlap PCR (section 3.2.7 (c) (ii)) was digested with *Eco*RI-*Bam*HI and ligated to *Eco*RI-*Bam*HI digested plasmid pcDNA 3.1(-) (Invitrogen) to create plasmid pc.52KΔ2.

(iii) Construction of pc.52KΔ3. The 989-bp PCR product created by two-step overlap PCR (section 3.2.7 (c) (iii)) was digested with *Eco*RI-*Bam*HI and ligated to *Eco*RI-*Bam*HI digested plasmid pcDNA 3.1(-) (Invitrogen) to create plasmid pc.52KΔ3.

(iv) Construction of pc.52KΔ4. The 962-bp PCR product created by two-step overlap PCR (section 3.2.7 (c) (iv)) was digested with *Eco*RI-*Bam*HI and ligated to *Eco*RI-*Bam*HI digested plasmid pcDNA 3.1(-) (Invitrogen) to create plasmid pc.52KΔ4.

(v) Construction of pc.52KΔ5. The 983-bp PCR product created by two-step overlap PCR (section 3.2.7 (c) (v)) was digested with *Eco*RI-*Bam*HI and ligated to *Eco*RI-*Bam*HI digested plasmid pcDNA 3.1(-) (Invitrogen) to create plasmid pc.52KΔ5.

(vi) Construction of pc.52KΔ6. The 983-bp PCR product created by two-step overlap PCR (section 3.2.7 (c) (vi)) was digested with *Eco*RI-*Bam*HI and ligated to *Eco*RI-*Bam*HI digested plasmid pcDNA 3.1(-) (Invitrogen) to create plasmid pc.52KΔ6.

(vii) Construction of pc.52KΔ7. The 959-bp PCR product created by two-step overlap PCR (section 3.2.7 (c) (vii)) was digested with *Eco*RI-*Bam*HI and ligated to *Eco*RI-*Bam*HI digested plasmid pcDNA 3.1(-) (Invitrogen) to create plasmid pc.52KΔ7.

(viii) Construction of pc.52KΔ8. A 940-bp fragment amplified by PCR using primers CP1 (table 3.1) and Δ8Rs (5'-GGATCCTCACTCCCGACGCCTGCCTATGC-3') and plasmid pcDNA.52K DNA as a template was digested with *Eco*RI-*Bam*HI and ligated to *Eco*RI-*Bam*HI digested plasmid pcDNA 3.1(-) (Invitrogen) to create plasmid pc.52KΔ8.

(c) Plasmids expressing NFBP. Plasmids expressing NFBP fused to a hemagglutinin (HA) epitope tag (pcDNA-NFBP-HA) or fused to enhanced yellow fluorescent protein (EYFP) (pEY.NFBP) were a gift from T. Sweet (Center for Neurovirology, Philadelphia, PA) and have been previously described (Sweet et al., 2005).

4.2.3 Antibodies

The production of anti-52K serum was previously described (section 3.2.4). To raise anti-pVII serum, two peptides corresponding to residues 24-47 and 89-117 (GenBank Accession #AAD09724) were synthesized on a Pioneer Peptide Synthesis system (Perkin Elmer). Immunization of a rabbit with the two peptides was carried out as described in section 3.2.4, using 500 μg of peptide for the initial immunization and 300μg for subsequent boosts.

4.2.4 Yeast two-hybrid system

A GAL4 Matchmaker yeast two-hybrid system (Clontech) was used to detect interactions between BAdV-3 52K and other viral proteins as previously described (Kulshreshtha and Tikoo, 2008). Briefly, plasmid pGBK.52K was co-transformed into yeast strain AH109 with individual pGADT7 plasmids expressing different BAdV-3 proteins. The co-transformed AH109 were

plated on low (Leu^-/Trp^-), medium ($Leu^-/Trp^-/His^-$), and high ($Leu^-/Trp^-/His^-/Ade^-$/X-α-gal) stringency selective dropout media to screen for protein-protein interactions.

4.2.5 GST pulldown assay

The plasmid pGEX-52K (section 3.2.7) expressing a GST-52K fusion protein or pGEX5x2 (GE Healthcare) expressing GST alone were individually transformed into *E. coli* BL21 cells and expression was induced as previously described (section 3.2.8). Cells were harvested by centrifugation (6,000x*g* for 15 min) and resuspended in GST binding buffer [540 mM NaCl, 2.7 mM KCl, 10.15 mM Na_2HPO_4, 1.75 mM KH_2PO_4, 10 mM $MgCl_2$, 1% Triton X-100, 1 µg/mL each aprotinin and leupeptin]. Cells were lysed by sonication (4 x 30 sec) and lysate was cleared by centrifugation (12,000x*g* for 15 min). The supernatant was added to 200 µL washed glutathione-sepharose beads (GE Healthcare) and incubated overnight at 4˚C on a nutator. Beads were washed four times in GST binding buffer and the amount of protein bound to the beads was quantitated. BAdV-3 genes (IVa2, pV, and pVII) cloned in pGADT7 (section 4.2.2) were translated *in vitro* using a TNT T7 Coupled Reticulocyte Lysate System (Promega) in the presence of [^{35}S]-methionine (Perkin Elmer), as per the manufacturer's instructions. *In vitro* translated proteins (10 µL) were individually added to 100 µg of GST-52K or GST bound to glutathione-sepharose beads and incubated overnight in GST binding buffer at 4˚C on a nutator. Beads were washed four times in GST binding buffer and resuspended in 2X SDS sample buffer [100 mM Tris-HCl (pH 6.8), 4% SDS, 0.2% bromophenol blue, 10% glycerol] containing 2% β-mercaptoethanol (βME). Samples were boiled for 5 min, vortexed to release protein from the sepharose beads, and briefly centrifuged. Samples were separated by 10% SDS-PAGE. The gel was fixed in destain solution [10% acetic acid, 40% methanol] containing 5% glycerol, dried onto filter paper, and exposed to a phosphor screen (Kodak). The phosphor screen was visualized on a Bio-Rad Molecular Imager FX using Quantity One software (Bio-Rad).

4.2.6 Western blotting

MDBK cells seeded in 6-well plates were infected with BAdV-3 at a multiplicity of infection (MOI) of 4 pfu/cell. Virus was allowed to adhere to the cells for 2 hrs in serum-free MEM, then FBS was added to a final concentration of 2%. At indicated times post infection, cells were harvested by centrifugation at 3,000 rpm (950 *g*) for 5 minutes and lysed by the addition of RIPA

buffer [0.15 M NaCl, 50 mM Tris-HCl (pH 8.0), 1% NP-40, 1% deoxycholate, 0.1% SDS] containing a protease inhibitor cocktail (Sigma-Aldrich), followed by sonication (4 x 30 sec). Cell lysates were cleared by centrifugation (10,000x*g* for 10 min), separated by 12% SDS-PAGE, and transferred to a polyvinylidene fluoride (PVDF) membrane. The membrane was blocked at 4˚C overnight in 10% skim milk in TBST [Tris-buffered saline (pH 8.0) containing 0.05% tween 20], and then probed with anti-pVII serum diluted 1:200 in TBST containing 1% skim milk for 1 hr at room temperature. After three TBST washes, the membrane were probed with alkaline phosphatase-conjugated goat anti-rabbit IgG (Jackson Immunoresearch) diluted 1:10,000 in TBST containing 1% skim milk for 1 hr at room temperature. Finally, the membrane was washed three times in TBST and developed using a BCIP/NBT chromagenic substrate (Sigma-Aldrich).

4.2.7 Co-immunoprecipitation of 52K and pVII

MDBK cells seeded into 10 cm plates were infected with BAdV-3 at a multiplicity of infection (MOI) of 5 pfu/cell as described in section 4.2.6. At 24 hrs post-infection, cells were incubated in 1 mL of E1A lysis buffer [50 mM HEPES (pH 7.0), 250 mM NaCl, 0.1% Nonidet P-40, 50 mM sodium fluoride, 1 µg/mL each aprotinin and leupeptin] for 30 min on ice. Lysates were transferred to a microcentrifuge tube and cleared by centrifugation at 10,000x*g* for 5 min. An aliquot of each lysate was used as an unimmunoprecipitated control. Samples were incubated with 30 µL of antibody (anti-52K serum, anti-pVII serum, or pre-immune serum as a control) for 1 hr on ice. Protein A sepharose beads rehydrated in E1A lysis buffer (0.1 g/mL) were added (50 µL/sample) and incubated for 4-6 hrs at 4˚C on a nutator. Beads were washed four times in E1A lysis buffer, then resuspended in 2X SDS sample buffer containing 2% βME and boiled for 5 min. Samples were separated by 10% SDS-PAGE and transferred to a PVDF membrane. The membrane was blocked overnight in 10% skim milk in TBST, then probed with anti-52K or anti-pVII serum diluted 1:200 in TBST with 1% skim milk for 1 hr. Membranes were washed three times for 1 hr each in TBST before probing with horseradish peroxidase conjugated goat anti-rabbit IgG light chain specific serum (Jackson Immunoresearch) diluted 1:10,000 in TBST with 1% skim milk for 1 hr at room temperature. Membranes were washed again in TBST (3 x 1 hr each) and developed with an ECL Advance kit (GE Healthcare) as per the manufacturer's instructions. Membranes were exposed to x-ray film for 5 minutes and developed.

4.2.8 Mass spectrometry analysis of proteins co-precipitating with 52K

MDBK cells were infected with BAdV-3 at a MOI of 5 pfu/cell as described in section 4.2.6. At 48 hrs post-infection, the cells were harvested by centrifugation at 3,000 rpm (1,950x*g*) for 10 min, washed in phosphate-buffered saline (PBS) and resuspended in 4 mL of radioimmunoprecipitation buffer (RIPA) [50 mM Tris-Cl (pH 8.0), 150 mM NaCl, 0.1% sodium dodecyl sulfate (SDS), 1% nonidet P 40, 1% deoxycholic acid] containing 1 µg/mL each aprotinin, leupeptin, and pepstatin A. The resuspended cells were sonicated (4 x 30 seconds) and lysate was cleared by centrifugation at 10,000x*g* for 5 minutes. Anti-52K serum (30 µL) was added to 200 µL of cell lysate supernatant and 200 µL RIPA, and incubated for 6-8 hours at 4˚C on a nutator. Protein A sepharose beads were rehydrated in RIPA (0.1g/mL), washed, and 100µL was added to each binding reaction and incubated overnight at 4˚C on a nutator. Finally, the beads were washed four times with RIPA and mixed with an equal volume of 2X SDS sample buffer. Samples were boiled for 5 min and separated by 10% SDS-PAGE. Gels were stained with Coomassie blue for 15 min and washed in several changes of destain solution for 4-6 hrs. Sections of the gel were excised and sent for mass spectrometry identification of proteins.

Mass spectrometry analysis of the gel fragments was performed at the National Research Council Plant Biotechnology Institute (Saskatoon, SK). Protein identification was performed using a workflow similar to that described by Sheoran *et al.* (2005). In brief, excised bands from the SDS-PAGE separation were subjected to an automated process of de-staining, reduction, and alkylation, followed by tryptic digestion, using a MassPrep II Proteomics Workstation (Micromass, UK). The resulting tryptic peptides were detected using on-line chromatography coupled to a Q-ToF Ultima Global mass spectrometer (Micromass, UK). The mass spectrometry data was processed and searched against the NCBInr database, hosted by NRC (Ottawa), using MASCOT Daemon (Matrix Science Ltd., London, UK) identifying proteins present in the gel band.

4.2.9 Co-immunoprecipitation of *in vitro* translated proteins

Proteins were translated using a TNT T7 Coupled Reticulocyte Lysate System (Promega). Plasmid pcDNA-NFBP-HA DNA (1 µg) was *in vitro* transcribed and translated in the absence of [^{35}S]-methionine. Similarly, individual plasmid (pcDNA.52K, pc52KΔ1 to pc52KΔ8) DNA (1 µg) was *in vitro* transcribed and translated in the presence of [^{35}S]-methionine (Perkin-Elmer).

For each *in vitro* binding reaction, 45 µL of unlabeled NFBP-HA was mixed with 45 µL radiolabeled wild-type or mutant 52K protein in GST binding buffer and incubated at 4˚C for 4 hrs on a nutator. The proteins were incubated with 10 µL of a mouse monoclonal anti-HA antibody (Sigma-Aldrich) or a mouse anti-c-myc antibody (Sigma-Aldrich) overnight at 4˚C on a nutator. GammaBind G Sepharose beads (GE Healthcare) were washed and added to binding reactions (50 µL per reaction) for 4 hrs at 4˚C on a nutator. Finally, the beads were washed three times in GST binding buffer and mixed with an equal volume of 2X SDS sample buffer containing 2% βME. Samples were boiled for 5 min and separated by 10% SDS-PAGE. Gels were fixed in destain solution containing 5% glycerol for 30 min and dried onto filter paper, then exposed to a phosphor screen (Kodak). The phosphor screen was visualized on a Bio-Rad Molecular Imager FX using Quantity One software (Bio-Rad).

4.2.10 Immunofluorescence microscopy

COS7 cells were seeded onto 4-well glass slides and transfected with 1 µg of indicated plasmid DNA using lipofectin (Invitrogen) in Opti-MEM (Invitrogen) per the manufacturer's instructions. After 24 hrs, cells were fixed in 3.7% paraformaldehyde for 15 minutes at room temperature, washed three times in PBS, and permeabilized with 0.2% Triton X-100 for 5 minutes. After three washes with PBS, the cells were blocked in 2% goat serum for 30 mins. The cells were incubated with rabbit anti-52K serum diluted 1:50 and/or a mouse anti-nucleolin monoclonal antibody (Stressgen) diluted to 1 µg/mL for 1 hr at room temperature. After three PBS washes, the cells were incubated with Cy2-conjugated goat anti-rabbit IgG (Jackson Immunoresearch) and/or Cy3-conjugated goat anti-mouse IgG diluted 1:800 for 1 hr at room temperature. After three PBS washes, cells were counterstained with 2 µg/mL DAPI for 5 min, mounted in Citifluor mounting reagent, and visualized on an Axiovert UV microscope using Zeiss AxioVision software.

4.3 Results

4.3.1 Yeast two-hybrid analysis of BAdV-3 proteins interacting with 52K

To identify BAdV-3 proteins that interact with BAdV-3 52K, a yeast two-hybrid system was used as previously described (Kulshreshtha and Tikoo, 2008). Briefly, viral proteins were

expressed in a pGADT7 vector fused to the activation domain of the yeast GAL4 protein. The BAdV-3 52K protein was expressed in a pGBKT7 vector fused to the DNA-binding domain of the GAL4 protein. Interactions between 52K and any of the other viral proteins brings the GAL4 activation domain in proximity to the GAL4 DNA binding domain and allows activation of yeast reporter genes that are used as selection markers. Yeast co-transformed with pGBK.52K and individual pGADT7 plasmids expressing BAdV-3 proteins were grown on low-, medium-, and high-stringency selective media to screen for interactions. As a control, pGBK.52K was also co-transformed with pGADT7 but did not permit growth on selective media (data not shown), indicating that pGBK.52K alone cannot activate expression of the reporter genes.

The results of the yeast two-hybrid screen are shown in figure 4.1. Yeast co-transformed with pGBK.52K and pGADT7-IVa2 were able to grow on medium-stringency media (figure 4.1, panel A) but not on high-stringency media (data not shown), suggesting that there could be a weak or transient interaction between 52K and IVa2. 52K has been shown to interact with IVa2 in HAdV-5 (Gustin et al., 1996). However, co-transformation of yeast with pGBKT7 and pGADT7-IVa2 also permits growth on medium-stringency media (figure 4.1, panel C), so this could also be a false positive. Similarly, co-transformation of yeast with pGBK.52K and pGADT7-pVI permitted growth on medium-stringency media (figure 4.1, panel A) but not high-stringency media (data not shown). However, co-transformation of pGADT7-pVI and pGBKT7 also permitted growth on medium-stringency media (figure 4.1, panel C), suggesting that this is a false positive and not indicative of an interaction between 52K and pVI.

Yeast co-transformed with pGBK.52K and pGADT7-V grew on medium-stringency (figure 4.1, panel A) and high-stringency media (figure 4.1, panel B), but did not hydrolyze X-α-gal. This suggests that while these co-transformed yeast were able to activate the two reporter genes required for survival on the high-stringency dropout media, the *MEL1* reporter gene was not activated despite being under the control of the same GAL4 promoter. Co-transformation of yeast with pGBKT7 and pGADT7-V did not permit growth on selective media (data not shown), indicating that pV alone is not activating the reporter genes.

Co-transformation with pGBK.52K and pGADT7-pVII permitted growth on medium-stringency (figure 4.1, panel A) and high-stringency media (figure 4.1, panel B). Yeast co-transformed with pGBKT7 and pGADT7-pVII were not able to grow on selective media (data

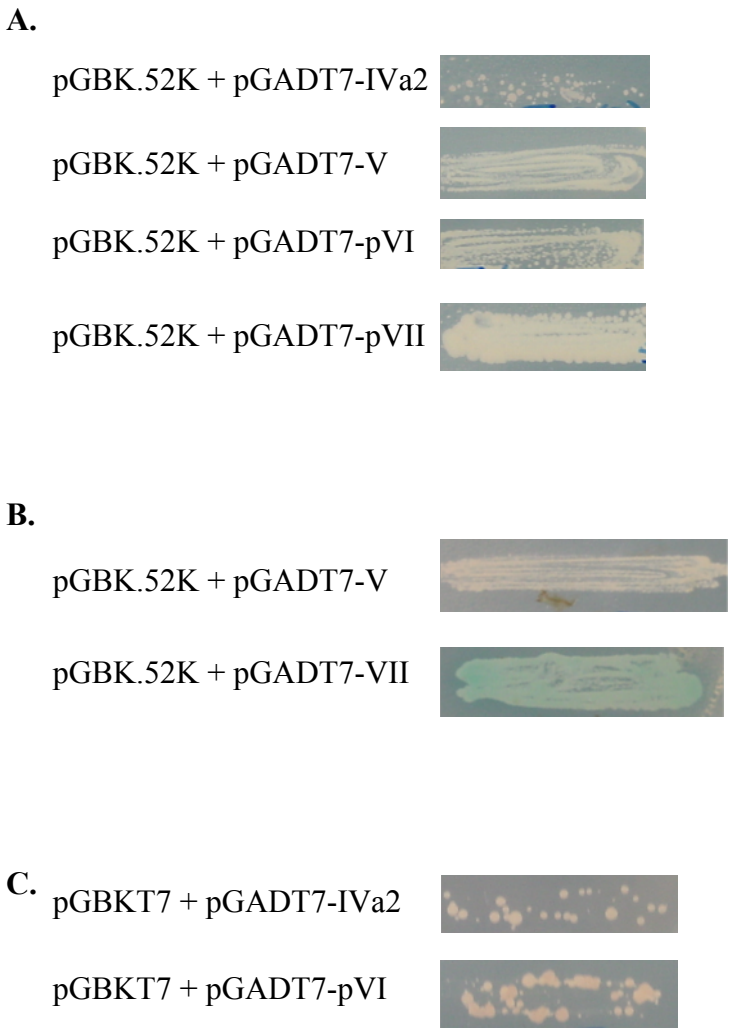

Figure 4.1 Yeast two-hybrid analysis of BAdV-3 proteins interacting with 52K. Yeast were co-transformed with indicated plasmids and plated on selective media. **A.** Growth on medium-stringency selective media ($Leu^-/Trp^-/His^-$). Interactions between 52K and IVa2, pV, pVI, and pVII were detected. **B.** Growth on high-stringency selective media ($Leu^-/Trp^-/His^-/Ade^-$/X-α-gal). Interactions between 52K and pV and pVII were detected. **C.** Co-transformation of pGBKT7 with pGADT7-IVa2 or pGADT7-pVI permits growth on medium-stringency media.

not shown), indicating that there is a specific interaction between 52K and pVII. An interaction between 52K and pVII has previously been demonstrated in HAdV-5 (Zhang and Arcos, 2005).

4.3.2 52K interacts with pVII

To confirm the interactions between 52K and IVa2, pV, and pVII detected by the yeast two-hybrid system, a GST pulldown assay was performed. A GST-52K fusion protein was expressed in bacteria and purified, then allowed to bind to *in vitro* translated, [^{35}S]-labeled IVa2, pV, or pVII. As shown in figure 4.2 (panel A), pVII is pulled down by the GST-52K fusion protein (lane 2) but not by GST alone (lane 3). However, GST-52K did not interact with pV or IVa2 (data not shown). This shows that pVII interacts specifically with 52K. Since this interaction occurs in an *in vitro* binding assay, it is a direct interaction that does not require other viral or cellular factors.

Next, we confirmed the interaction of 52K with pVII during BAdV-3 infection. Initially, we examined pVII expression during BAdV-3 infection. As shown in figure 4.2 (panel B), anti-pVII serum recognizes two proteins of 22 kDa and 20 kDa, slightly larger than the predicted molecular weights of uncleaved pVII (19 kDa) and cleaved VII (16.6 kDa). No such proteins are detected in lysate from uninfected cells (figure 4.2 panel B). The proteins could be detected after 24-48 hrs post-infection but were not detected at 12 hrs post infection. Next, we determined if 52K and pVII interact in BAdV-3 infected cells. Proteins from lysates of BAdV-3 infected cells were immunoprecipitated with anti-pVII serum. The co-immunoprecipitated proteins were separated by 10% SDS-PAGE, transferred to PVDF membranes, and probed in Western blot using anti-52K serum. As seen in figure 4.2 (panel C), the 52K protein could be detected in BAdV-3 infected cell lysates immunoprecipitated with anti-pVII serum and probed in Western blot with anti-52K serum (lane 2). As expected, 52K protein could be detected in BAdV-3 infected cell lysates that were left untreated (lane 4) or immunoprecipitated with anti-52K serum (lane 3) and probed in Western blot with anti-52K serum. No such protein could be detected in BAdV-3 infected cell lysates immunoprecipitated with pre-immune serum and probed in Western blot with anti-52K serum (lane 1). However, as shown in figure 4.2 (panel D), pVII protein could not be detected in BAdV-3 infected cell lysates immunoprecipitated with anti-52K serum and probed in Western blot with anti-pVII serum (lane 2). As expected, pVII (cleaved and uncleaved) could be detected in BAdV-3 infected cell lysates that were unimmunoprecipitated and probed in Western blot with anti-pVII serum (lane 4), while uncleaved pVII protein could be detected in

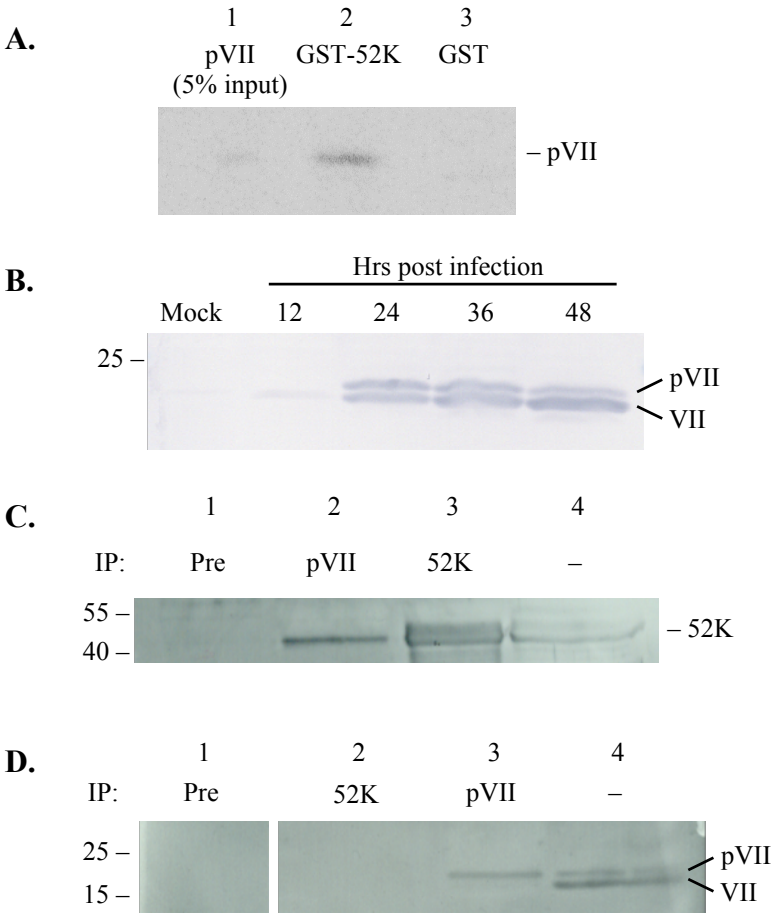

Figure 4.2 Interaction of 52K with pVII. **A.** GST pulldown assay. *In vitro* translated pVII (lane 1) is pulled down by GST-52K (lane 2) but not GST (lane 3). **B.** Expression of pVII during BAdV-3 infection. Cell lysates were separated by SDS-PAGE and probed in Western blot with anti-pVII serum. Molecular weight standards are indicated in kDa. **C.** Co-immunoprecipitation of 52K and pVII from BAdV-3 infected MDBK cells. Lysate from BAdV-3 infected cells was immunoprecipitated with pre-immune serum (Pre, lane 1), anti-pVII serum (lane 2), or anti-52K serum (lane 3). Untreated lysate was run as a positive control (lane 4). Proteins were separated by SDS-PAGE and probed with anti-52K serum by Western blot. Molecular weight standards are indicated in kDa. **D.** Infected cell lysates immunoprecipitated with pre-immune serum (Pre, lane 1), anti-52K serum (lane 2) or anti-pVII serum were separated by SDS-PAGE along with unimmunoprecipitated lysate (lane 4) and probed with anti-pVII serum by Western blot. Molecular weight standards are indicated in kDa.

BAdV-3 infected cell lysates that were immunoprecipitated with anti-pVII serum and probed in Western blot with anti-pVII serum (lane 3). No such protein could be detected in BAdV-3 infected cell lysates immunoprecipitated with prebleed serum and probed in Western blot with anti-pVII serum (lane 1).

4.3.3 Mass spectrometry identification of cellular proteins interacting with BAdV-3 52K

To identify cellular proteins that may interact with 52K during BAdV-3 infection, proteins from lysates of BAdV-3 infected MDBK cells were immunoprecipitated with anti-52K serum. Immunoprecipitated samples were separated by SDS-PAGE, and fragments of the gel were sent for mass spectrometry analysis. Three peaks were identified by a Mascot database search. A rabbit transferrin precursor and a rabbit serum albumin precursor were identified, but neither of these hits were statistically significant according to the Mascot search. Peptides corresponding to an S1 RNA-binding domain-containing protein from *Arabidopsis thaliana* (GenBank accession number 15229915) and the pre-rRNA processing protein Rrp5p of *Arabidopsis thaliana* (GenBank accession number 10998136) were identified and found to be statistically significant by the Mascot search ($p=0.00079$ and $p=0.04$, respectively).

The identified proteins from *Arabidopsis* have known homologs in yeast and humans. The yeast homolog, Rrp5p, is known to be involved in ribosomal RNA processing (Venema and Tollervey, 1996). A mammalian protein with significant homology to Rrp5p has been identified (Venema and Tollervey, 1996), and given a number of different names by different groups, including apoptosis-linked gene 4 (ALG-4), programmed cell death protein 11 (PDCD11), and NFκB-binding protein (NFBP) (Lacana and D'Adamio, 1999; Sweet et al., 2003). Like yeast Rrp5p, human NFBP contains S1 RNA-binding domains and the C-terminus also contains a histone acetyl transferase repeat (Sweet et al., 2003). A bovine homolog of NFBP also exists (NCBI reference sequence NP_001095573.1). The bovine NFBP has high sequence identity with the human NFBP (NCBI reference sequence NP_005791.1), with 84% sequence identity and only 3 amino acids difference in length (1871 and 1874 for human and bovine NFBP, respectively).

4.3.4 *In vitro* interaction of 52K and NFκB-binding protein (NFBP)

To confirm the mass spectrometry results, we determined if 52K and NFBP could interact directly in an *in vitro* binding assay. Plasmid pcDNA-NFBP-HA (expressing human NFBP fused to an HA epitope tag) or plasmid pcDNA.52K were transcribed and translated *in vitro* in the absence or presence of [^{35}S]-methionine, respectively. After incubating the *in vitro* translated labeled (52K) and unlabeled (NFBP-HA) proteins for 4 hrs at 4˚C, the unlabeled NFBP-HA protein was immunoprecipitated using an anti-HA antibody. The immunoprecipitated proteins were separated by SDS-PAGE and radiolabeled protein was visualized by exposure to a phosphor screen using a phosphorimager. The anti-HA serum immunoprecipitated a faint band corresponding to the 52K protein (figure 4.3), indicating that 52K is bound to NFBP-HA. An anti-c-myc serum did not immunoprecipitate the 52K protein, showing that the 52K band was specific to NFBP-HA. These results confirm the mass spectrometry identification of NFBP as a cellular protein that interacts with 52K, and the *in vitro* binding shows that this interaction is direct and not mediated by another cellular or viral protein or other co-factors such as RNA.

4.3.5 Identification of NFBP-binding region of 52K

To identify the region of 52K involved in binding to NFBP, a series of mutant 52K proteins were expressed. Initially, individual deletions in the 52K ORF were cloned into plasmid pcDNA and the expression of mutant proteins was examined by SDS-PAGE analysis of mutant proteins *in vitro* transcribed and translated in the presence of [^{35}S]-methionine. As seen in figure 4.4 (panel A), *in vitro* translation produced mutant 52K proteins of expected sizes. Finally, NFBP-HA was translated *in vitro* and incubated with *in vitro* translated, [^{35}S]-labeled individual mutant 52K proteins. The ability of NFBP-HA to interact with each mutant 52K protein was determined by separating the HA-immunoprecipitated samples by SDS-PAGE and exposing the gel to a phosphor screen to detect the radiolabeled 52K proteins. As seen in figure 4.4 (panel B), all mutants except deletions Δ1, Δ2, and Δ3 (amino acids 2 to 134) showed significant binding of NFBP-HA with 52K. However, deletions Δ1, Δ2, and Δ3 showed significantly reduced binding of 52K to NFBP-HA (figure 4.4, panel B). This could not be due to differences in the expression level of *in vitro* translated mutant 52K proteins, as all *in vitro* translated mutant proteins showed similar levels of expression (figure 4.4, panel A). These results suggest that the N-terminal 134 amino acids of 52K contain domain(s) involved in the interaction of 52K with NFBP.

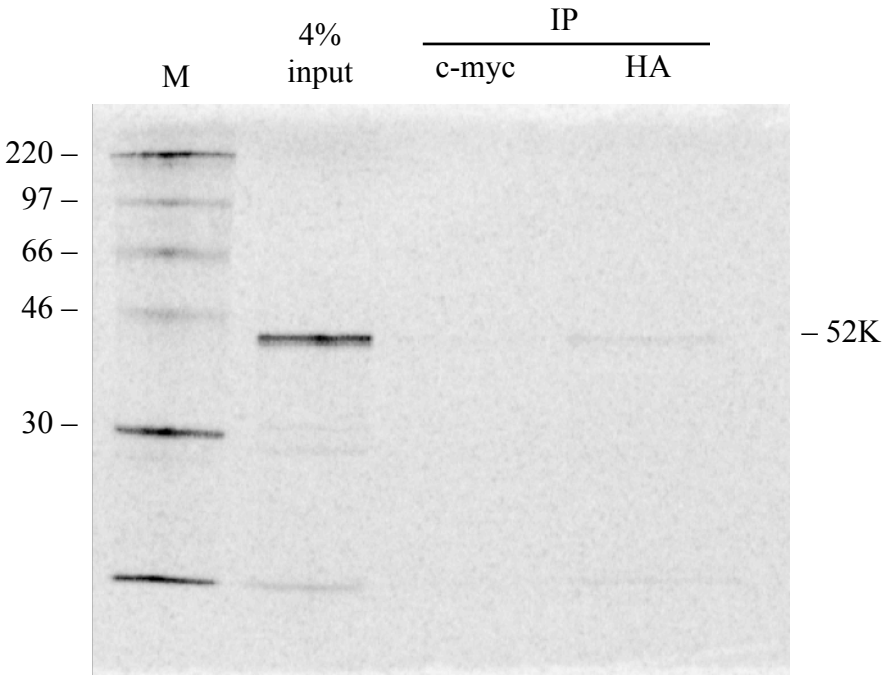

Figure 4.3 *In vitro* interaction of NFBP with 52K. *In vitro* translated NFBP-HA was mixed with *in vitro* translated, [^{35}S]-methionine-labeled 52K, and immunoprecipitated with an anti-HA antibody. Immunoprecipitation with an anti-c-myc antibody was used as a negative control. Molecular weight standards are indicated in kDa.

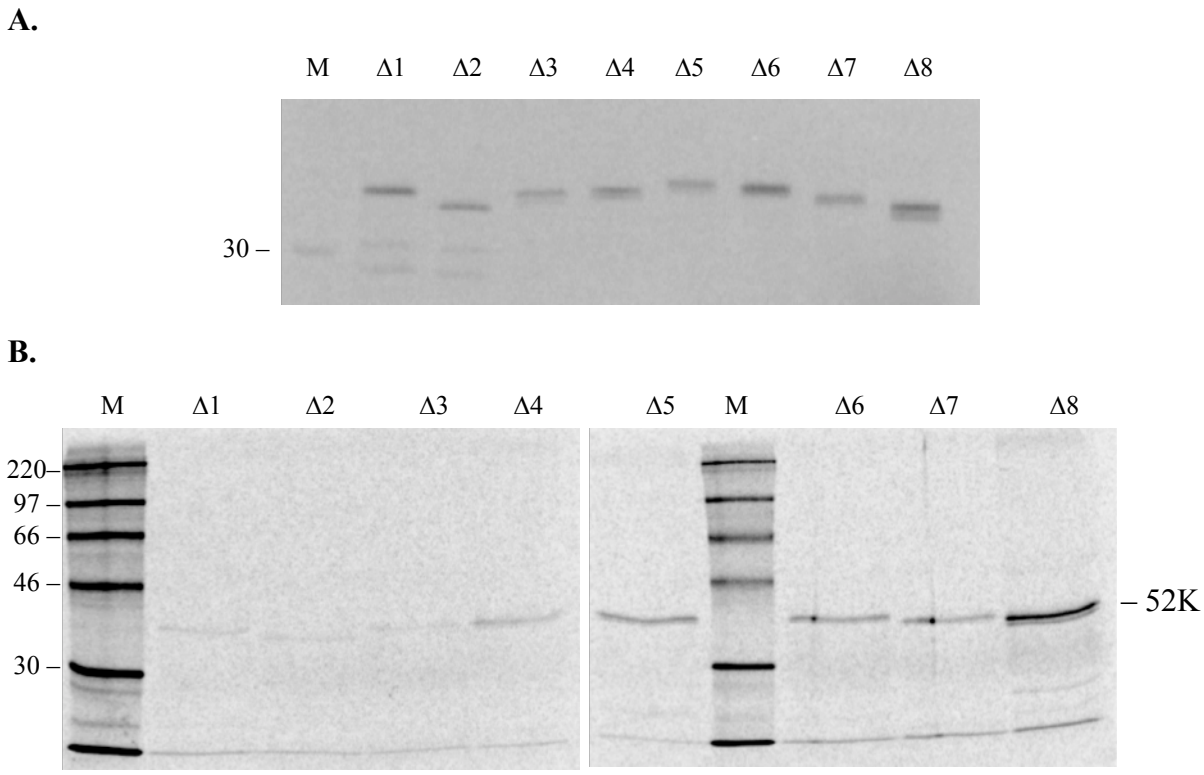

Figure 4.4 The N-terminus of 52K is involved in binding NFBP. **A.** 52K mutants were translated *in vitro* in the presence of [^{35}S]-methionine. Equal volumes of the translation mixture were separated by SDS-PAGE and visualized to determine the level of protein expression. **B.** Immunoprecipitation of 52K mutants by NFBP-HA. *In vitro* translated radiolabeled 52K mutants were mixed with *in vitro* translated unlabeled NFBP-HA, then immunoprecipitated with an anti-HA antibody. Samples were separated by SDS-PAGE and exposed to a phosphor screen to visualize the immunoprecipitated radiolabeled 52K constructs. Molecular weight standards (M) are indicated in kDa.

4.3.6 Co-localization of 52K and NFBP

Since 52K and NFBP were shown to interact *in vitro*, we determined if they co-localize in transfected cells. NFBP has been shown to localize in distinct regions of the nucleus presumed to be the nucleolus (Sweet et al., 2005), while 52K localizes in the nucleus but appears to be excluded from the nucleolus (section 3.3.3).

First, to determine if NFBP does localize to nucleoli, COS7 cells were transfected with the plasmid pEY.NFBP that expresses NFBP fused to enhanced yellow-green fluorescent protein (EYFP). Cells were fixed in paraformaldehyde, permeabilized, and stained with a mouse antibody against nucleolin, a cellular protein known to localize in the nucleolus. As previously reported (Sweet et al., 2005), NFBP localized in distinct centers of the nucleus, and co-localizes with nucleolin (figure 4.5). This confirms that NFBP does localize to the nucleolus.

To examine if 52K and NFBP co-localize, cells were co-transfected with pcDNA.52K and pEY.NFBP, then fixed in paraformaldehyde, permeabilized, and stained with anti-52K serum. In the cells expressing both 52K and NFBP, NFBP appeared diffused throughout the nucleus (figure 4.6, filled arrow). In cells expressing only NFBP, it accumulated in the nucleoli (figure 4.6, empty arrows). This re-distribution of NFBP in the presence of 52K was seen in the majority of co-transfected cells and suggests that 52K relocalizes some of the NFBP to other parts of the nucleus.

4.4 Discussion

Protein-DNA and protein-protein interactions are important for capsid assembly and DNA packaging, leading to the production of progeny adenovirus. A number of proteins, including IVa2 (Zhang and Imperiale, 2000; Zhang et al., 2001; Zhang and Imperiale, 2003; Perez-Romero et al., 2005; Tyler et al., 2007), IIIa (D'Halluin et al., 1978b), pVII (Zhang and Arcos, 2005), 22K (Ostapchuk et al., 2006), and 52K (Hasson et al., 1989; Gustin and Imperiale, 1998), are potentially involved in the packaging of adenovirus DNA. Of these, 52K has been suggested to be involved in serotype specific adenoviral DNA packaging (Wohl and Hearing, 2008). Although interaction of 52K with other DNA packaging proteins including IVa2 (Gustin et al., 1996) and pVII (Zhang and Arcos, 2005) has been reported, the importance of these interactions in DNA packaging is not clear yet. Since 52K is detected in empty capsids, assembly intermediates, and

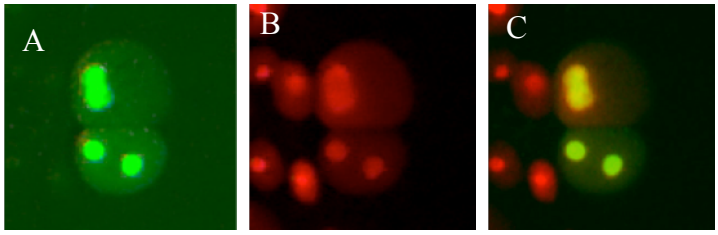

Figure 4.5 NFBP localizes in the nucleolus of transfected cells. A plasmid expressing an EYFP-NFBP fusion protein was transfected into COS7 cells, which were then fixed and stained with a mouse anti-nucleolin antibody followed by a Cy3 conjugated goat anti-mouse IgG antibody to visualize the nucleoli. **A.** Intracellular localization of EYFP-NFBP. **B.** Nucleolin stain to identify nucleoli. **C.** Merge of EYFP and nucleolin staining.

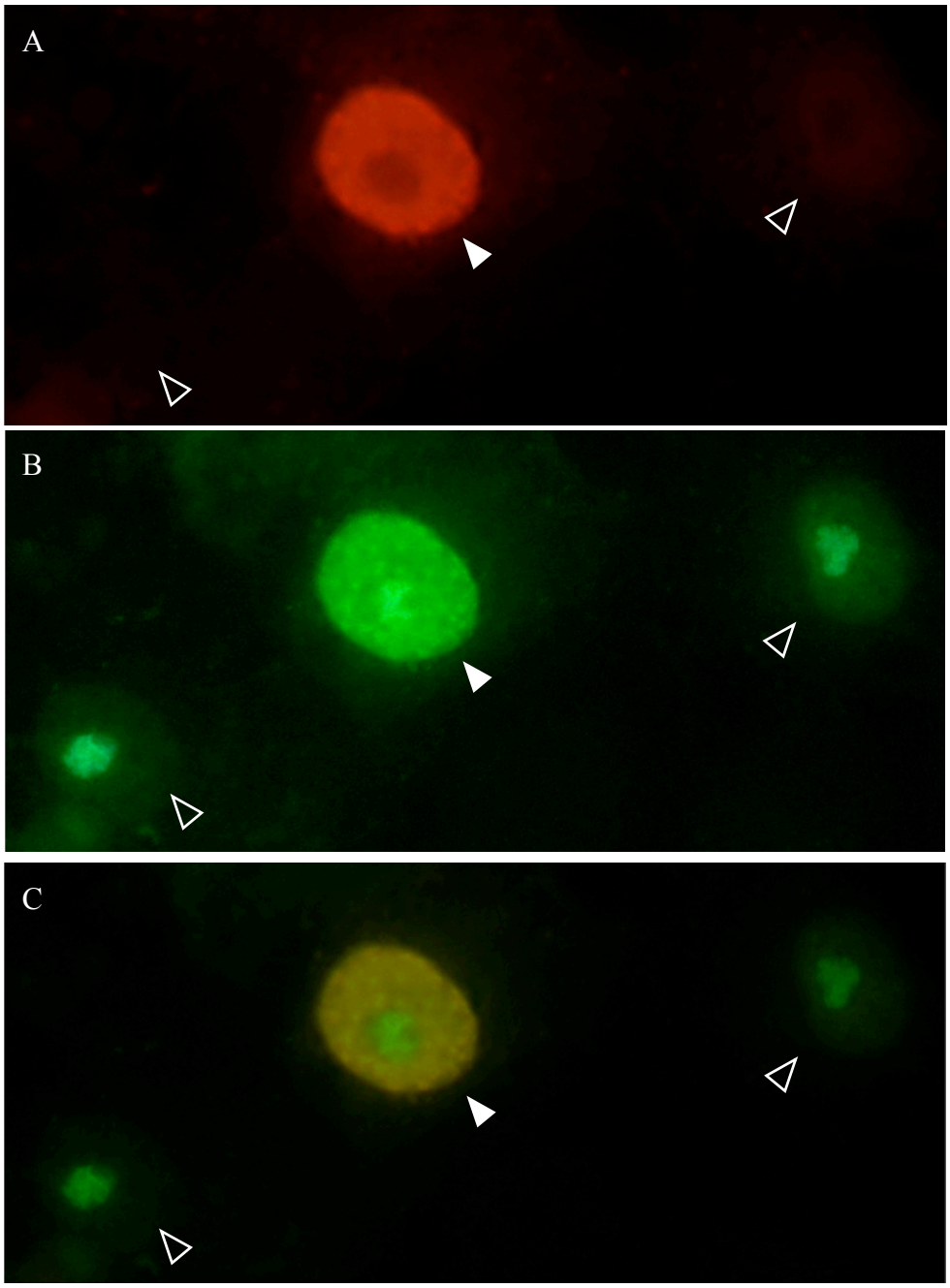

Figure 4.6 Co-localization of 52K and NFBP in transfected cells. COS7 cells were transfected with pcDNA.52K and pEY.NFBP, fixed, and stained with anti-52K serum and Cy3-conjugated goat anti-rabbit IgG (panel A). The NFBP-EYFP fusion protein was visualized directly (panel B). A merge of the Cy3 and EYFP images is shown (panel C). In cells expressing both 52K and NFBP (filled arrow), NFBP is diffused throughout the nucleus with some NFBP still present in the nucleolus. However, cells expressing NFBP alone (empty arrows) show nucleolar accumulation of NFBP.

young virions but not in mature virions (Hasson et al., 1992), it may interact with other proteins (viral/cellular) and perform additional functions. In the present report, we confirm the interaction of 52K with pVII previously reported in HAdV-5. In addition, we report for the first time that 52K interacts with the cellular protein NFBP.

A yeast two-hybrid system was used to screen for interactions between BAdV-3 52K and other viral proteins. On medium- or high-stringency selective media, specific interactions were detected between 52K and IVa2, pV, and pVII. In HAdV-5, 52K has been shown to interact with IVa2 and pVII (Gustin et al., 1996; Zhang and Arcos, 2005). However, in BAdV-3, only the interaction between 52K and pVII could be confirmed by an *in vitro* GST pulldown assay. If 52K and IVa2 interact in BAdV-3, the interaction could be transient or too weak to be detectable by the *in vitro* GST pulldown assay.

Anti-pVII serum was able to specifically co-precipitate 52K from infected cells, suggesting that 52K and pVII interact in BAdV-3 infected cells. However, anti-pVII serum appears to only immunoprecipitate the uncleaved form of pVII. Interestingly, GST-52K also interacted with the uncleaved form of pVII. These results suggest that 52K interacts with the uncleaved form of pVII, although our results do not exclude the possibility that 52K also interacts with the cleaved form of protein VII. It is possible that adenovirus protease cleavage of pVII to produce mature VII protein during processing of young virions to mature virions removes 52K from the nucleus. Support for this comes from the fact that 52K is detected in empty capsids, assembly intermediates, and young virions but not in mature virions, and that in the absence of active viral protease 52K remains associated with young virions (Hasson et al., 1992). Surprisingly, anti-52K serum was not able to co-precipitate pVII from BAdV-3 infected cells. This could be due to epitope masking. Binding of pVII to 52K could block access to epitopes recognized by the anti-52K serum and prevent the pVII/52K complex from being precipitated by anti-52K serum. It is also possible that the high affinity binding of antibodies to 52K disrupts the interaction between 52K and pVII or that only a small percentage of 52K may bind to pVII, making it difficult to detect pVII co-precipitated with 52K.

Mass spectrometry analysis of proteins co-immunoprecipitating with 52K identified a cellular protein, NFκB binding protein (NFBP). This interaction appears to be direct and does not require other cellular or viral proteins or other factors such as RNA. However, since the detected *in vitro* interaction is very weak, it is possible that other cellular or viral proteins could enhance the

interaction between 52K and NFBP *in vivo*. It is also possible that 52K would bind with higher affinity to the bovine NFBP homolog than to the human NFBP protein used for the *in vitro* assays. Although human and bovine NFBP proteins show 84% amino acid sequence identity, small differences in the protein sequence could affect the binding affinity of 52K for human NFBP compared to bovine NFBP. Deletions within the N-terminal 134 amino acids of 52K significantly reduce the *in vitro* interaction of 52K with NFBP, suggesting that these interactions involve residues spanning different regions of the 52K protein. The NFBP binding site of 52K could be highly conformation dependent, and thus the deletions may affect proper folding of 52K. Alternatively, interaction of 52K with NFBP may involve extensive protein-protein contacts.

NFBP localizes to the nucleolus of transfected cells. However, a significant amount of NFBP appears to be localized in the nucleus of transfected cells co-expressing 52K and NFBP. Since NFBP is involved in normal rRNA processing in the nucleolus (Sweet et al., 2008), it is possible that significant redistribution of NFBP to other parts of the nucleus in cells expressing 52K may decrease rRNA processing. Thus, the 52K protein may be involved in the disruption of rRNA processing observed in HAdV-5 infected cells (Castiglia and Flint, 1983). Alternatively, interaction of 52K and NFBP could alter NFκB activity (Sweet et al., 2003) or modulate the apoptosis response through NFκB-mediated transcription of the Fas ligand (Lacana and D'Adamio, 1999).

5.0 52K AND RIBOSOMAL RNA PROCESSING

5.1 Introduction

Adenovirus infection inhibits a number of normal cellular processes, including host ribosomal RNA (rRNA) processing (Raskas et al., 1970; Ledinko, 1972; Castiglia and Flint, 1983; Lawler et al., 1989). Normally, a single rRNA precursor is synthesized and processed in the nucleolus by cleavage and covalent modification into three smaller rRNA molecules (5.8S, 18S, and 28S) that are associated with ribosomes (Gerbi and Borovjagin, 2004; Nazar, 2004; Henras et al., 2008). In adenovirus infected cells, the production of new 28S, 18S, and 5.8S rRNA species from the pre-rRNA precursor is inhibited, indicating a block in rRNA processing (Raskas et al., 1970; Ledinko, 1972; Castiglia and Flint, 1983; Lawler et al., 1989). Export of the rRNA to the cytoplasm may also be inhibited (Castiglia and Flint, 1983). Whether rRNA transcription is also decreased is unclear. While several viral proteins such as IVa2, pV, IVa2, and μ have been shown to localize to the nucleolus (Lutz et al., 1996; Matthews, 2001; Lee et al., 2003; Lee et al., 2004b), where rRNA transcription and processing occurs, the viral protein responsible for inhibiting rRNA processing during virus infection has not been identified.

The processing of rRNA requires the association of many ribosomal and non-ribosomal proteins and ribonucleoprotein molecules with the pre-RNA, and occurs in a step-wise manner. The NFκB-binding protein (NFBP) has been shown to be essential for rRNA processing (Sweet et al., 2008). Knocking down the expression of NFBP by small interfering RNA inhibits the appearance of 18S rRNA but not of pre-rRNA precursors, suggesting that NFBP has an essential role in the processing of the pre-rRNA. Similarly, Rrp5p, a yeast homolog of NFBP, is required for the recruitment of several other factors required for rRNA processing (Venema and Tollervey, 1996; Vos et al., 2004; de Boer et al., 2006; Pérez-Fernández et al., 2007).

The L1 region of human adenovirus (HAdV) -5 encodes a nonstructural 52/55K protein which is present as two differentially phosphorylated forms of a 48 kDa precursor (Lucher et al., 1986; Hasson et al., 1992). The 52K protein is involved in the packaging of adenovirus DNA (Hasson et al., 1989; Gustin and Imperiale, 1998). The N-terminal half of the 52K protein mediates serotype specificity for packaging of the viral genome into the capsid (Wohl and Hearing, 2008). Recently, we demonstrated that the 52K protein of bovine adenovirus (BAdV)-3 interacts with NFBP (section 4.3), which is involved in rRNA processing (Sweet et al., 2008). Co-expression of

52K and NFBP in transfected cells results in significant redistribution of NFBP from the nucleolus to other parts of the nucleus. This suggested that relocalization of NFBP away from the nucleolus may affect rRNA processing occurring in the nucleolus (Henras et al., 2008). Here, we determined if the 52K protein is involved in the inhibition of rRNA processing during BAdV-3 infection of bovine cells.

5.2 Materials and Methods

5.2.1 Cell lines and viruses

Madin-Darby bovine kidney (MDBK) cells were propagated in minimal essential medium (MEM; Sigma-Aldrich) supplemented with 10% fetal bovine serum (FBS; SeraCare Life Sciences). 293T cells were propagated in Dulbecco's modified Eagle's medium (DMEM; Sigma-Aldrich) supplemented with 10% FBS.

Wild-type BAdV-3 (WBR-1 strain) was grown in MDBK cells in MEM supplemented with 2% FBS and was purified by cesium chloride density-gradient centrifugation (Reddy et al., 1999a). The virus titer was determined by plaque assay (Mittal et al., 1995) to be $1x10^8$ plaque-forming units (pfu)/mL.

HAdV-5 mutant viruses were propagated in 293T cells grown in DMEM supplemented with 2% FBS. A replication-defective HAdV-5 vector expressing GFP (AdGFP) was provided by M. Cotten and has been previously described (Michou et al., 1999). 293T cells infected with AdGFP in three $150cm^2$ flasks were lysed by five freeze-thaw cycles and the titer of the lysate was determined by $TCID_{50}$ assay (Both et al., 2007) to be $1x10^7$ $TCID_{50}$/mL.

5.2.2 Plasmid construction

A second generation lentivirus system was a gift from Dr. Robert Brownlie (Vaccine and Infectious Disease Organization, University of Saskatchewan) and included plasmids pTRIP-WRE-pur [a modified lentiviral vector (Brownlie et al., 2009) containing the encapsidation signal] pXPAX2 [encoding HIV Gag and Pol proteins; (al Yacoub et al., 2007)] and pMD2.G [encoding the VSV G protein; (al Yacoub et al., 2007)]. The plasmid pTRIP.GFP [expressing green fluorescent protein [GFP]) was also a gift from Dr. Brownlie (unpublished data). A 1.1-kb *Xho*I-*Bam*HI fragment containing the BAdV-3 52K ORF was isolated from plasmid pcDNA.52K

(section 3.2.7) and ligated to *Xho*I-*Bam*HI digested plasmid pTRIP-WRE-pur creating plasmid pTRIP.52K.

A 599-bp *Bsr*GI-*Nco*I fragment containing the internal ribosome entry site (IRES) from encephalomyocarditis virus (Bochkov and Palmenberg, 2006) was isolated from plasmid pGIPz (Open Biosystems) and ligated to *Bsi*WI-*Nco*I digested plasmid Litmus28i (New England Biolabs) to create plasmid pL28i.IRES. Similarly, a 1.1-kb *Eco*RV-*Bam*HI fragment containing the BAdV-3 52K ORF was isolated from plasmid pcDNA.52K and ligated to *Sna*BI-*Bgl*II digested plasmid pL28i.IRES creating plasmid pL28i.52K.IRES. Finally, a 745-bp *Age*I-*Xba*I fragment containing enhanced yellow fluorescent protein (EYFP) was isolated from plasmid pEYFPN1 (Clontech) and ligated to *Age*I-*Xba*I digested plasmid pL28i.52K.IRES creating plasmid pL28i.52K.IRES.EY. The entire 2.5-kb *Eco*RI-*Stu*I fragment containing 52K-IRES-EYFP was isolated from plasmid pL28i.52K.IRES.EY and ligated to *Eco*RI-*Eco*RV digested plasmid pH5L (Zakhartchouk et al., 2005) creating plasmid pH5L.52K.EY (figure 5.1). This plasmid is predicted to express BAdV-3 52K and EYFP from a single bicistronic mRNA transcript.

5.2.3 Rescue of replication-defective lentivirus vectors

Plasmid pTRIP.52K DNA (1.5 μg) or plasmid pTRIP.GFP DNA (1.5 μg) was co-transfected with plasmid pXPAX2 DNA (1 μg) and plasmid pMD2.G DNA (0.5 μg) into 293T cells in 100-mm dishes using lipofectin (Invitrogen) in Opti-MEM (Invitrogen) as per the manufacturer's instructions. Supernatant was collected at 48 and 72 hrs post-transfection. Cell debris was cleared by centrifugation at 3,000 rpm (1,950x*g*) for 20 min at 4˚C. Virus was harvested by centrifugation at 23,000 rpm for 1.5 hrs in a Beckman SW28 rotor and resuspended in DMEM.

5.2.4 MDBK cell lines expressing 52K or GFP

Purified pseudotyped lentivirus vectors (TRIP.52K or TRIP.GFP) were mixed with 8 μg/mL Sequa-brene (Sigma-Aldrich) and incubated at room temperature for at least 30 minutes.

The virus mixtures were added to MDBK cells in serum-free MEM in 6 wells (TRIP.52K) or 1 well (TRIP.GFP) of a 24-well plate. After 6 hrs, media was supplemented with FBS to a final concentration of 2%. At 24 hrs post-infection, cells were split into 100-mm dishes. At 48 hrs

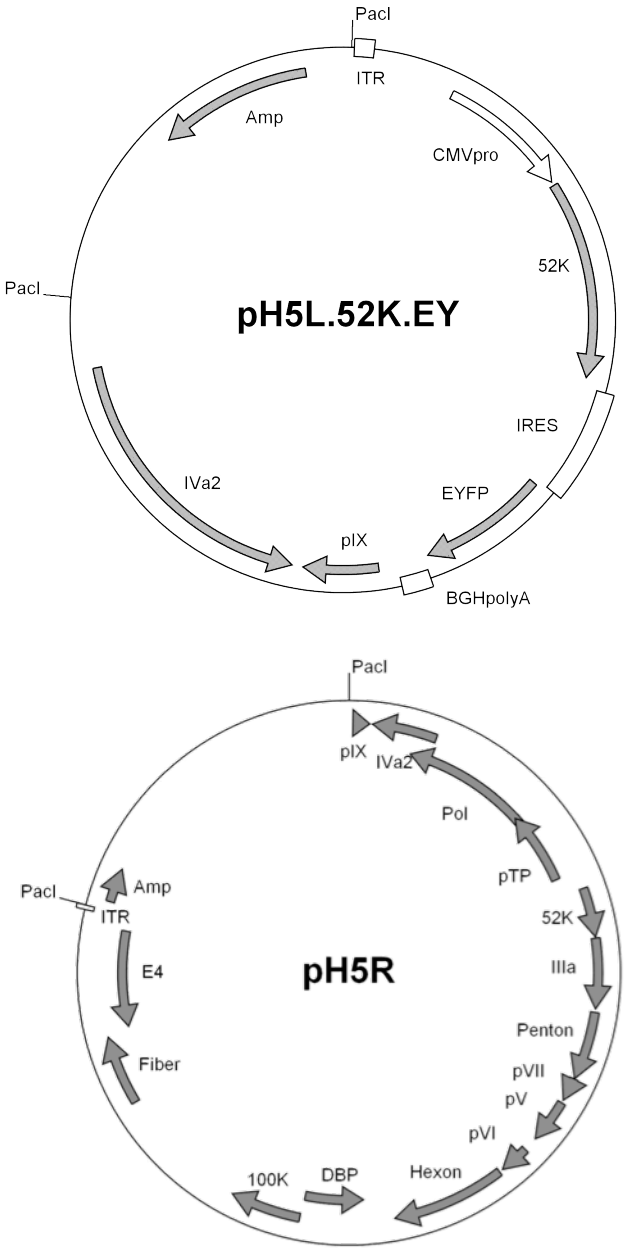

Figure 5.1 Plasmids used to generate a replication-defective HAdV-5 vector expressing 52K and EYFP. Plasmid pH5L.52K.EY contains the left-hand portion of the HAdV-5 genome including the ITR but is deleted for the E1 region and instead contains 52K and EYFP under the control of a CMV promoter and separated by an IRES. Plasmid pH5R contains the right-hand portion of the HAdV-5 genome from pIX onward, including the right ITR. Plasmids are linearized by digestion with *Pac*I and homologous recombination between the pIX/IVa2 regions generates a linear genome with an ITR and both ends that is replication-competent in cells expressing adenovirus E1 proteins.

post-infection, media was replaced with MEM containing 10% dialyzed FBS (Invitrogen) and 2 μg/mL puromycin for selection. Media was changed every 3 days. After 7-10 days, puromycin concentration was increased to 8 μg/mL. When the puromycin-selected cells were confluent, they were split into 100-mm plates to reach a confluence of 20% the next day and the puromycin concentration was increased to 50μg/mL after 24 hrs. For TRIP.52K-transduced cells, after 7-10 days puromycin-resistant colonies were harvested and transferred to individual wells of a 96-well plate. Out of 30 clones isolated, a single clone which showed adequate growth was selected for use in further experiments. Expression of BAdV-3 52K in this cell line (MDBK:52K) was confirmed by indirect immunofluorescence using anti-52K serum as described in section 3.2.6 and by Western blot using anti-52K serum as described in section 3.2.5.

For TRIP.GFP-transduced cells, the puromycin-selected cells in two 100-mm dishes were allowed to reach confluence and were passaged in the presence of 50μg/mL puromycin and used for further experiments. Expression of GFP in this cell line (MDBK:GFP) was confirmed by visualizing cells directly on an AxioVert UV microscope.

5.2.5 Rescue of a replication-defective HAdV-5 vector expressing BAdV-3 52K

Plasmids pH5L.52K.EY and pH5R (Zakhartchouk et al., 2005) (figure 5.1) were linearized by *Pac*I digestion and DNA was purified by phenol-chloroform extraction followed by ethanol precipitation. To rescue recombinant virus by homologous recombination, 293T cells in one well of a 6-well plate were co-transfected with 1 μg each of linearized pH5R and pH5L.52K.EY DNA using lipofectin (Invitrogen) in serum-free Opti-MEM (Invitrogen) as per the manufacturer's instructions. At 8 hrs post-transfection, Opti-MEM was replaced with DMEM containing 2% FBS. Cells were passaged as required post-transfection. After 24 days, fluorescent cells were visible but no cytopathic effects (CPE) were observed. Cells in a 75cm^2 flask were lysed by five freeze-thaw cycles and used to infect new 293T cells in a 25cm^2 flask. Visible CPE and fluorescence were visible after several days, indicating rescue of the recombinant virus (HAdV5-52K). The infected cells in a 75cm^2 flask were lysed by five freeze-thaw cycles and the lysate was passaged several more times in 293T cells to amplify the virus. At the end of amplification, the virus was released from cells in three 150cm^2 flasks by five freeze-thaw cycles and titered. The titer of the lysate was determined by $TCID_{50}$ assay (Both et al., 2007) and was determined to be $1x10^9$ $TCID_{50}$/mL.

To confirm the expression of BAdV-3 52K, 293T cells in one well of a 6-well plate were infected with HAdV5-52K lysate (50 $TCID_{50}$/cell) in MEM. Two hrs post infection, media was supplemented with 2% FBS. After 24 hrs post infection, the cells were harvested, lysed, and analyzed by Western blot using anti-52K serum as described in section 3.2.5. In addition, 293T cells infected with HAdV5-52K were fixed 24 hrs post infection in methanol for 20 min at -20˚C and the intracellular localization of 52K was examined by indirect immunofluorescence using anti-52K serum and Cy3-conjugated goat anti-rabbit IgG (diluted 1:800) as described in section 3.2.6.

5.2.6 Ribosomal RNA processing assay

Analysis of cellular rRNA processing was carried out based on a previously described method (Sweet et al., 2008). MDBK cells were grown to approximately 80% confluency and rinsed in MEM before incubating with wild-type BAdV-3 (MOI of 5 pfu/cell), AdGFP (MOI of 50 $TCID_{50}$/cell), or HAdV5-52K (MOI of 50 $TCID_{50}$/cell) in MEM for 2 hrs. Media was then replaced with MEM supplemented with 2% FBS.

At the indicated time post infection, the cells were starved in phosphate-free DMEM (Invitrogen) in 10% FBS for 30 min before pulsing with MEM containing 15μCi/mL [^{32}P]-orthophosphate (Perkin Elmer) and 10% FBS for 45 minutes. The [^{32}P] pulsed cells were chased with MEM supplemented with 10% FBS for 2 hrs. Finally, the cells were harvested, lysed, and total RNA was extracted using either an RNeasy purification system (Qiagen) or TRIzol reagent (Invitrogen). The cpm/mL of each RNA sample was calculated by measuring radioactivity of a mixture of an aliquot of the purified RNA and scintillation fluid in a Beckman scintillation counter.

Equal cpms of purified RNAs in 8 μL of RNase-free water were mixed with 2 μL of 5X RNA loading buffer [0.16% bromophenol blue, 4 mM EDTA (pH 8.0), 7.2% formaldehyde, 20% glycerol, 30% formamide, 10X formaldehyde agarose gel buffer (200 mM MOPS, 50 mM sodium acetate, 10 mM EDTA, pH adjusted to 7.0) at a final concentration of 4X] and separated on a 1.2% formaldehyde-agarose gel by electrophoresis. Finally, the gel was dried onto filter paper and exposed to a phosphor screen overnight. The phosphor screen was visualized on a Bio-Rad Molecular Imager FX using Quantity One software (Bio-Rad). Densitometric analysis of the gels was also performed using the Quantity One program.

5.3 Results

5.3.1 Inhibition of ribosomal RNA processing during BAdV-3 infection

To determine if BAdV-3 infection of bovine cells affects rRNA processing, MDBK cells were infected with BAdV-3 at an MOI of 5 pfu/cell and ribosomal RNA processing was examined at various times post-infection in a pulse-chase experiment. At 0 hrs post infection, 47S and 32S precursor rRNA is efficiently processed into 28S and 18S rRNA (figure 5.2, panel A). By 24 hrs post infection, there is a significant reduction in the amounts of 28S and 18S rRNA with a significant increase in the amount of 32S and 47S precursors. This reduction in processing is also apparent at 36 and 48 hrs post infection. There also appears to be less total labeled rRNA at 36 and 48 hrs post infection, suggesting a reduction in rRNA synthesis in proportion to total RNA synthesis.

5.3.2 Construction of an MDBK cell line expressing BAdV-3 52K

Due to the low transfection efficiency of MDBK cells, our initial attempts to study the effects of BAdV-3 52K in the absence of other BAdV-3 viral proteins using a transient expression system proved futile. As such, we chose to construct a stable MDBK cell line expressing BAdV-3 52K using a replication-defective lentivirus system (Brownlie et al., 2009).

BAdV-3 52K was cloned into a plasmid from a second generation lentivirus expression system (pTRIP-WRE-pur) and pseudotyped lentivirus TRIP.52K was produced by co-transfection of 293T cells with plasmids pTRIP.52K, pXPAX2, and pMD2.G. Similarly, pseudotyped lentivirus TRIP.GFP was produced by co-transfection of 293T cells with plasmids pTRIP.GFP, pXPAX2, and pMD2.G. The TRIP.52K or TRIP.GFP lentiviruses were used to transduce MDBK cells and puromycin resistant clones were selected by culturing the lentivirus-transduced cells in the presence of puromycin (50 μg/mL). A single puromycin-resistant clone was selected and checked for the expression of 52K by Western blot analysis and indirect immunofluorescence or expression of GFP by fluorescent microscopy. Cell lines expressing GFP (MDBK:GFP) or BAdV-3 52K (MDBK:52K) were selected for further analysis. As shown in figure 5.3, the level of expression of BAdV-3 52K in the MDBK:52K cell line is significantly lower than that seen in BAdV-3 infected MDBK cells (panel A) and does not appear to be expressed in 100% of cells (panel B).

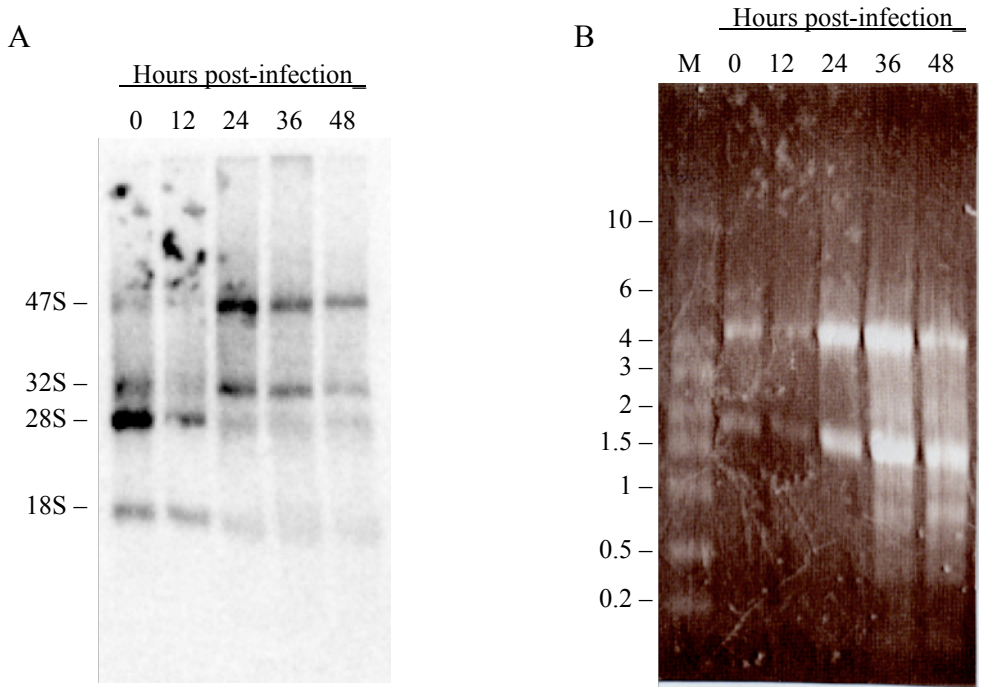

Figure 5.2 Inhibition of ribosomal RNA processing during BAdV-3 infection. MDBK cells infected with BAdV-3 were labeled at 12, 24, 36, or 48 hours post-infection with media containing [^{32}P] and chased in MEM for 2 hours. Uninfected cells (0 hrs post-infection) were similarly labeled and chased. Total RNA was harvested and 2.5x10^3 cpm were loaded in each lane and separated by formaldahyde-agarose electrophoresis, then visualized by exposure to a phosphor screen. **A.** Ribosomal RNA species in uninfected (0 hrs) and infected cells (12-48 hrs) are marked. **B.** Total RNA visualized by ethidium bromide staining. Molecular weight standards (M) are indicated in kilobases.

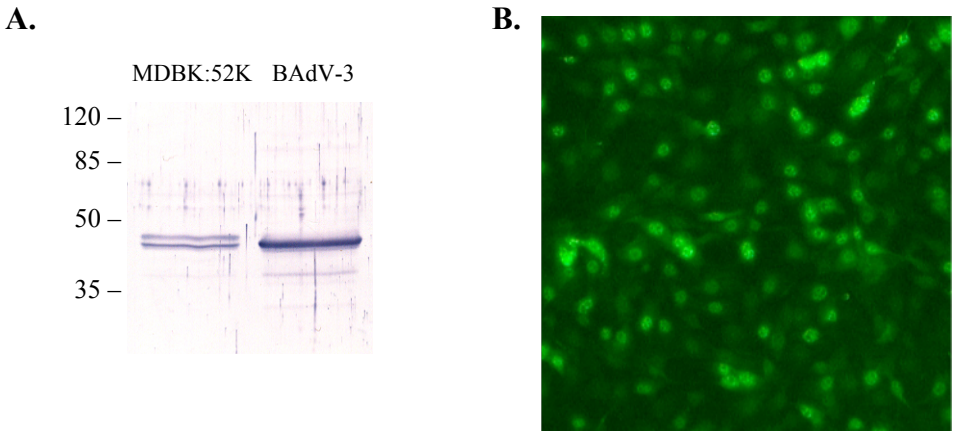

Figure 5.3 Expression of 52K in MDBK:52K cells. A. The expression of 52K in MDBK:52K cells and BAdV-3 infected MDBK cells was examined by Western blot using anti-52K serum. Molecular weight standards are indicated in kDa. **B.** Expression of 52K in MDBK:52K cell line visualized by indirect immunofluorescence of fixed cells using anti-52K serum and Cy2 conjugated goat anti-rabbit IgG.

5.3.3 Construction of a replication-defective HAdV-5 vector expressing BAdV-3 52K

To attempt to express BAdV-3 52K in close to 100% of cells, we chose to construct a replication-defective HAdV-5 expressing BAdV-3 52K and EYFP on a single bicistronic transcript under the control of the CMV promoter, with EYFP translation under the control of an IRES (figure 5.1).

To rescue recombinant virus, we used two plasmids. The plasmid pH5L.52K.EY contains the left-hand portion of the HAdV-5 genome including pIX and IVa2, while the plasmid pH5R contains the rest of the genome containing overlap of the pIX and IVa2 regions. Briefly, 293T cells were transfected with *Pac*I-linearized plasmids pH5R and pH5L.52K.EY. The homologous recombination in the co-transfected cells between the two linearized plasmids generates a linear viral genome containing an inverted terminal repeat at both ends that permits virus replication and allows the recombinant virus to be rescued. Cells showing cytopathic effects and green fluorescence were collected, freeze-thawed, and cell lysate was used to infect MDBK cells.

The expression of BAdV-3 52K was analyzed by Western blot using anti-52K serum. As seen in figure 5.4, anti-52K serum detected two proteins of 35 kDa and 36 kDa in HAdV5-52K infected (figure 5.4, panel A) or pH5L.52K.EY transfected (data not shown) 293T cells. However, a protein of 40 kDa was detected in BAdV-3 infected MDBK cells (figure 5.4, panel A). The difference in the molecular weight of BAdV-3 52K expressed in BAdV-3 infected MDBK cells and HAdV5-52K infected or pH5L.52K.EY transfected 293T cells suggested that an error in the 52K ORF had been introduced during cloning. DNA sequencing revealed a four nucleotide deletion (nucleotides 10,984 to 10,897 in Genbank AF030154) in the 52K ORF in plasmid pH5L.52K.EY which caused a frame shift and introduced a stop codon, truncating the 52K ORF at amino acid 302. While it is possible that this could affect BAdV-3 52K function for the ribosomal RNA assay, considering that the NFBP-binding domain of 52K appears to be located in the N-terminus of the protein and that the truncated BAdV-3 52K protein still localizes to the nucleus (figure 5.4, panel B), the HAdV5-52K virus was used for the following ribosomal RNA experiments.

5.3.4 Effect of 52K expression on ribosomal RNA processing

To determine if expression of BAdV-3 52K in MDBK:52K cells inhibits rRNA processing, cellular rRNA was labeled with [^{32}P] and analyzed by formaldehyde-agarose gel electrophoresis.

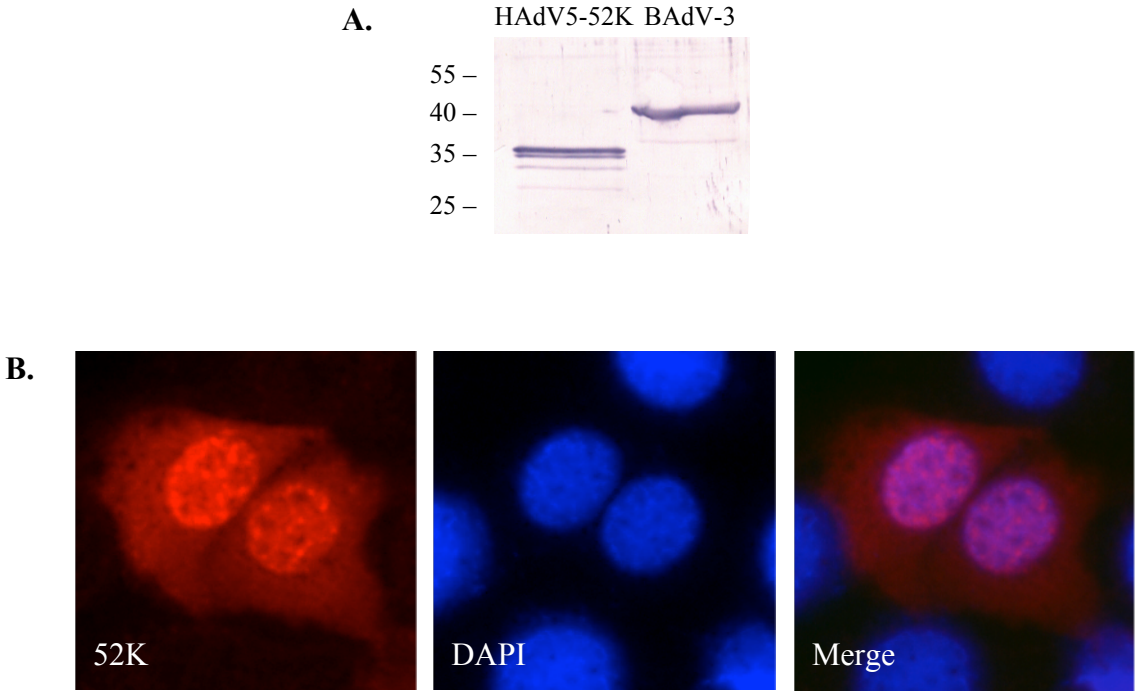

Figure 5.4 Expression of 52K by the recombinant virus HAdV5-52K. A. Lysates from 293T cells infected with HAdV5-52K (lane 1) or MDBK cells infected with 5 pfu/cell BAdV-3 (lane 2) were separated by SDS-PAGE and analyzed by Western blot using anti-52K serum. Molecular weight standards (M) are indicated in kDa. **B.** The intracellular localization of 52K in MDBK cells infected with HAdV5-52K was determined by indirect immunofluorescence using anti-52K serum and Cy3-conjugated goat anti-rabbit IgG.

As seen in figure 5.5, at 24 hrs post infection there is no detectable amount of 28S and 18S rRNA produced in MDBK cells infected with 5 pfu/cell of BAdV-3 (panel A, lane 4). However, detectable amounts of 28S and 18S rRNAs are produced in normal MDBK cells (panel A, lane 1). Interestingly, similar detectable amounts of 28S and 18S rRNA are also produced in MDBK:GFP (panel A, lane 2) or MDBK:52K (panel A, lane 3) cells.

To determine if expression of the truncated BAdV-3 52K in HAdV5-52K infected cells inhibits cellular rRNA processing, cellular rRNAs in uninfected, HAdV5-52K infected, AdGFP infected, or BAdV-3 infected MDBK cells were labeled with [^{32}P] and analyzed by formaldehyde-agarose gel electrophoresis. As seen in figure 5.6, at 24 hrs post infection there was significant increase in the amount of 47S rRNA precursor and a slight decrease in the amount of 28S and 18S rRNA in BAdV-3 infected cells (panel A, lane 4). However, there was no detectable 47S rRNA precursor in normal MDBK (panel A, lane 1) or AdGFP infected MDBK (panel A, lane 2) cells. Similarly, there was no detectable 47S rRNA precursor in HAdV5-52K infected MDBK cells expressing BAdV-3 52K (panel A, lane 3). Taken together, our data suggests that the expression of the full-length or truncated 52K in the absence of other viral proteins does not inhibit rRNA processing.

5.4 Discussion

Although inhibition of ribosomal RNA processing during adenovirus infection was first discovered in the 1970s, the mechanism of this inhibition remains poorly understood (Ledinko, 1972; Castiglia and Flint, 1983). Earlier, we demonstrated that the 52K protein of BAdV-3 interacts with the cellular protein NFBP (section 4.3), which is known to be essential for rRNA processing (Sweet et al., 2008). Since co-expression of 52K and NFBP in transfected cells disrupts the nucleolar localization of NFBP (section 4.3.6), we hypothesized that the interaction between 52K and NFBP may inhibit rRNA processing during BAdV-3 infection.

Like HAdV-5 (Ledinko, 1972; Castiglia and Flint, 1983; Lawler et al., 1989), processing of cellular precursor rRNA into 28S and 18S rRNAs is inhibited in BAdV-3 infected cells. This suggests that inhibition of precursor rRNA processing may be a common phenomenon conserved across adenoviruses, including members of the *Mastadenovirus* genus.

Expression of a truncated BAdV-3 52K (amino acids 1-302) in MDBK cells using replication-defective HAdV5-52K did not affect the efficiency of processing of precursor rRNA to 28S and

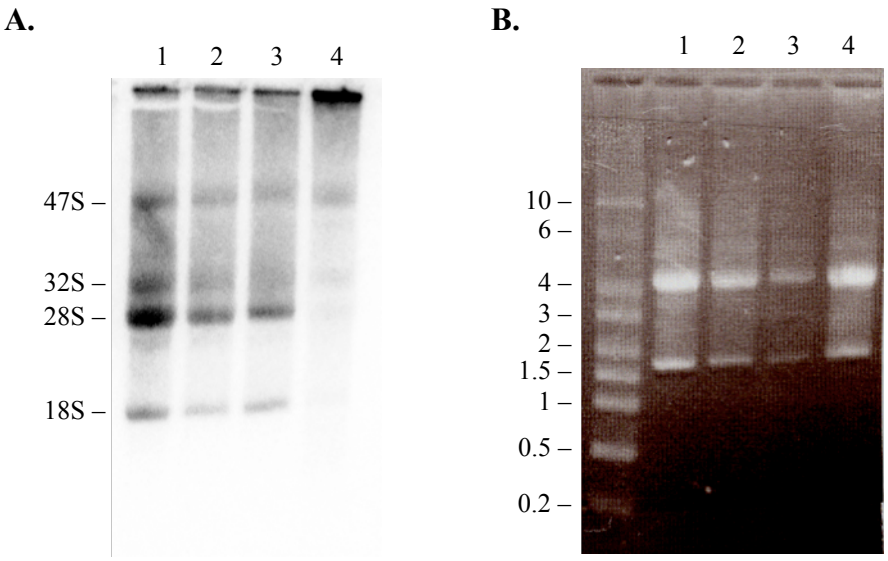

Figure 5.5 Ribosomal RNA processing in a 52K-expressing cell line. A. MDBK (lane 1), MDBK:GFP (lane 2), or MDBK:52K cells (lane 3), along with BAdV-3 infected MDBK cells 24 hrs post-infection (lane 4) were phosphate starved, labeled with ^{32}P, and chased for 2 hrs in complete media. Total RNA was harvested and $4.7x10^3$ cpms were loaded into each lane of a formaldehyde-agarose gel and separated by electrophoresis. The gel was dried and exposed to a phosphor screen to visualize rRNA species. **B.** Ethidium bromide stain of the formaldehyde-agarose gel to visualize total RNA loaded. Molecular weight standards are indicated in kilobases.

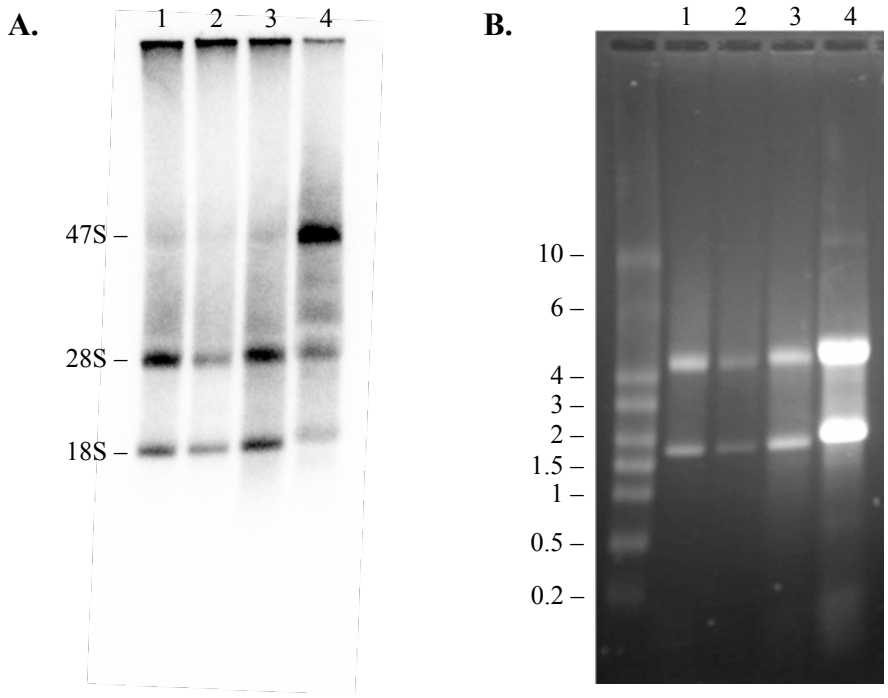

Figure 5.6 Ribosomal RNA processing in HAdV5-52K infected cells. MDBK cells were mock-infected (lane 1) or infected with AdGFP (lane 2), HAdV5-52K (lane 3), or BAdV-3 (lane 4). After 24 hours, cells were starved in phosphate-free media, labeled with ^{32}P, and chased for 2 hrs in complete media before total RNA was harvested. **A.** 1.2 x 10^4 cpms were and separated on a formaldehyde-agarose gel to visualize rRNA. **B.** Total RNA was visualized by ethidium bromide staining. Molecular weight standards are shown in kilobases.

18S rRNAs. It is possible that amino acids 303-370 may be required for inhibiting the processing of precursor rRNA. However, we have demonstrated that the N-terminal 134 amino acids of BAdV-3 52K may be involved in binding to NFBP. Alternatively, it is possible that the amount of 52K required to inhibit rRNA processing is not sufficient in HAdV5-52K infected cells as seen in figure 5.4.

Surprisingly, expression of the complete BAdV-3 52K ORF in MDBK cells also did not affect the efficiency of processing of precursor rRNA to 28S and 18S rRNAs. Since immunofluorescent staining showed that not all cells were expressing 52K, it was possible that the lack of inhibition of rRNA processing was due to not enough cells expressing 52K, or cells not expressing 52K at a high enough level. Alternatively, it is possible that 52K co-operates with other viral proteins to inhibit rRNA processing but is unable to exert this effect when expressed alone. Viral proteins IVa2, pV, pVII, and μ have been shown to localize to the nucleolus in HAdV (Lutz et al., 1996; Matthews, 2001; Lee et al., 2003; Lee et al., 2004b) and could potentially be involved in inhibition of rRNA processing.

It is also possible that the interaction between 52K and NFBP may have other effects during BAdV-3 infection, such as altering NFκB transcriptional activity (Sweet et al., 2003) or modulating the apoptosis response through transcription of the Fas ligand (Lacana and D'Adamio, 1999).

6.0 GENERAL DISCUSSION AND CONCLUSIONS

Bovine adenovirus (BAdV)-3 has potential as a vector for gene delivery and vaccination (Reddy et al., 1999b). Because of the observed differences between human and non-human adenoviruses, including differences in cell entry (Bangari et al., 2005), transcriptional organization of the genome (Reddy et al., 1998), location of DNA packaging signals (Xing et al., 2003; Xing and Tikoo, 2007), proteins encoded by the E3 and E4 regions (Reddy et al., 1998; Idamakanti et al., 1999), and the absence of the virus-associated RNAs in BAdV-3 (Reddy et al., 1998), it is important to characterize the structure and function of individual BAdV-3 proteins in order to develop improved and efficient BAdV-3 vectors.

Adenoviruses encode a non-structural late protein named 52K, which is conserved in members of the family *Adenoviridae* (Davison et al., 2003). Earlier reports have suggested a role for 52K in serotype specific packaging of adenovirus DNA (Hasson et al., 1989; Gustin and Imperiale, 1998; Wohl and Hearing, 2008). Moreover, 52K has been shown to interact with the viral IVa2 and pVII proteins (Gustin et al., 1996; Zhang and Arcos, 2005). Despite significant sequence identity among 52K proteins encoded by adenoviruses including BAdV-3 52K, the 52K protein has been suggested to determine the serotype specificity of adenovirus DNA packaging (Wohl and Hearing, 2008).

Thus, the main aim of the present investigation was to characterize the BAdV-3 52K protein and determine its interaction with other viral and cellular proteins.

DNA sequence analysis revealed that the BAdV-3 52K ORF encoded a protein of 370 amino acids rather than 331 amino acids as previously reported (Reddy et al., 1998). A high degree of sequence identity (50-60%) among 52K proteins encoded by members of the *Mastadenovirus* genus including BAdV-3 suggests that some functions of 52K may be conserved among members of the *Mastadenovirus* genus.

Anti-52K serum detected a protein of 40 kDa at 24 to 72 hrs post-infection. This is similar to the expression pattern of other late genes of BAdV-3 (Reddy et al., 1998; Kulshreshtha et al., 2004; Patel and Tikoo, 2006). BAdV-3 52K localizes predominantly to the nucleus of infected cells. Moreover, localization of 52K to the nucleus in transfected cells suggests that the transport of 52K to the nucleus is independent of other viral proteins. Due to its small size (40kDa), 52K could be capable of diffusing across the nuclear pores. However, free diffusion of the protein

across the nuclear pores would distrubute 52K equally in the cytoplasm and nucleus of the cell. Localization of 52K predominantly in the nucleus of infected or transfected cells suggests that the protein uses active import pathways, or is retained preferentially in the nucleus. To create a large protein incapable of entering the nucleus without using active transport pathways, we constructed a plasmid expressing 52K fused to enhanced yellow fluorescent protein (EYFP) to analyze the nuclear localization of 52K. The EYFP-52K fusion protein localized to the nucleus, indicating that 52K contains a nuclear localization signal (NLS) that can direct its nuclear import. Deletions and point mutagenesis of 52K demonstrated that a cluster of basic residues (^{105}RKR^{107}) was essential for nuclear localization, but that residues ^{102}GMPRKRVLT^{110} were not sufficient to direct nuclear import of an unrelated protein. This suggests that either upstream or downstream residues of the 52K NLS are required, or the NLS is dependent on its conformation within 52K.

The nuclear import of 52K could be reconstituted in an *in vitro* nuclear import assay. Nuclear accumulation of 52K was significantly but not completely dependent on soluble factors, ATP, and temperature. In contrast, a protein with the nuclear localization signal of the simian virus 40 T antigen, which uses a classical importin α/importin β pathway, was completely dependent on soluble factors, ATP, and temperature. The nuclear import of 52K could be significantly inhibited by a peptide that competes for binding to importin β and slightly inhibited by a peptide containing the NLS from Ycbp80, but could not be blocked by a dominant negative mutant of Ran. This suggests that 52K uses the classical importin α/importin β pathway for nuclear import. A specific interaction of 52K with importin α3 supports this conclusion.

52K could also localize to the nucleus in the absence of soluble factors and ATP when the nuclear membrane was permeabilized with detergent, suggesting that it can bind to nuclear components. This suggests that 52K is imported into the nucleus not only by the importin α3/importin β pathway, but is also retained there by binding to nuclear components. Since 52K interacts with the nucleolar protein NFBP, it is tempting to speculate that NFBP could be one of the nuclear components which may help in the localization of 52K to the nucleus. The matrix protein of respiratory syncytial virus and the integrase protein of human immunodeficiency virus have similar mechanisms of nuclear import, using the importin α/importin β pathway in addition to accumulating in the nucleus independently of soluble factors by binding to nuclear components (Ghildyal et al., 2005; Hearps and Jans, 2006).

A yeast two-hybrid system was used to identify viral proteins interacting with BAdV-3 52K, and interactions of 52K with pV, pVI, pVII, and IVa2 proteins of BAdV-3 were detected. However, only the interaction of 52K with pVII could be confirmed by GST pulldown. Moreover, 52K and pVII also interact in BAdV-3 infected cells. Although similar results have been reported in HAdV-5 infected cells (Zhang and Arcos, 2005), the importance of these protein interactions are not known. Thus, future work should focus on isolating and analyzing mutant BAdV-3s containing deletions or point mutations to identify protein domains/motifs involved in these interactions.

Interactions of adenovirus proteins with cellular proteins during different stages of viral replication have been shown to be required for efficient production of progeny adenovirus. These interactions may alter the cell cycle (Berk, 2005), inhibit apoptosis (Berk, 2005) or host cell protein synthesis (Cuesta et al., 2000), and may help to defend against antiviral cellular responses (Horwitz, 2004). Mass spectrometry analysis of proteins co-immunoprecipitating with 52K from BAdV-3 infected cells identified a cellular protein, NFBP, which interacts with 52K. This interaction was confirmed *in vitro* and *in vivo*.

NFBP has been shown to be essential for ribosomal RNA (rRNA) processing (Sweet et al., 2008) and is normally localized in the nucleolus (Sweet et al., 2005). Co-expression of 52K and NFBP results in redistribution of NFBP from the nucleolus to other parts of the nucleus. Since NFBP is essential for rRNA processing in the nucleolus, it is possible that 52K inhibits rRNA processing by redistributing NFBP away from the nucleolus. However, we could not detect any difference in rRNA processing in cells expressing truncated or full length 52K. Further experiments are required to determine if other viral proteins are required along with 52K to inhibit rRNA processing in BAdV-3 infected cells.

NFBP appears to be a multifunctional protein. The interaction between 52K and NFBP could therefore have other functions during BAdV-3 infection. NFBP binds to the p50 and p65 subunits of NFκB (Sweet et al., 2003). The interaction between 52K and NFBP could potentially modulate NFκB activity in BAdV-3 infected cells. NFBP has also been shown to bind the human immunodeficiency virus Tat protein and is able to modulate Tat- and NFκB-mediated transcriptional activation from the viral long terminal repeat (Sweet et al., 2005). The mouse homolog of NFBP, apoptosis-linked gene 4, induces apoptosis through increased transcription of the Fas ligand when overexpressed (Lacana and D'Adamio, 1999). It is therefore possible that the

interaction between 52K and NFBP inhibits apoptosis during virus infection. The 33K protein of BAdV-3 has been shown to inhibit apoptosis through its interaction with the bovine presenilin-1-associated protein, a cellular mitochondrial protein that has pro-apoptotic effects (Kulshreshtha, 2009). Further investigation will be required to determine the biological significance, if any, of the interaction between 52K and NFBP.

7.0 REFERENCES

Adam SA, Marr RS, Gerace L. 1990. Nuclear protein import in permeabilized mammalian cells requires soluble cytoplasmic factors. J Cell Biol 111: 807-816.

Ahmed M, Lyles DS. 1998. Effect of vesicular stomatitis virus matrix protein on transcription directed by host RNA polymerases I, II, and III. J Virol 72: 8413-8419.

Akusjärvi G, Persson H. 1981. Controls of RNA splicing and termination in the major late adenovirus transcription unit. Nature 292: 420-426.

al Yacoub N, Romanowska M, Haritonova N, Foerster J. 2007. Optimized production and concentration of lentiviral vectors containing large inserts. J Gene Med 9: 579-584.

Albinsson B, Kidd AH. 1999. Adenovirus type 41 lacks an RGD alpha(v)-integrin binding motif on the penton base and undergoes delayed uptake in A549 cells. Virus Res 64: 125-136.

Alemany R, Curiel DT. 2001. CAR-binding ablation does not change biodistribution and toxicity of adenoviral vectors. Gene Ther 8: 1347-1353.

Ali H, LeRoy G, Bridge G, Flint SJ. 2007. The adenovirus L4 33-kilodalton protein binds to intragenic sequences of the major late promoter required for late phase-specific stimulation of transcription. J Virol 81: 1327-1338.

Anderson CW, Young ME, Flint SJ. 1989. Characterization of the adenovirus 2 virion protein, mu. Virology 172: 506-512.

Andersson MG, Haasnoot PCJ, Xu N, Berenjian S, Berkhout B, Akusjärvi G. 2005. Suppression of RNA interference by adenovirus virus-associated RNA. J Virol 79: 9556-9565.

Aparicio O, Carnero E, Abad X, Razquin N, Guruceaga E, Segura V, Fortes P. 2010. Adenovirus VA RNA-derived miRNAs target cellular genes involved in cell growth, gene expression and DNA repair. Nucleic Acids Res 38: 750-763.

Armentero MT, Horwitz M, Mermod N. 1994. Targeting of DNA polymerase to the adenovirus origin of DNA replication by interaction with nuclear factor I. Proc Natl Acad Sci USA 91: 11537-11541.

Arnberg N. 2009. Adenovirus receptors: implications for tropism, treatment and targeting. Rev Med Virol 19: 165-178.

Arnberg N, Kidd AH, Edlund K, Olfat F, Wadell G. 2000. Initial interactions of subgenus D adenoviruses with A549 cellular receptors: sialic acid versus alpha(v) integrins. J Virol 74: 7691-7693.

Avvakumov N, Kajon AE, Hoeben RC, Mymryk JS. 2004. Comprehensive sequence analysis of the E1A proteins of human and simian adenoviruses. Virology 329: 477-492.

Babich A, Feldman LT, Nevins JR, Darnell JE, Weinberger C. 1983. Effect of adenovirus on metabolism of specific host mRNAs: transport control and specific translational discrimination. Mol Cell Biol 3: 1212-1221.

Bai M, Harfe B, Freimuth P. 1993. Mutations that alter an Arg-Gly-Asp (RGD) sequence in the adenovirus type 2 penton base protein abolish its cell-rounding activity and delay virus reproduction in flat cells. J Virol 67: 5198-5205.

Banerjee R, Weidman MK, Navarro S, Comai L, Dasgupta A. 2005. Modifications of both selectivity factor and upstream binding factor contribute to poliovirus-mediated inhibition of RNA polymerase I transcription. J Gen Virol 86: 2315-2322.

Bangari DS, Sharma A, Mittal SK. 2005. Bovine adenovirus type 3 internalization is independent of primary receptors of human adenovirus type 5 and porcine adenovirus type 3. Biochem Biophys Res Commun 331: 1478-1484.

Baxi MK, Babiuk LA, Mehtali M, Tikoo SK. 1999. Transcription map and expression of bovine herpesvirus-1 glycoprotein D in early region 4 of bovine adenovirus-3. Virology 261: 143-152.

Baxi MK, Reddy PS, Zakhartchouk AN, Idamakanti N, Pyne C, Babiuk LA, Tikoo SK. 1998. Characterization of bovine adenovirus type 3 early region 2B. Virus Genes 16: 313-316.

Baxi MK, Robertson J, Babiuk LA, Tikoo SK. 2001. Mutational analysis of early region 4 of bovine adenovirus type 3. Virology 290: 153-163.

Bayliss R, Littlewood T, Stewart M. 2000. Structural basis for the interaction between FxFG nucleoporin repeats and importin-beta in nuclear trafficking. Cell 102: 99-108.

Benedict CA, Norris PS, Prigozy TI, Bodmer JL, Mahr JA, Garnett CT, Martinon F, Tschopp J, Gooding LR, Ware CF. 2001. Three adenovirus E3 proteins cooperate to evade apoptosis by tumor necrosis factor-related apoptosis-inducing ligand receptor-1 and -2. J Biol Chem 276: 3270-3278.

Benko M, Elo P, Ursu K, Ahne W, LaPatra SE, Thomson D, Harrach B. 2002. First molecular evidence for the existence of distinct fish and snake adenoviruses. J Virol 76: 10056-10059.

Benko M, Harrach B. 1998. A proposal for a new (third) genus within the family Adenoviridae. Arch virology 143: 829-837.

Bergelson JM, Cunningham JA, Droguett G, Kurt-Jones EA, Krithivas A, Hong JS, Horwitz MS, Crowell RL, Finberg RW. 1997. Isolation of a common receptor for Coxsackie B viruses and adenoviruses 2 and 5. Science 275: 1320-1323.

Berk AJ. 2005. Recent lessons in gene expression, cell cycle control, and cell biology from adenovirus. Oncogene 24: 7673-7685.

Berk AJ. 2007. Adenoviridae: The viruses and their replication. In: Fields Virology, 5th ed. D. Knipe and P. Howley (Ed.). Philadelphia: Wolters Kluwer Health/Lippincott Williams & Wilkins. pp.2355-2394.

Besse S, Puvion-Dutilleul F. 1996. Intranuclear retention of ribosomal RNAs in response to herpes simplex virus type 1 infection. J Cell Sci 109: 119-129.

Binger MH, Flint SJ. 1984. Accumulation of early and intermediate mRNA species during subgroup C adenovirus productive infections. Virology 136: 387-403.

Blackford AN, Grand RJA. 2009. Adenovirus E1B 55-kilodalton protein: multiple roles in viral infection and cell transformation. J Virol 83: 4000-4012.

Bochkov YA, Palmenberg AC. 2006. Translational efficiency of EMCV IRES in bicistronic vectors is dependent upon IRES sequence and gene location. Biotechniques 41: 283-284, 286, 288 passim.

Both GW. 2002. Identification of a unique family of F-box proteins in atadenoviruses. Virology 304: 425-433.

Both GW. 2004. Ovine atadenovirus: a review of its biology, biosafety profile and application as a gene delivery vector. Immunol Cell Biol 82: 189-195.

Both GW, Cameron F, Collins A, Lockett LJ, Shaw J. 2007. Production and release testing of ovine atadenovirus vectors. In: Adenovirus Methods and Protocols. W. S. M. Wold and A. E. Tollefson (Ed.). Totowa, New Jersey: Humana Press. pp.69-90.

Bremner KH, Scherer J, Yi J, Vershinin M, Gross SP, Vallee RB. 2009. Adenovirus transport via direct interaction of cytoplasmic dynein with the viral capsid hexon subunit. Cell Host Microbe 6: 523-535.

Brown MT, Mangel WF. 2004. Interaction of actin and its 11-amino acid C-terminal peptide as cofactors with the adenovirus proteinase. FEBS Lett 563: 213-218.

Brownlie R, Zhu J, Allan B, Mutwiri GK, Babiuk LA, Potter A, Griebel P. 2009. Chicken TLR21 acts as a functional homologue to mammalian TLR9 in the recognition of CpG oligodeoxynucleotides. Mol Immunol 46: 3163-3170.

Castiglia CL, Flint SJ. 1983. Effects of adenovirus infection on rRNA synthesis and maturation in HeLa cells. Mol Cell Biol 3: 662-671.

Cavanaugh A, Hirschler-Laszkiewicz I, Rothblum L. 2004. Ribosomal DNA transcription in mammals. In: The Nucleolus. M. Olson (Ed.). New York: Kluwer Academic/Plenum Publishers. pp.88-127.

Chardonnet Y, Dales S. 1970. Early events in the interaction of adenoviruses with HeLa cells. II. Comparative observations on the penetration of types 1, 5, 7, and 12. Virology 40: 478-485.

Chen H, Vinnakota R, Flint SJ. 1994. Intragenic activating and repressing elements control transcription from the adenovirus IVa2 initiator. Mol Cell Biol 14: 676-685.

Chen J, Morral N, Engel DA. 2007. Transcription releases protein VII from adenovirus chromatin. Virology 369: 411-422.

Chen M, Mermod N, Horwitz MS. 1990. Protein-protein interactions between adenovirus DNA polymerase and nuclear factor I mediate formation of the DNA replication preinitiation complex. J Biol Chem 265: 18634-18642.

Chen PH, Ornelles DA, Shenk T. 1993. The adenovirus L3 23-kilodalton proteinase cleaves the amino-terminal head domain from cytokeratin 18 and disrupts the cytokeratin network of HeLa cells. J Virol 67: 3507-3514.

Chin YR, Horwitz MS. 2006. Adenovirus RID complex enhances degradation of internalized tumour necrosis factor receptor 1 without affecting its rate of endocytosis. J Gen Virol 87: 3161-3167.

Chiocca S, Kurzbauer R, Schaffner G, Baker A, Mautner V, Cotten M. 1996. The complete DNA sequence and genomic organization of the avian adenovirus CELO. J Virol 70: 2939-2949.

Chow LT, Gelinas RE, Broker TR, Roberts RJ. 1977. An amazing sequence arrangement at the 5' ends of adenovirus 2 messenger RNA. Cell 12: 1-8.

Christophe D, Christophe-Hobertus C, Pichon B. 2000. Nuclear targeting of proteins: how many different signals? Cell Signal 12: 337-341.

Chroboczek J, Bieber F, Jacrot B. 1992. The sequence of the genome of adenovirus type 5 and its comparison with the genome of adenovirus type 2. Virology 186: 280-285.

Cingolani G, Petosa C, Weis K, Müller CW. 1999. Structure of importin-beta bound to the IBB domain of importin-alpha. Nature 399: 221-229.

Coenjaerts FE, van Oosterhout JA, van der Vliet PC. 1994. The Oct-1 POU domain stimulates adenovirus DNA replication by a direct interaction between the viral precursor terminal protein-DNA polymerase complex and the POU homeodomain. EMBO J 13: 5401-5409.

Cook A, Bono F, Jinek M, Conti E. 2007. Structural biology of nucleocytoplasmic transport. Annu Rev Biochem 76: 647-671.

Crawford-Miksza L, Schnurr DP. 1996. Analysis of 15 adenovirus hexon proteins reveals the location and structure of seven hypervariable regions containing serotype-specific residues. J Virol 70: 1836-1844.

Cuesta R, Xi Q, Schneider RJ. 2000. Adenovirus-specific translation by displacement of kinase Mnk1 from cap-initiation complex eIF4F. EMBO J 19: 3465-3474.

Cuesta R, Xi Q, Schneider RJ. 2004. Structural basis for competitive inhibition of eIF4G-Mnk1 interaction by the adenovirus 100-kilodalton protein. J Virol 78: 7707-7716.

D'Halluin JC, Martin GR, Torpier G, Boulanger PA. 1978a. Adenovirus type 2 assembly analyzed by reversible cross-linking of labile intermediates. J Virol 26: 357-363.

D'Halluin JC, Milleville M, Boulanger PA, Martin GR. 1978b. Temperature-sensitive mutant of adenovirus type 2 blocked in virion assembly: accumulation of light intermediate particles. J Virol 26: 344-356.

Darbyshire JH, Dawson PS, Lamont PH, Ostler DC, Pereira HG. 1965. A new adenovirus serotype of bovine origin. J Comp Pathol 75: 327-330.

Davison AJ, Benko M, Harrach B. 2003. Genetic content and evolution of adenoviruses. J Gen Virol 84: 2895-2908.

Davison AJ, Wright KM, Harrach B. 2000. DNA sequence of frog adenovirus. J Gen Virol 81: 2431-2439.

de Boer P, Vos HR, Faber AW, Vos JC, Raue HA. 2006. Rrp5p, a trans-acting factor in yeast ribosome biogenesis, is an RNA-binding protein with a pronounced preference for U-rich sequences. RNA 12: 263-271.

de Jong RN, van der Vliet PC, Brenkman AB. 2003. Adenovirus DNA replication: protein priming, jumping back and the role of the DNA binding protein DBP. Curr Top Microbiol Immunol 272: 187-211.

Deng W, Roberts SGE. 2007. TFIIB and the regulation of transcription by RNA polymerase II. Chromosoma 116: 417-429.

Depping R, Steinhoff A, Schindler SG, Friedrich B, Fagerlund R, Metzen E, Hartmann E, Köhler M. 2008. Nuclear translocation of hypoxia-inducible factors (HIFs): involvement of the classical importin alpha/beta pathway. Biochim Biophys Acta 1783: 394-404.

Ding J, McGrath WJ, Sweet RM, Mangel WF. 1996. Crystal structure of the human adenovirus proteinase with its 11 amino acid cofactor. EMBO J 15: 1778-1783.

Dobbelstein M, Roth J, Kimberly WT, Levine AJ, Shenk T. 1997. Nuclear export of the E1B 55-kDa and E4 34-kDa adenoviral oncoproteins mediated by a rev-like signal sequence. EMBO J 16: 4276-4284.

Dou S, Zeng X, Cortes P, Erdjument-Bromage H, Tempst P, Honjo T, Vales LD. 1994. The recombination signal sequence-binding protein RBP-2N functions as a transcriptional repressor. Mol Cell Biol 14: 3310-3319.

Efthymiadis A, Briggs LJ, Jans DA. 1998. The HIV-1 Tat nuclear localization sequence confers novel nuclear import properties. J Biol Chem 273: 1623-1628.

Enders JF, Bell JA, Dingle JH, Francis T, Hilleman MR, Huebner RJ, Payne AM. 1956. Adenoviruses: group name proposed for new respiratory-tract viruses. Science 124: 119-120.

Erturk E, Ostapchuk P, Wells SI, Yang J, Gregg K, Nepveu A, Dudley JP, Hearing P. 2003. Binding of CCAAT displacement protein CDP to adenovirus packaging sequences. J Virol 77: 6255-6264.

Everitt E, Lutter L, Philipson L. 1975. Structural proteins of adenoviruses. XII. Location and neighbor relationship among proteins of adenovirion type 2 as revealed by enzymatic iodination, immunoprecipitation and chemical cross-linking. Virology 67: 197-208.

Ewing SG, Byrd SA, Christensen JB, Tyler RE, Imperiale MJ. 2007. Ternary complex formation on the adenovirus packaging sequence by the IVa2 and L4 22-kilodalton proteins. J Virol 81: 12450-12457.

Ewton D, Hodes ME. 1967. Nucleic acid synthesis in HeLa cells infected with Shope fibroma virus. Virology 33: 77-83.

Fabry CMS, Rosa-Calatrava M, Conway JF, Zubieta C, Cusack S, Ruigrok RWH, Schoehn G. 2005. A quasi-atomic model of human adenovirus type 5 capsid. EMBO J 24: 1645-1654.

Fabry CMS, Rosa-Calatrava M, Moriscot C, Ruigrok RWH, Boulanger P, Schoehn G. 2009. The C-terminal domains of adenovirus serotype 5 protein IX assemble into an antiparallel structure on the facets of the capsid. J Virol 83: 1135-1139.

Fagotto F, Glück U, Gumbiner BM. 1998. Nuclear localization signal-independent and importin/karyopherin-independent nuclear import of beta-catenin. Curr Biol 8: 181-190.

Favier A-L, Schoehn G, Jaquinod M, Harsi C, Chroboczek J. 2002. Structural studies of human enteric adenovirus type 41. Virology 293: 75-85.

Fontes MR, Teh T, Kobe B. 2000. Structural basis of recognition of monopartite and bipartite nuclear localization sequences by mammalian importin-alpha. J Mol Biol 297: 1183-1194.

Fontoura BM, Blobel G, Yaseen NR. 2000. The nucleoporin Nup98 is a site for GDP/GTP exchange on ran and termination of karyopherin beta 2-mediated nuclear import. J Biol Chem 275: 31289-31296.

Fried H, Kutay U. 2003. Nucleocytoplasmic transport: taking an inventory. Cell Mol Life Sci 60: 1659-1688.

Friedrich B, Quensel C, Sommer T, Hartmann E, Kohler M. 2006. Nuclear localization signal and protein context both mediate importin alpha specificity of nuclear import substrates. Mol Cell Biol 26: 8697-8709.

Gallimore PH, Turnell AS. 2001. Adenovirus E1A: remodelling the host cell, a life or death experience. Oncogene 20: 7824-7835.

Gastaldelli M, Imelli N, Boucke K, Amstutz B, Meier O, Greber UF. 2008. Infectious adenovirus type 2 transport through early but not late endosomes. Traffic 9: 2265-2278.

Gerbi S, Borovjagin A. 2004. Pre-ribosomal RNA processing in multicellular organisms. In: The Nucleolus. M. Olson (Ed.). New York: Kluwer Academic/Plenum Publishers. pp.170-198.

Ghildyal R, Ho A, Wagstaff KM, Dias MM, Barton CL, Jans P, Bardin P, Jans DA. 2005. Nuclear import of the respiratory syncytial virus matrix protein is mediated by importin beta1 independent of importin alpha. Biochemistry 44: 12887-12895.

Gluzman Y. 1981. SV40-transformed simian cells support the replication of early SV40 mutants. Cell 23: 175-182.

Goff SP. 2007. Retroviridae: The retroviruses and their replication. In: Fields Virology, 5th ed. D. Knipe and P. Howley (Ed.). Philadelphia: Wolters Kluwer Health/Lippincott Williams & Wilkins. pp.2000-2069.

Goldberg S, Nevins J, Darnell JE. 1978. Evidence from UV transcription mapping that late adenovirus type 2 mRNA is derived from a large precursor molecule. J Virol 25: 806-810.

Goldfarb DS, Corbett AH, Mason DA, Harreman MT, Adam SA. 2004. Importin alpha: a multipurpose nuclear-transport receptor. Trends Cell Biol 14: 505-514.

Gooding LR, Elmore LW, Tollefson AE, Brady HA, Wold WS. 1988. A 14,700 MW protein from the E3 region of adenovirus inhibits cytolysis by tumor necrosis factor. Cell 53: 341-346.

Görlich D, Henklein P, Laskey RA, Hartmann E. 1996a. A 41 amino acid motif in importin-alpha confers binding to importin-beta and hence transit into the nucleus. EMBO J 15: 1810-1817.

Görlich D, Kraft R, Kostka S, Vogel F, Hartmann E, Laskey RA, Mattaj IW, Izaurralde E. 1996b. Importin provides a link between nuclear protein import and U snRNA export. Cell 87: 21-32.

Görlich D, Panté N, Kutay U, Aebi U, Bischoff FR. 1996c. Identification of different roles for RanGDP and RanGTP in nuclear protein import. EMBO J 15: 5584-5594.

Gorman JJ, Wallis TP, Whelan DA, Shaw J, Both GW. 2005. LH3, a "homologue" of the mastadenoviral E1B 55-kDa protein is a structural protein of atadenoviruses. Virology 342: 159-166.

Gräble M, Hearing P. 1990. Adenovirus type 5 packaging domain is composed of a repeated element that is functionally redundant. J Virol 64: 2047-2056.

Gräble M, Hearing P. 1992. cis and trans requirements for the selective packaging of adenovirus type 5 DNA. J Virol 66: 723-731.

Grand RJ, Parkhill J, Szestak T, Rookes SM, Roberts S, Gallimore PH. 1999. Definition of a major p53 binding site on Ad2E1B58K protein and a possible nuclear localization signal on the Ad12E1B54K protein. Oncogene 18: 955-965.

Greber U. 1998. Virus assembly and disassembly: the adenovirus cysteine protease as a trigger factor. Rev Med Virol 8: 213-222.

Greber UF, Willetts M, Webster P, Helenius A. 1993. Stepwise dismantling of adenovirus 2 during entry into cells. Cell 75: 477-486.

Gupta S, Mangel WF, McGrath WJ, Perek JL, Lee DW, Takamoto K, Chance MR. 2004. DNA binding provides a molecular strap activating the adenovirus proteinase. Mol Cell Proteomics 3: 950-959.

Gustin KE, Imperiale MJ. 1998. Encapsidation of viral DNA requires the adenovirus L1 52/55-kilodalton protein. J Virol 72: 7860-7870.

Gustin KE, Lutz P, Imperiale MJ. 1996. Interaction of the adenovirus L1 52/55-kilodalton protein with the IVa2 gene product during infection. J Virol 70: 6463-6467.

Hadjiolova KV, Nicoloso M, Mazan S, Hadjiolov AA, Bachellerie JP. 1993. Alternative pre-rRNA processing pathways in human cells and their alteration by cycloheximide inhibition of protein synthesis. Eur J Biochem 212: 211-215.

Hanover JA, Love DC, Prinz WA. 2009. Calmodulin-driven nuclear entry: trigger for sex determination and terminal differentiation. J Biol Chem 284: 12593-12597.

Harrach B. 2000. Reptile adenoviruses in cattle? Acta Vet Hung 48: 485-490.

Hasson TB, Ornelles DA, Shenk T. 1992. Adenovirus L1 52- and 55-kilodalton proteins are present within assembling virions and colocalize with nuclear structures distinct from replication centers. J Virol 66: 6133-6142.

Hasson TB, Soloway PD, Ornelles DA, Doerfler W, Shenk T. 1989. Adenovirus L1 52- and 55-kilodalton proteins are required for assembly of virions. J Virol 63: 3612-3621.

Hearps AC, Jans DA. 2006. HIV-1 integrase is capable of targeting DNA to the nucleus via an importin alpha/beta-dependent mechanism. Biochem J 398: 475-484.

Henras AK, Soudet J, Gérus M, Lebaron S, Caizergues-Ferrer M, Mougin A, Henry Y. 2008. The post-transcriptional steps of eukaryotic ribosome biogenesis. Cell Mol Life Sci 65: 2334-2359.

Herold A, Truant R, Wiegand H, Cullen BR. 1998. Determination of the functional domain organization of the importin alpha nuclear import factor. J Cell Biol 143: 309-318.

Hilleman MR, Werner JH. 1954. Recovery of new agent from patients with acute respiratory illness. Proc Soc Exp Biol Med 85: 183-188.

Hindley CE, Lawrence FJ, Matthews DA. 2007. A role for transportin in the nuclear import of adenovirus core proteins and DNA. Traffic 8: 1313-1322.

Hiscox JA. 2002. The nucleolus--a gateway to viral infection? Arch Virol 147: 1077-1089.

Hong JS, Engler JA. 1991. The amino terminus of the adenovirus fiber protein encodes the nuclear localization signal. Virology 185: 758-767.

Hong SS, Szolajska E, Schoehn G, Franqueville L, Myhre S, Lindholm L, Ruigrok RWH, Boulanger P, Chroboczek J. 2005. The 100K-chaperone protein from adenovirus serotype 2 (Subgroup C) assists in trimerization and nuclear localization of hexons from subgroups C and B adenoviruses. J Mol Biol 352: 125-138.

Horwitz MS. 2004. Function of adenovirus E3 proteins and their interactions with immunoregulatory cell proteins. J Gene Med 6 (Suppl 1): S172-183.

Horwitz MS, Scharff MD, Maizel JV. 1969. Synthesis and assembly of adenovirus 2. I. Polypeptide synthesis, assembly of capsomeres, and morphogenesis of the virion. Virology 39: 682-694.

Hu SL, Hays WW, Potts DE. 1984. Sequence homology between bovine and human adenoviruses. J Virol 49: 604-608.

Idamakanti N, Reddy PS, Babiuk LA, Tikoo SK. 1999. Transcription mapping and characterization of 284R and 121R proteins produced from early region 3 of bovine adenovirus type 3. Virology 256: 351-359.

Iftode C, Flint SJ. 2004. Viral DNA synthesis-dependent titration of a cellular repressor activates transcription of the human adenovirus type 2 IVa2 gene. Proc Natl Acad Sci USA 101: 17831-17836.

Imamoto N, Shimamoto T, Takao T, Tachibana T, Kose S, Matsubae M, Sekimoto T, Shimonishi Y, Yoneda Y. 1995. In vivo evidence for involvement of a 58 kDa component of nuclear pore-targeting complex in nuclear protein import. EMBO J 14: 3617-3626.

Imperiale MJ, Akusjnärvi G, Leppard KN. 1995. Post-transcriptional control of adenovirus gene expression. Curr Top Microbiol Immunol 199: 139-171.

Ishiko H, Aoki K. 2009. Spread of epidemic keratoconjunctivitis due to a novel serotype of human adenovirus in Japan. J Clin Microbiol 47: 2678-2679.

Ishiko H, Shimada Y, Konno T, Hayashi A, Ohguchi T, Tagawa Y, Aoki K, Ohno S, Yamazaki S. 2008. Novel human adenovirus causing nosocomial epidemic keratoconjunctivitis. J Clin Microbiol 46: 2002-2008.

Jäkel S, Görlich D. 1998. Importin beta, transportin, RanBP5 and RanBP7 mediate nuclear import of ribosomal proteins in mammalian cells. EMBO J 17: 4491-4502.

Jenkins Y, McEntee M, Weis K, Greene WC. 1998. Characterization of HIV-1 vpr nuclear import: analysis of signals and pathways. J Cell Biol 143: 875-885.

Johnson JS, Osheim YN, Xue Y, Emanuel MR, Lewis PW, Bankovich A, Beyer AL, Engel DA. 2004. Adenovirus protein VII condenses DNA, represses transcription, and associates with transcriptional activator E1A. J Virol 78: 6459-6468.

Jones MS, 2nd, Harrach B, Ganac RD, Gozum MM, Dela Cruz WP, Riedel B, Pan C, Delwart EL, Schnurr DP. 2007. New adenovirus species found in a patient presenting with gastroenteritis. J Virol 81: 5978-5984.

Kalderon D, Richardson WD, Markham AF, Smith AE. 1984. Sequence requirements for nuclear location of simian virus 40 large-T antigen. Nature 311: 33-38.

Katoh H, Ohya K, Kubo M, Murata K, Yanai T, Fukushi H. 2009. A novel budgerigar-adenovirus belonging to group II avian adenovirus of Siadenovirus. Virus Res 144: 294-297.

Kauffman RS, Ginsberg HS. 1976. Characterization of a temperature-sensitive, hexon transport mutant of type 5 adenovirus. J Virol 19: 643-658.

King AJ, Teertstra WR, Blanco L, Salas M, van der Vliet PC. 1997. Processive proofreading by the adenovirus DNA polymerase. Association with the priming protein reduces exonucleolytic degradation. Nucleic Acids Res 25: 1745-1752.

King AJ, van der Vliet PC. 1994. A precursor terminal protein-trinucleotide intermediate during initiation of adenovirus DNA replication: regeneration of molecular ends in vitro by a jumping back mechanism. EMBO J 13: 5786-5792.

Klebe C, Bischoff FR, Ponstingl H, Wittinghofer A. 1995. Interaction of the nuclear GTP-binding protein Ran with its regulatory proteins RCC1 and RanGAP1. Biochemistry 34: 639-647.

Kobe B. 1999. Autoinhibition by an internal nuclear localization signal revealed by the crystal structure of mammalian importin alpha. Nat Struct Biol 6: 388-397.

Kohler M, Gorlich D, Hartmann E, Franke J. 2001. Adenoviral E1A protein nuclear import is preferentially mediated by importin alpha3 in vitro. Virology 289: 186-191.

Köhler M, Speck C, Christiansen M, Bischoff FR, Prehn S, Haller H, Görlich D, Hartmann E. 1999. Evidence for distinct substrate specificities of importin alpha family members in nuclear protein import. Mol Cell Biol 19: 7782-7791.

Kojaoghlanian T, Flomenberg P, Horwitz MS. 2003. The impact of adenovirus infection on the immunocompromised host. Rev Med Virol 13: 155-171.

Kose S, Imamoto N, Tachibana T, Shimamoto T, Yoneda Y. 1997. Ran-unassisted nuclear migration of a 97-kD component of nuclear pore-targeting complex. J Cell Biol 139: 841-849.

Kovács ER, Benko M. 2009. Confirmation of a novel siadenovirus species detected in raptors: partial sequence and phylogenetic analysis. Virus Res 140: 64-70.

Kovács ER, Jánoska M, Dán A, Harrach B, Benko M. 2010. Recognition and partial genome characterization by non-specific DNA amplification and PCR of a new siadenovirus species in a sample originating from Parus major, a great tit. J Virol Methods 163: 262-268.

Kovács GM, LaPatra SE, D'Halluin JC, Benko M. 2003. Phylogenetic analysis of the hexon and protease genes of a fish adenovirus isolated from white sturgeon (Acipenser transmontanus) supports the proposal for a new adenovirus genus. Virus Res 98: 27-34.

Koyuncu OO, Dobner T. 2009. Arginine methylation of human adenovirus type 5 L4 100-kilodalton protein is required for efficient virus production. J Virol 83: 4778-4790.

Kulshreshtha V. 2009. Molecular characterization of 33K protein of bovine adenovirus type 3. PhD Thesis, University of Saskatchewan, Saskatoon. 132 p.

Kulshreshtha V, Babiuk LA, Tikoo SK. 2004. Role of bovine adenovirus-3 33K protein in viral replication. Virology 323: 59-69.

Kulshreshtha V, Tikoo SK. 2008. Interaction of bovine adenovirus-3 33K protein with other viral proteins. Virology 381: 29-35.

Kutay U, Bischoff FR, Kostka S, Kraft R, Görlich D. 1997. Export of importin alpha from the nucleus is mediated by a specific nuclear transport factor. Cell 90: 1061-1071.

Kutay U, Lipowsky G, Izaurralde E, Bischoff FR, Schwarzmaier P, Hartmann E, Görlich D. 1998. Identification of a tRNA-specific nuclear export receptor. Mol Cell 1: 359-369.

La Rosa AM, Champlin RE, Mirza N, Gajewski J, Giralt S, Rolston KV, Raad I, Jacobson K, Kontoyiannis D, Elting L, Whimbey E. 2001. Adenovirus infections in adult recipients of blood and marrow transplants. Clin Infect Dis 32: 871-876.

Lacana E, D'Adamio L. 1999. Regulation of Fas ligand expression and cell death by apoptosis-linked gene 4. Nat Med 5: 542-547.

Lai MC, Lin RI, Tarn WY. 2001. Transportin-SR2 mediates nuclear import of phosphorylated SR proteins. Proc Natl Acad Sci USA 98: 10154-10159.

Lam YW, Evans VC, Heesom KJ, Lamond AI, Matthews DA. 2010. Proteomics analysis of the nucleolus in adenovirus-infected cells. Mol Cell Proteomics 9: 117-130.

Lawler SH, Jones RW, Eliceiri BP, Eliceiri GL. 1989. Adenovirus infection retards ribosomal RNA processing. J Cell Physiol 138: 205-207.

Lawrence FJ, McStay B, Matthews DA. 2006. Nucleolar protein upstream binding factor is sequestered into adenovirus DNA replication centres during infection without affecting RNA polymerase I location or ablating rRNA synthesis. J Cell Sci 119: 2621-2631.

Lechner RL, Kelly TJ. 1977. The structure of replicating adenovirus 2 DNA molecules. Cell 12: 1007-1020.

Ledinko N. 1972. Nucleolar ribosomal precursor RNA and protein metabolism in human embryo kidney cultures infected with adenovirus 12. Virology 49: 79-89.

Lee J, Lee HJ, Shin MK, Ryu WS. 2004a. Versatile PCR-mediated insertion or deletion mutagenesis. Biotechniques 36: 398-400.

Lee TW, Blair GE, Matthews DA. 2003. Adenovirus core protein VII contains distinct sequences that mediate targeting to the nucleus and nucleolus, and colocalization with human chromosomes. J Gen Virol 84: 3423-3428.

Lee TW, Lawrence FJ, Dauksaite V, Akusjarvi G, Blair GE, Matthews DA. 2004b. Precursor of human adenovirus core polypeptide Mu targets the nucleolus and modulates the expression of E2 proteins. J Gen Virol 85: 185-196.

Leen AM, Rooney CM. 2005. Adenovirus as an emerging pathogen in immunocompromised patients. Br J Haematol 128: 135-144.

Lehmkuhl HD, Hobbs LA. 2008. Serologic and hexon phylogenetic analysis of ruminant adenoviruses. Arch virology 153: 891-897.

Lehmkuhl HD, Smith MH, Dierks RE. 1975. A bovine adenovirus type 3: isolation, characterization, and experimental infection in calves. Arch virology 48: 39-46.

Lehrmann H, Cotten M. 1999. Characterization of CELO virus proteins that modulate the pRb/E2F pathway. J Virol 73: 6517-6525.

Lempiäinen H, Shore D. 2009. Growth control and ribosome biogenesis. Curr Opin Cell Biol 21: 855-863.

Leong K, Lee W, Berk AJ. 1990. High-level transcription from the adenovirus major late promoter requires downstream binding sites for late-phase-specific factors. J Virol 64: 51-60.

Leopold PL, Crystal RG. 2007. Intracellular trafficking of adenovirus: many means to many ends. Adv Drug Deliv Rev 59: 810-821.

Leopold PL, Kreitzer G, Miyazawa N, Rempel S, Pfister KK, Rodriguez-Boulan E, Crystal RG. 2000. Dynein- and microtubule-mediated translocation of adenovirus serotype 5 occurs after endosomal lysis. Hum Gene Ther 11: 151-165.

Li E, Stupack D, Bokoch GM, Nemerow GR. 1998a. Adenovirus endocytosis requires actin cytoskeleton reorganization mediated by Rho family GTPases. J Virol 72: 8806-8812.

Li E, Stupack D, Klemke R, Cheresh DA, Nemerow GR. 1998b. Adenovirus endocytosis via alpha(v) integrins requires phosphoinositide-3-OH kinase. J Virol 72: 2055-2061.

Li X, Bangari DS, Sharma A, Mittal SK. 2009. Bovine adenovirus serotype 3 utilizes sialic acid as a cellular receptor for virus entry. Virology 392: 162-168.

Lim RYH, Aebi U, Fahrenkrog B. 2008. Towards reconciling structure and function in the nuclear pore complex. Histochem Cell Biol 129: 105-116.

Lin HJ, Flint SJ. 2000. Identification of a cellular repressor of transcription of the adenoviral late IVa(2) gene that is unaltered in activity in infected cells. Virology 277: 397-410.

Liu F, Green MR. 1994. Promoter targeting by adenovirus E1a through interaction with different cellular DNA-binding domains. Nature 368: 520-525.

Lucher LA, Symington JS, Green M. 1986. Biosynthesis and properties of the adenovirus 2 L1-encoded 52,000- and 55,000-Mr proteins. J Virol 57: 839-847.

Lutz P, Kedinger C. 1996. Properties of the adenovirus IVa2 gene product, an effector of late-phase-dependent activation of the major late promoter. J Virol 70: 1396-1405.

Lutz P, Puvion-Dutilleul F, Lutz Y, Kedinger C. 1996. Nucleoplasmic and nucleolar distribution of the adenovirus IVa2 gene product. J Virol 70: 3449-3460.

Lyles DS, Rupprecht CE. 2007. Rhabdoviridae. In: Fields Virology, 5th ed. D. Knipe and P. Howley (Ed.). Philadelphia: Wolters Kluwer Health/Lippincott Williams & Wilkins. pp.1364-1408.

Lyons RH, Ferguson BQ, Rosenberg M. 1987. Pentapeptide nuclear localization signal in adenovirus E1a. Mol Cell Biol 7: 2451-2456.

Mangel WF, Toledo DL, Ding J, Sweet RM, McGrath WJ. 1997. Temporal and spatial control of the adenovirus proteinase by both a peptide and the viral DNA. Trends Biochem Sci 22: 393-398.

Marttila M, Persson D, Gustafsson D, Liszewski MK, Atkinson JP, Wadell G, Arnberg N. 2005. CD46 is a cellular receptor for all species B adenoviruses except types 3 and 7. J Virol 79: 14429-14436.

Mathews MB, Shenk T. 1991. Adenovirus virus-associated RNA and translation control. J Virol 65: 5657-5662.

Matthews DA. 2001. Adenovirus protein V induces redistribution of nucleolin and B23 from nucleolus to cytoplasm. J Virol 75: 1031-1038.

Mautner V, Steinthorsdottir V, Bailey A. 1995. Enteric adenoviruses. Curr Top Microbiol Immunol 199: 229-282.

McLaughlin-Drubin ME, Munger K. 2008. Viruses associated with human cancer. Biochim Biophys Acta 1782: 127-150.

McSharry BP, Burgert H-G, Owen DP, Stanton RJ, Prod'homme V, Sester M, Koebernick K, Groh V, Spies T, Cox S, Little A-M, Wang ECY, Tomasec P, Wilkinson GWG. 2008. Adenovirus E3/19K promotes evasion of NK cell recognition by intracellular sequestration of the NKG2D ligands major histocompatibility complex class I chain-related proteins A and B. J Virol 82: 4585-4594.

Melen K, Fagerlund R, Franke J, Kohler M, Kinnunen L, Julkunen I. 2003. Importin alpha nuclear localization signal binding sites for STAT1, STAT2, and influenza A virus nucleoprotein. J Biol Chem 278: 28193-28200.

Mettenleiter TC, Klupp BG, Granzow H. 2009. Herpesvirus assembly: an update. Virus Res 143: 222-234.

Michael WM, Eder PS, Dreyfuss G. 1997. The K nuclear shuttling domain: a novel signal for nuclear import and nuclear export in the hnRNP K protein. EMBO J 16: 3587-3598.

Michou AI, Lehrmann H, Saltik M, Cotten M. 1999. Mutational analysis of the avian adenovirus CELO, which provides a basis for gene delivery vectors. J Virol 73: 1399-1410.

Miller JS, Ricciardi RP, Roberts BE, Paterson BM, Mathews MB. 1980. Arrangement of messenger RNAs and protein coding sequences in the major late transcription unit of adenovirus 2. J Mol Biol 142: 455-488.

Mittal SK, Middleton DM, Tikoo SK, Babiuk LA. 1995. Pathogenesis and immunogenicity of bovine adenovirus type 3 in cotton rats (Sigmodon hispidus). Virology 213: 131-139.

Mittal SK, Prevec L, Babiuk LA, Graham FL. 1992. Sequence analysis of bovine adenovirus type 3 early region 3 and fibre protein genes. J Gen Virol 73 (Pt 12): 3295-3300.

Mittal SK, Tikoo SK, Van Donkersgoed J, Beskorwayne T, Godson DL, Babiuk LA. 1999. Experimental inoculation of heifers with bovine adenovirus type 3. Can J Vet Res 63: 153-156.

Miyamoto Y, Imamoto N, Sekimoto T, Tachibana T, Seki T, Tada S, Enomoto T, Yoneda Y. 1997. Differential modes of nuclear localization signal (NLS) recognition by three distinct classes of NLS receptors. J Biol Chem 272: 26375-26381.

Miyazawa N, Crystal RG, Leopold PL. 2001. Adenovirus serotype 7 retention in a late endosomal compartment prior to cytosol escape is modulated by fiber protein. J Virol 75: 1387-1400.

Morris SJ, Leppard KN. 2009. Adenovirus serotype 5 L4-22K and L4-33K proteins have distinct functions in regulating late gene expression. J Virol 83: 3049-3058.

Moss B. 2007. Poxviridae: The viruses and their replication. In: Fields Virology, 5th ed. D. Knipe and P. Howley (Ed.). Philadelphia: Wolters Kluwer Health/Lippincott Williams & Wilkins. pp.2906-2945.

Mul YM, van der Vliet PC. 1992. Nuclear factor I enhances adenovirus DNA replication by increasing the stability of a preinitiation complex. EMBO J 11: 751-760.

Mul YM, Verrijzer CP, van der Vliet PC. 1990. Transcription factors NFI and NFIII/oct-1 function independently, employing different mechanisms to enhance adenovirus DNA replication. J Virol 64: 5510-5518.

Nagata K, Guggenheimer RA, Hurwitz J. 1983. Adenovirus DNA replication in vitro: synthesis of full-length DNA with purified proteins. Proc Natl Acad Sci USA 80: 4266-4270.

Nakano MY, Boucke K, Suomalainen M, Stidwill RP, Greber UF. 2000. The first step of adenovirus type 2 disassembly occurs at the cell surface, independently of endocytosis and escape to the cytosol. J Virol 74: 7085-7095.

Nakielny S, Dreyfuss G. 1998. Import and export of the nuclear protein import receptor transportin by a mechanism independent of GTP hydrolysis. Curr Biol 8: 89-95.

Nazar RN. 2004. Ribosomal RNA processing and ribosome biogenesis in eukaryotes. IUBMB Life 56: 457-465.

Nemergut ME, Mizzen CA, Stukenberg T, Allis CD, Macara IG. 2001. Chromatin docking and exchange activity enhancement of RCC1 by histones H2A and H2B. Science 292: 1540-1543.

Nevins JR, Ginsberg HS, Blanchard JM, Wilson MC, Darnell JE. 1979. Regulation of the primary expression of the early adenovirus transcription units. J Virol 32: 727-733.

Niiyama Y, Igarashi K, Tsukamoto K, Kurokawa T, Sugino Y. 1975. Biochemical studies on bovine adenovirus type 3. I. Purification and properties. J Virol 16: 621-633.

O'Brien TP, Jeng BH, McDonald M, Raizman MB. 2009. Acute conjunctivitis: truth and misconceptions. Curr Med Res Opin 25: 1953-1961.

O'Malley RP, Mariano TM, Siekierka J, Mathews MB. 1986. A mechanism for the control of protein synthesis by adenovirus VA RNAI. Cell 44: 391-400.

O'Shea C, Klupsch K, Choi S, Bagus B, Soria C, Shen J, McCormick F, Stokoe D. 2005. Adenoviral proteins mimic nutrient/growth signals to activate the mTOR pathway for viral replication. EMBO J 24: 1211-1221.

Obert S, O'Connor RJ, Schmid S, Hearing P. 1994. The adenovirus E4-6/7 protein transactivates the E2 promoter by inducing dimerization of a heteromeric E2F complex. Mol Cell Biol 14: 1333-1346.

Ojkic D, Nagy E. 2000. The complete nucleotide sequence of fowl adenovirus type 8. J Gen Virol 81: 1833-1837.

Ostapchuk P, Anderson ME, Chandrasekhar S, Hearing P. 2006. The L4 22-kilodalton protein plays a role in packaging of the adenovirus genome. J Virol 80: 6973-6981.

Ostapchuk P, Hearing P. 2005. Control of adenovirus packaging. J Cell Biochem 96: 25-35.

Ostapchuk P, Hearing P. 2008. Adenovirus IVa2 protein binds ATP. J Virol 82: 10290-10294.

Ostapchuk P, Yang J, Auffarth E, Hearing P. 2005. Functional interaction of the adenovirus IVa2 protein with adenovirus type 5 packaging sequences. J Virol 79: 2831-2838.

Pääbo S, Bhat BM, Wold WS, Peterson PA. 1987. A short sequence in the COOH-terminus makes an adenovirus membrane glycoprotein a resident of the endoplasmic reticulum. Cell 50: 311-317.

Palmeri D, Malim MH. 1999. Importin beta can mediate the nuclear import of an arginine-rich nuclear localization signal in the absence of importin alpha. Mol Cell Biol 19: 1218-1225.

Parks CL, Shenk T. 1997. Activation of the adenovirus major late promoter by transcription factors MAZ and Sp1. J Virol 71: 9600-9607.

Patel AK, Tikoo SK. 2006. 293T cells expressing simian virus 40 T antigen are semi-permissive to bovine adenovirus type 3 infection. J Gen Virol 87: 817-821.

Pellett PE, Roizman B. 2007. The Family Herpesviridae: A Brief Introduction. In: Fields Virology, 5th ed. D. Knipe and P. Howley (Ed.). Philadelphia: Wolters Kluwer Health/Lippincott Williams & Wilkins.

Pérez-Fernández J, Román A, De Las Rivas J, Bustelo XR, Dosil M. 2007. The 90S preribosome is a multimodular structure that is assembled through a hierarchical mechanism. Mol Cell Biol 27: 5414-5429.

Perez-Romero P, Gustin KE, Imperiale MJ. 2006. Dependence of the encapsidation function of the adenovirus L1 52/55-kilodalton protein on its ability to bind the packaging sequence. J Virol 80: 1965-1971.

Perez-Romero P, Tyler RE, Abend JR, Dus M, Imperiale MJ. 2005. Analysis of the interaction of the adenovirus L1 52/55-kilodalton and IVa2 proteins with the packaging sequence in vivo and in vitro. J Virol 79: 2366-2374.

Perricaudet M, Akusjärvi G, Virtanen A, Pettersson U. 1979. Structure of two spliced mRNAs from the transforming region of human subgroup C adenoviruses. Nature 281: 694-696.

Pitcovski J, Mualem M, Rei-Koren Z, Krispel S, Shmueli E, Peretz Y, Gutter B, Gallili GE, Michael A, Goldberg D. 1998. The complete DNA sequence and genome organization of the avian adenovirus, hemorrhagic enteritis virus. Virology 249: 307-315.

Pollard VW, Michael WM, Nakielny S, Siomi MC, Wang F, Dreyfuss G. 1996. A novel receptor-mediated nuclear protein import pathway. Cell 86: 985-994.

Ponti D, Troiano M, Bellenchi GC, Battaglia PA, Gigliani F. 2008. The HIV Tat protein affects processing of ribosomal RNA precursor. BMC Cell Biol 9: 32.

Querido E, Morrison MR, Chu-Pham-Dang H, Thirlwell SW, Boivin D, Branton PE, Morisson MR. 2001. Identification of three functions of the adenovirus e4orf6 protein that mediate p53 degradation by the E4orf6-E1B55K complex. J Virol 75: 699-709.

Rajendra Kumar P, Singhal PK, Vinod SS, Mahalingam S. 2003. A non-canonical transferable signal mediates nuclear import of simian immunodeficiency virus Vpx protein. J Mol Biol 331: 1141-1156.

Rao VB, Feiss M. 2008. The bacteriophage DNA packaging motor. Annu Rev Genet 42: 647-681.

Raskas HJ, Thomas DC, Green M. 1970. Biochemical studies on adenovirus multiplication. XVII. Ribosome synthesis in uninfected and infected KB cells. Virology 40: 893-902.

Rasmussen UB, Benchaibi M, Meyer V, Schlesinger Y, Schughart K. 1999. Novel human gene transfer vectors: evaluation of wild-type and recombinant animal adenoviruses in human-derived cells. Hum Gene Ther 10: 2587-2599.

Reach M, Xu LX, Young CS. 1991. Transcription from the adenovirus major late promoter uses redundant activating elements. EMBO J 10: 3439-3446.

Reddy PS, Chen Y, Idamakanti N, Pyne C, Babiuk LA, Tikoo SK. 1999a. Characterization of early region 1 and pIX of bovine adenovirus-3. Virology 253: 299-308.

Reddy PS, Idamakanti N, Chen Y, Whale T, Babiuk LA, Mehtali M, Tikoo SK. 1999b. Replication-defective bovine adenovirus type 3 as an expression vector. J Virol 73: 9137-9144.

Reddy PS, Idamakanti N, Zakhartchouk AN, Baxi MK, Lee JB, Pyne C, Babiuk LA, Tikoo SK. 1998. Nucleotide sequence, genome organization, and transcription map of bovine adenovirus type 3. J Virol 72: 1394-1402.

Rekosh DM, Russell WC, Bellet AJ, Robinson AJ. 1977. Identification of a protein linked to the ends of adenovirus DNA. Cell 11: 283-295.

Rivera S, Wellehan JFX, McManamon R, Innis CJ, Garner MM, Raphael BL, Gregory CR, Latimer KS, Rodriguez CE, Diaz-Figueroa O, Marlar AB, Nyaoke A, Gates AE, Gilbert K, Childress AL, Risatti GR, Frasca S. 2009. Systemic adenovirus infection in Sulawesi tortoises (Indotestudo forsteni) caused by a novel siadenovirus. J Vet Diagn Invest 21: 415-426.

Robbins J, Dilworth SM, Laskey RA, Dingwall C. 1991. Two interdependent basic domains in nucleoplasmin nuclear targeting sequence: identification of a class of bipartite nuclear targeting sequence. Cell 64: 615-623.

Roelvink PW, Lizonova A, Lee JG, Li Y, Bergelson JM, Finberg RW, Brough DE, Kovesdi I, Wickham TJ. 1998. The coxsackievirus-adenovirus receptor protein can function as a cellular attachment protein for adenovirus serotypes from subgroups A, C, D, E, and F. J Virol 72: 7909-7915.

Rowe WP, Huebner RJ, Gilmore LK, Parrott RH, Ward TG. 1953. Isolation of a cytopathogenic agent from human adenoids undergoing spontaneous degeneration in tissue culture. Proc Soc Exp Biol Med 84: 570-573.

Ruigrok RW, Barge A, Mittal SK, Jacrot B. 1994. The fibre of bovine adenovirus type 3 is very long but bent. J Gen Virol 75: 2069-2073.

Russell WC. 2009. Adenoviruses: update on structure and function. J Gen Virol 90: 1-20.

Sachdev S, Bagchi S, Zhang DD, Mings AC, Hannink M. 2000. Nuclear import of IkappaBalpha is accomplished by a ran-independent transport pathway. Mol Cell Biol 20: 1571-1582.

Salzman NP, Shatkin AJ, Sebring ED. 1964. The synthesis of a DNA-like RNA in the cytoplasm of HeLa cells infected with vaccinia virus. J Mol Biol 8: 405-416.

San Martín C, Glasgow JN, Borovjagin A, Beatty MS, Kashentseva EA, Curiel DT, Marabini R, Dmitriev IP. 2008. Localization of the N-terminus of minor coat protein IIIa in the adenovirus capsid. J Mol Biol 383: 923-934.

Saphire AC, Guan T, Schirmer EC, Nemerow GR, Gerace L. 2000. Nuclear import of adenovirus DNA in vitro involves the nuclear protein import pathway and hsc70. J Biol Chem 275: 4298-4304.

Sawadogo M, Roeder RG. 1985. Interaction of a gene-specific transcription factor with the adenovirus major late promoter upstream of the TATA box region. Cell 43: 165-175.

Schaack J, Schedl P, Shenk T. 1990. Topoisomerase I and II cleavage of adenovirus DNA in vivo: both topoisomerase activities appear to be required for adenovirus DNA replication. J Virol 64: 78-85.

Schaley JE, Polonskaia M, Hearing P. 2005. The adenovirus E4-6/7 protein directs nuclear localization of E2F-4 via an arginine-rich motif. J Virol 79: 2301-2308.

Schmid SI, Hearing P. 1997. Bipartite structure and functional independence of adenovirus type 5 packaging elements. J Virol 71: 3375-3384.

Schmid SI, Hearing P. 1998. Cellular components interact with adenovirus type 5 minimal DNA packaging domains. J Virol 72: 6339-6347.

Schneider-Brachert W, Tchikov V, Merkel O, Jakob M, Hallas C, Kruse M-L, Groitl P, Lehn A, Hildt E, Held-Feindt J, Dobner T, Kabelitz D, Krönke M, Schütze S. 2006. Inhibition of TNF receptor 1 internalization by adenovirus 14.7K as a novel immune escape mechanism. J Clin Invest 116: 2901-2913.

Seki T, Tada S, Katada T, Enomoto T. 1997. Cloning of a cDNA encoding a novel importin-alpha homologue, Qip1: discrimination of Qip1 and Rch1 from hSrp1 by their ability to interact with DNA helicase Q1/RecQL. Biochem Biophys Res Commun 234: 48-53.

Sekimoto T, Imamoto N, Nakajima K, Hirano T, Yoneda Y. 1997. Extracellular signal-dependent nuclear import of Stat1 is mediated by nuclear pore-targeting complex formation with NPI-1, but not Rch1. EMBO J 16: 7067-7077.

Sessler RJ, Noy N. 2005. A ligand-activated nuclear localization signal in cellular retinoic acid binding protein-II. Mol Cell 18: 343-353.

Shaw AR, Ziff EB. 1980. Transcripts from the adenovirus-2 major late promoter yield a single early family of 3' coterminal mRNAs and five late families. Cell 22: 905-916.

Shayakhmetov DM, Li Z-Y, Ternovoi V, Gaggar A, Gharwan H, Lieber A. 2003. The interaction between the fiber knob domain and the cellular attachment receptor determines the intracellular trafficking route of adenoviruses. J Virol 77: 3712-3723.

Shenk T. 2001. Adenoviridae: The viruses and their replication. In: Fields Virology, 4th ed. D. Knipe and P. Howley (Ed.). Philadelphia: Lippincott Williams & Wilkins. pp.2265-2300.

Sheoran IS, Olson DJ, Ross AR, Sawhney VK. 2005. Proteome analysis of embryo and endosperm from germinating tomato seeds. Proteomics 5: 3752-3764.

Shinagawa M, Iida Y, Matsuda A, Tsukiyama T, Sato G. 1987. Phylogenetic relationships between adenoviruses as inferred from nucleotide sequences of inverted terminal repeats. Gene 55: 85-93.

Shisler J, Yang C, Walter B, Ware CF, Gooding LR. 1997. The adenovirus E3-10.4K/14.5K complex mediates loss of cell surface Fas (CD95) and resistance to Fas-induced apoptosis. J Virol 71: 8299-8306.

Short JJ, Vasu C, Holterman MJ, Curiel DT, Pereboev A. 2006. Members of adenovirus species B utilize CD80 and CD86 as cellular attachment receptors. Virus Res 122: 144-153.

Singh M, Shmulevitz M, Tikoo SK. 2005. A newly identified interaction between IVa2 and pVIII proteins during porcine adenovirus type 3 infection. Virology 336: 60-69.

Siomi H, Dreyfuss G. 1995. A nuclear localization domain in the hnRNP A1 protein. J Cell Biol 129: 551-560.

Smyth JA, Benkö M, Moffett DA, Harrach B. 1996. Bovine adenovirus type 10 identified in fatal cases of adenovirus-associated enteric disease in cattle by in situ hybridization. J Clin Microbiol 34: 1270-1274.

Soudais C, Boutin S, Hong SS, Chillon M, Danos O, Bergelson JM, Boulanger P, Kremer EJ. 2000. Canine adenovirus type 2 attachment and internalization: coxsackievirus-adenovirus receptor, alternative receptors, and an RGD-independent pathway. J Virol 74: 10639-10649.

Soudais C, Boutin S, Kremer EJ. 2001. Characterization of cis-acting sequences involved in canine adenovirus packaging. Mol Ther 3: 631-640.

Spurgeon ME, Ornelles DA. 2009. The adenovirus E1B 55-kilodalton and E4 open reading frame 6 proteins limit phosphorylation of eIF2alpha during the late phase of infection. J Virol 83: 9970-9982.

Stochaj U, Rother K. 1999. Nucleocytoplasmic trafficking of proteins: With or without Ran? Bioessays 21: 579-589.

Strunze S, Trotman LC, Boucke K, Greber UF. 2005. Nuclear targeting of adenovirus type 2 requires CRM1-mediated nuclear export. Mol Biol Cell 16: 2999-3009.

Stuiver MH, van der Vliet PC. 1990. Adenovirus DNA-binding protein forms a multimeric protein complex with double-stranded DNA and enhances binding of nuclear factor I. J Virol 64: 379-386.

Sundquist B, Everitt E, Philipson L, Hoglund S. 1973. Assembly of adenoviruses. J Virol 11: 449-459.

Sweet T, Khalili K, Sawaya BE, Amini S. 2003. Identification of a novel protein from glial cells based on its ability to interact with NF-kappaB subunits. J Cell Biochem 90: 884-891.

Sweet T, Sawaya BE, Khalili K, Amini S. 2005. Interplay between NFBP and NF-kappaB modulates tat activation of the LTR. J Cell Physiol 204: 375-380.

Sweet T, Yen W, Khalili K, Amini S. 2008. Evidence for involvement of NFBP in processing of ribosomal RNA. J Cell Physiol 214: 381-388.

Sweitzer TD, Hanover JA. 1996. Calmodulin activates nuclear protein import: a link between signal transduction and nuclear transport. Proc Natl Acad Sci USA 93: 14574-14579.

Tachibana T, Hieda M, Miyamoto Y, Kose S, Imamoto N, Yoneda Y. 2000. Recycling of importin alpha from the nucleus is suppressed by loss of RCC1 function in living mammalian cells. Cell Struct Funct 25: 115-123.

Temperley SM, Hay RT. 1992. Recognition of the adenovirus type 2 origin of DNA replication by the virally encoded DNA polymerase and preterminal proteins. EMBO J 11: 761-768.

Tibbetts C, Giam CZ. 1979. In vitro association of empty adenovirus capsids with double-stranded DNA. J Virol 32: 995-1005.

Tollefson AE, Hermiston TW, Lichtenstein DL, Colle CF, Tripp RA, Dimitrov T, Toth K, Wells CE, Doherty PC, Wold WS. 1998. Forced degradation of Fas inhibits apoptosis in adenovirus-infected cells. Nature 392: 726-730.

Tollefson AE, Scaria A, Hermiston TW, Ryerse JS, Wold LJ, Wold WS. 1996. The adenovirus death protein (E3-11.6K) is required at very late stages of infection for efficient cell lysis and release of adenovirus from infected cells. J Virol 70: 2296-2306.

Tollefson AE, Scaria A, Saha SK, Wold WS. 1992. The 11,600-MW protein encoded by region E3 of adenovirus is expressed early but is greatly amplified at late stages of infection. J Virol 66: 3633-3642.

Tollefson AE, Stewart AR, Yei SP, Saha SK, Wold WS. 1991. The 10,400- and 14,500-dalton proteins encoded by region E3 of adenovirus form a complex and function together to down-regulate the epidermal growth factor receptor. J Virol 65: 3095-3105.

Törmänen H, Backström E, Carlsson A, Akusjärvi G. 2006. L4-33K, an adenovirus-encoded alternative RNA splicing factor. J Biol Chem 281: 36510-36517.

Toth M, Doerfler W, Shenk T. 1992. Adenovirus DNA replication facilitates binding of the MLTF/USF transcription factor to the viral major late promoter within infected cells. Nucleic Acids Res 20: 5143-5148.

Tran EJ, Wente SR. 2006. Dynamic nuclear pore complexes: life on the edge. Cell 125: 1041-1053.

Trentin JJ, Yabe Y, Taylor G. 1962. The quest for human cancer viruses. Science 137: 835-841.

Tribouley C, Lutz P, Staub A, Kedinger C. 1994. The product of the adenovirus intermediate gene IVa2 is a transcriptional activator of the major late promoter. J Virol 68: 4450-4457.

Trotman LC, Mosberger N, Fornerod M, Stidwill RP, Greber UF. 2001. Import of adenovirus DNA involves the nuclear pore complex receptor CAN/Nup214 and histone H1. Nat Cell Biol 3: 1092-1100.

Truant R, Cullen BR. 1999. The arginine-rich domains present in human immunodeficiency virus type 1 Tat and Rev function as direct importin beta-dependent nuclear localization signals. Mol Cell Biol 19: 1210-1217.

Tsuji T, Sheehy N, Gautier VW, Hayakawa H, Sawa H, Hall WW. 2007. The nuclear import of the human T lymphotropic virus type I (HTLV-1) tax protein is carrier- and energy-independent. J Biol Chem 282: 13875-13883.

Tyler RE, Ewing SG, Imperiale MJ. 2007. Formation of a multiple protein complex on the adenovirus packaging sequence by the IVa2 protein. J Virol 81: 3447-3454.

van Breukelen B, Brenkman AB, Holthuizen PE, van der Vliet PC. 2003. Adenovirus type 5 DNA binding protein stimulates binding of DNA polymerase to the replication origin. J Virol 77: 915-922.

Varga MJ, Weibull C, Everitt E. 1991. Infectious entry pathway of adenovirus type 2. J Virol 65: 6061-6070.

Vayda ME, Flint SJ. 1987. Isolation and characterization of adenovirus core nucleoprotein subunits. J Virol 61: 3335-3339.

Vellinga J, Van der Heijdt S, Hoeben RC. 2005. The adenovirus capsid: major progress in minor proteins. J Gen Virol 86: 1581-1588.

Venema J, Tollervey D. 1996. RRP5 is required for formation of both 18S and 5.8S rRNA in yeast. EMBO J 15: 5701-5714.

Vetter IR, Arndt A, Kutay U, Görlich D, Wittinghofer A. 1999. Structural view of the Ran-Importin beta interaction at 2.3 A resolution. Cell 97: 635-646.

Vos HR, Bax R, Faber AW, Vos JC, Raue HA. 2004. U3 snoRNP and Rrp5p associate independently with Saccharomyces cerevisiae 35S pre-rRNA, but Rrp5p is essential for association of Rok1p. Nucleic Acids Res 32: 5827-5833.

Wagner EK, Roizman B. 1969. Ribonucleic acid synthesis in cells infected with herpes simplex virus. I. Patterns of ribonucleic acid synthesis in productively infected cells. J Virol 4: 36-46.

Walsh MP, Chintakuntlawar A, Robinson CM, Madisch I, Harrach B, Hudson NR, Schnurr D, Heim A, Chodosh J, Seto D, Jones MS. 2009. Evidence of molecular evolution driven by recombination events influencing tropism in a novel human adenovirus that causes epidemic keratoconjunctivitis. PLoS One 4: e5635.

Walters RW, Freimuth P, Moninger TO, Ganske I, Zabner J, Welsh MJ. 2002. Adenovirus fiber disrupts CAR-mediated intercellular adhesion allowing virus escape. Cell 110: 789-799.

Wang G, Berk AJ. 2002. In vivo association of adenovirus large E1A protein with the human mediator complex in adenovirus-infected and -transformed cells. J Virol 76: 9186-9193.

Wang K, Huang S, Kapoor-Munshi A, Nemerow G. 1998. Adenovirus internalization and infection require dynamin. J Virol 72: 3455-3458.

Wang P, Palese P, O'Neill RE. 1997. The NPI-1/NPI-3 (karyopherin alpha) binding site on the influenza a virus nucleoprotein NP is a nonconventional nuclear localization signal. J Virol 71: 1850-1856.

Weber J. 1976. Genetic analysis of adenovirus type 2 III. Temperature sensitivity of processing viral proteins. J Virol 17: 462-471.

Weber J, Philipson L. 1984. Protein composition of adenovirus nucleoprotein complexes extracted from infected cells. Virology 136: 321-327.

Weber JM. 1995. Adenovirus endopeptidase and its role in virus infection. Curr Top Microbiol Immunol 199: 227-235.

Webster A, Russell S, Talbot P, Russell WC, Kemp GD. 1989. Characterization of the adenovirus proteinase: substrate specificity. J Gen Virol 70: 3225-3234.

Weeks DL, Jones NC. 1985. Adenovirus E3-early promoter: sequences required for activation by E1A. Nucleic Acids Res 13: 5389-5402.

Weinberg RA, Loening U, Willems M, Penman S. 1967. Acrylamide gel electrophoresis of HeLa cell nucleolar RNA. Proc Natl Acad Sci USA 58: 1088-1095.

Weitzman MD, Ornelles DA. 2005. Inactivating intracellular antiviral responses during adenovirus infection. Oncogene 24: 7686-7696.

Wellehan JFX, Greenacre CB, Fleming GJ, Stetter MD, Childress AL, Terrell SP. 2009. Siadenovirus infection in two psittacine bird species. Avian Pathol 38: 413-417.

Wellehan JFX, Johnson AJ, Harrach B, Benkö M, Pessier AP, Johnson CM, Garner MM, Childress A, Jacobson ER. 2004. Detection and analysis of six lizard adenoviruses by consensus primer PCR provides further evidence of a reptilian origin for the atadenoviruses. J Virol 78: 13366-13369.

White E. 2001. Regulation of the cell cycle and apoptosis by the oncogenes of adenovirus. Oncogene 20: 7836-7846.

Wickham TJ, Mathias P, Cheresh DA, Nemerow GR. 1993. Integrins alpha v beta 3 and alpha v beta 5 promote adenovirus internalization but not virus attachment. Cell 73: 309-319.

Wiethoff CM, Wodrich H, Gerace L, Nemerow GR. 2005. Adenovirus protein VI mediates membrane disruption following capsid disassembly. J Virol 79: 1992-2000.

Wodrich H, Cassany A, D'Angelo MA, Guan T, Nemerow G, Gerace L. 2006. Adenovirus core protein pVII is translocated into the nucleus by multiple import receptor pathways. J Virol 80: 9608-9618.

Wodrich H, Guan T, Cingolani G, Von Seggern D, Nemerow G, Gerace L. 2003. Switch from capsid protein import to adenovirus assembly by cleavage of nuclear transport signals. EMBO J 22: 6245-6255.

Wohl BP, Hearing P. 2008. Role for the L1-52/55K protein in the serotype specificity of adenovirus DNA packaging. J Virol 82: 5089-5092.

Wold WS, Tollefson AE, Hermiston TW. 1995. E3 transcription unit of adenovirus. Curr Top Microbiol Immunol 199: 237-274.

Wu Q, Chen Y, Kulshreshtha V, Tikoo S. 2004. Characterization and nuclear localization of the fiber protein encoded by the late region 7 of bovine adenovirus type 3. Arch virology 149: 1783-1799.

Wu Q, Tikoo SK. 2004. Altered tropism of recombinant bovine adenovirus type-3 expressing chimeric fiber. Virus Res 99: 9-15.

Wu WW, Pante N. 2009. The directionality of the nuclear transport of the influenza A genome is driven by selective exposure of nuclear localization sequences on nucleoprotein. Virol J 6: 68.

Xing L, Tikoo SK. 2003. Characterization of cis-acting sequences involved in packaging porcine adenovirus type 3. Virology 314: 650-661.

Xing L, Tikoo SK. 2004. cis-Acting packaging motifs of porcine adenovirus type 3. Virus Res 104: 207-214.

Xing L, Tikoo SK. 2006. E1A promoter of bovine adenovirus type 3. J Gen Virol 87: 3539-3544.

Xing L, Tikoo SK. 2007. Bovine adenovirus-3 E1A coding region contain cis-acting DNA packaging motifs. Virus Res 130: 315-320.

Xing L, Zhang L, Van Kessel J, Tikoo SK. 2003. Identification of cis-acting sequences required for selective packaging of bovine adenovirus type 3 DNA. J Gen Virol 84: 2947-2956.

Xu ZZ, Nevels M, MacAvoy ES, Lockett LJ, Curiel D, Dobner T, Both GW. 2000. An ovine adenovirus vector lacks transforming ability in cells that are transformed by AD5 E1A/B sequences. Virology 270: 162-172.

Yokoya F, Imamoto N, Tachibana T, Yoneda Y. 1999. beta-catenin can be transported into the nucleus in a Ran-unassisted manner. Mol Biol Cell 10: 1119-1131.

Yun C-O, Kim E, Koo T, Kim H, Lee Y-s, Kim J-H. 2005. ADP-overexpressing adenovirus elicits enhanced cytopathic effect by induction of apoptosis. Cancer Gene Ther 12: 61-71.

Zakhartchouk A, Connors W, van Kessel A, Tikoo SK. 2004. Bovine adenovirus type 3 containing heterologous protein in the C-terminus of minor capsid protein IX. Virology 320: 291-300.

Zakhartchouk AN, Godson DL, Babiuk LA, Tikoo SK. 2001. 121R protein from the E3 region of bovine adenovirus-3 inhibits cytolysis of mouse cells by human tumor necrosis factor. Intervirology 44: 29-35.

Zakhartchouk AN, Pyne C, Mutwiri GK, Papp Z, Baca-Estrada ME, Griebel P, Babiuk LA, Tikoo SK. 1999. Mucosal immunization of calves with recombinant bovine adenovirus-3: induction of protective immunity to bovine herpesvirus-1. J Gen Virol 80 (Pt 5): 1263-1269.

Zakhartchouk AN, Reddy PS, Baxi M, Baca-Estrada ME, Mehtali M, Babiuk LA, Tikoo SK. 1998. Construction and characterization of E3-deleted bovine adenovirus type 3 expressing full-length and truncated form of bovine herpesvirus type 1 glycoprotein gD. Virology 250: 220-229.

Zakhartchouk AN, Viswanathan S, Mahony JB, Gauldie J, Babiuk LA. 2005. Severe acute respiratory syndrome coronavirus nucleocapsid protein expressed by an adenovirus vector is phosphorylated and immunogenic in mice. J Gen Virol 86: 211-215.

Zan M, Evans P, Lucas-Lenard J. 1990. The inhibition of mouse L-cell 45 S ribosomal RNA processing is a highly uv-resistant property of vesicular stomatitis virus. Virology 177: 75-84.

Zhang W, Arcos R. 2005. Interaction of the adenovirus major core protein precursor, pVII, with the viral DNA packaging machinery. Virology 334: 194-202.

Zhang W, Imperiale MJ. 2000. Interaction of the adenovirus IVa2 protein with viral packaging sequences. J Virol 74: 2687-2693.

Zhang W, Imperiale MJ. 2003. Requirement of the adenovirus IVa2 protein for virus assembly. J Virol 77: 3586-3594.

Zhang W, Low JA, Christensen JB, Imperiale MJ. 2001. Role for the adenovirus IVa2 protein in packaging of viral DNA. J Virol 75: 10446-10454.

Zhang X, Yamada M, Mabuchi N, Shida H. 2003. Cellular requirements for CRM1 import and export. J Biochem 134: 759-764.

Zhang Y, Bergelson JM. 2005. Adenovirus receptors. J Virol 79: 12125-12131.

Zheng B, Mittal SK, Graham FL, Prevec L. 1994. The E1 sequence of bovine adenovirus type 3 and complementation of human adenovirus type 5 E1A function in bovine cells. Virus Res 31: 163-186.

Zheng BJ, Graham FL, Prevec L. 1999. Transcription units of E1a, E1b and pIX regions of bovine adenovirus type 3. J Gen Virol 80: 1735-1742.

Zhou Y, Pyne C, Tikoo SK. 2001a. Determination of bovine adenovirus-3 titer based on immunohistochemical detection of DNA binding protein in infected cells. J Virol Methods 94: 147-153.

Zhou Y, Reddy PS, Babiuk LA, Tikoo SK. 2001b. Bovine adenovirus type 3 E1B(small) protein is essential for growth in bovine fibroblast cells. Virology 288: 264-274.

Zijderveld DC, d'Adda di Fagagna F, Giacca M, Timmers HT, van der Vliet PC. 1994. Stimulation of the adenovirus major late promoter in vitro by transcription factor USF is enhanced by the adenovirus DNA binding protein. J Virol 68: 8288-8295.

Zijderveld DC, van der Vliet PC. 1994. Helix-destabilizing properties of the adenovirus DNA-binding protein. J Virol 68: 1158-1164.